

NEURODEGENERATION RISK FACTOR TREM2 R47H MUTATION CAUSES
DISTINCT SEX- AND AGE- DEPENDENT MUSCULOSKELETAL PHENOTYPE

Alyson Lola Essex

Submitted to the faculty of the University Graduate School
in partial fulfillment of the requirements
for the degree
Doctor of Philosophy
in the Department of Anatomy and Cell Biology,
Indiana University

May 2022

Accepted by the Graduate Faculty of Indiana University, in partial fulfillment of the requirements for the degree of Doctor of Philosophy.

Doctoral Committee

Lilian I. Plotkin, PhD, Co-Chair

Andrea Bonetto, PhD, Co-Chair

March 14, 2022

Matthew Allen, PhD

Gary E. Landreth, PhD

© 2022

Alyson Lola Essex

DEDICATION

To my college counselor at Winter Haven High School, Mrs. Ware, who looked me in the eye in 2012 and told me not to study science in college because “science was for the boys. It’s hard, let them do it. Be the secretary instead, they need smart people to be secretaries!”. I have spent a full decade proving you wrong. Every time I wanted to quit, I thought of that moment in your office when you crushed the dreams of an 18 year old excited to begin her career, the dreams of a 5 year old who came home every day to watch Bill Nye the Science Guy on TV with her grandmother.

This is dedicated to all the girls in Polk County and Winter Haven who took your terrible advice and never pursued careers in science. For all the researchers, doctors, and engineers that could have been but were stifled by sexist, outdated “advice”. For all the innovation, discovery, and lives changed that will never happen because of the rampant sexism that continues to oppress women, particularly women of color.

Finally, this is dedicated to my mom, the strongest woman I know, who reminded me that I can do anything I set my mind to and convinced me to still go to school for science. You taught me all I know, made me who I am, and taught me how to fight (literally and figuratively). I love you more than anything, and everything I do I owe in part to you.

ACKNOWLEDGEMENT

I would like to formally acknowledge that IUPUI stands on the historic homelands of the Miami people, but also displaced a vibrant Black community. This work was done on the ancestral lands of Native peoples who were removed unjustly, and that we in this community are the beneficiaries of that removal. We honor the heritage of Native peoples, what they teach us about stewardship of the earth and their continuing efforts today to protect the planet.

I would like to acknowledge the work of students mentored by me and others in the lab whose work contributed to this project, including Jorge Figueras, Allison Wagner, Azaria Davis, Harry Sidhu, Raquel Ciprian, Sylvia Robertson, Austin Magley, and the many high school students who came through the lab during the summers. You taught me as much as we (hopefully) taught you.

More than an acknowledgement belongs to Padmini, Joshua Huot, and Fabrizio Pin for being so patient with me over the last few years. You have been instrumental in teaching me everything about doing research and how to do science. I won't miss having someone screaming "Legs" at me, though.

Zach, you deserve more than a line in a paper to thank you for all you have done to help me through this process, so I'll marry you instead. Who else would let me bring a cat into the house in the middle of winter right before a pandemic?

Alyson Lola Essex

NEURODEGENERATION RISK FACTOR TREM2 R47H MUTATION CAUSES A
DISTINCT SEX- AND AGE- DEPENDENT MUSCULOSKELETAL PHENOTYPE

Triggering Receptor Expressed on Myeloid Cells 2 (TREM2), a receptor expressed in myeloid cells including microglia in brain and osteoclasts in bone has been proposed as a link between brain and bone disease. Previous studies identified an AD-associated mutation (R47H) which is known to confer an increased risk for developing AD. In these studies, we used a heterozygous model of the TREM2 R47H variant (TREM2^{R47H/+}), which does not exhibit cognitive defects, as a translational model of genetic risk factors that contribute to AD, and investigated whether alterations to TREM2 signaling could also contribute to bone and skeletal muscle loss, independently of central nervous system defects. Our study found that female TREM2^{R47H/+} animals experience bone loss in the femoral mid-diaphysis between 4 and 13 months of age as measured by microCT, which stalls out by 20 months of age. Female TREM2^{R47H/+} animals also experience significant decreases in the mechanical and material properties of the femur measured by three-point bending at 13 months of age, but not at 4 or 20 months. Interestingly, male TREM2^{R47H/+} animals do not demonstrate any discernable differences in bone geometry or strength until 20 months of age, where we observed slight changes in the bone volume and material properties of male TREM2^{R47H/+} bones. *Ex vivo* osteoclast differentiation assays demonstrate that only male TREM2^{R47H/+} osteoclasts differentiate more after 7 days with osteoclast differentiation factors compared to WT, but qPCR follow-up showed sex-dependent differences in intracellular signaling. However, bone is not the only musculoskeletal tissue affected by the TREM2 R47H variant. Skeletal muscle strength

measured by both in vivo plantar flexion and ex vivo contractility of the soleus is increased and body composition is altered in female TREM2^{R47H/+} mice compared to WT, and this is not likely due to bone-muscle crosstalk. These studies suggests that TREM2 R47H expression in the bone and skeletal muscle are likely impacting each tissue independently. These data demonstrate that AD-associated variants in TREM2 can alter bone and skeletal muscle strength in a sex-dimorphic manner independent of the presence of central neuropathology.

Lilian I. Plotkin, PhD, Co-Chair

Andrea Bonetto, PhD, Co-Chair

Matthew Allen, PhD

Gary E. Landreth, PhD

TABLE OF CONTENTS

LIST OF TABLES	ix
LIST OF FIGURES	x
LIST OF ABBREVIATIONS.....	xii
CHAPTER ONE: Background	1
CHAPTER TWO: Sex-dependent bone loss and weakness occur between 4 and 20 months of age in TREM2 ^{R47H/+} mice	6
Introduction	6
Methods	16
Results.....	21
CHAPTER THREE: Sex-dependent increase in skeletal muscle strength with TREM2 R47H variant	40
Introduction	40
Methods	47
Results.....	53
CHAPTER FOUR: Discussion.....	68
Conclusions	77
REFERENCES	80
CURRICULUM VITAE	

LIST OF TABLES

Table 1: ANOVA analysis from Figure 1-11.	39
Table 2: ANOVA analysis from Figure 2-1.	66
Table 3: ANOVA analysis from Figure 2-3.	66
Table 4: ANOVA analysis from Figure 2-4.	66
Table 5: ANOVA analysis from Figure 2-5.	67

LIST OF FIGURES

Figure 1-1: TREM2 mRNA expression is not altered in brain, marrow-flushed tibias, ex vivo differentiated osteoclast cultures, or whole gastrocnemius muscle lysates from male or female TREM2 ^{R47H/+} mice compared to WT.	27
Figure 1-2: TREM2 ^{R47H/+} has no effect on cortical or trabecular bone volume in male or female mice at 4 months of age.	28
Figure 1-3: TREM2 ^{R47H/+} has minimal effect on femoral bone strength in female but not male mice as assessed by three-point bending.	29
Figure 1-4: BMD accrual is reduced in female but not male TREM2 ^{R47H/+} animals.	30
Figure 1-5: Female TREM2 ^{R47H/+} mice have cortical and trabecular bone loss at 13 months of age.	31
Figure 1-6: Female TREM2 ^{R47H/+} mice have less mechanical and material strength compared to WT littermates at 13 months of age.	32
Figure 1-7: Age-induced bone loss in male and female TREM2 ^{R47H/+} animals at 20 months of age.	33
Figure 1-8: Mechanical and material strength of bone from TREM2 ^{R47H/+} animals at 20 months of age.	34
Figure 1-9: TRAP-stained scoring of cortical bone from female TREM2 ^{R47H/+} and WT femurs.	35
Figure 1-10: Dynamic histomorphometry analysis of cortical bone from female TREM2 ^{R47H/+} femurs.	36

Figure 1-11: Sex-dependent alterations in osteoclast differentiation and sex-hormone receptor expression in TREM2 ^{R47H/+} osteoclasts.	37
Figure 1-12: Sex-dependent alterations in intracellular signaling in TREM2 ^{R47H/+} osteoclasts.	38
Figure 2-1: Body composition and strength are altered in female, but not male TREM2 ^{R47H/+} animals.	57
Figure 2-2: Activity monitoring of male and female TREM2 ^{R47H/+} animals at 12 months of age.....	59
Figure 2-3: Increased in vivo plantar flexion in female and male TREM2 ^{R47H/+} animals at 12 months of age.....	60
Figure 2-4: Nerve input does not contribute to changes in muscle strength, and EDL muscle is unaffected by TREM2 R47H variant in female animals at 13 months of age...61	
Figure 2-5: Increased ex vivo soleus contractility muscle strength in female TREM2 ^{R47H/+} animals at 12 months of age.....	62
Figure 2-6: Serum TGF-β levels decreased in aged but not young male and female TREM2 ^{R47H/+} mice compared to WT littermates.	63
Figure 2-7: C2C12 myotubes exposed to conditioned media from marrow-flushed TREM2 ^{R47H/+} and WT bones.	64

LIST OF ABBREVIATIONS

- TREM2 – Triggering Receptor Expressed on Myeloid Cells 2
- R47H – Amino acid variant (arginine to histidine substitution at the 47th amino acid)
- TREM2^{-/-} - Complete deletion of TREM2 gene (TREM2 knockout)
- WT – Wild type, used interchangeably with control or littermate control
- KO – Knockout
- AD – Alzheimer’s Disease
- BMD – Bone mineral density
- RANKL – Receptor activator of nuclear factor kappa-B ligand
- M-CSF – Macrophage colony stimulating factor
- qPCR – Real-time polymerase chain reaction
- C3 – Complement component 3
- μCT – Micro computed tomography
- SNP – Single nucleotide polymorphism
- RNA – Ribonucleic acid
- GAPDH - Glyceraldehyde 3-phosphate dehydrogenase
- PBS – Phosphate buffered saline
- FBS – Fetal bovine serum
- P/S – Penicillin/Streptomycin
- α-MEM – Alpha-minimum essential media
- TRAP – Tartrate resistant acid phosphatase
- EMG - Electromyography
- CMAP - Compound muscle action potential

ANOVA - Analysis of variance

mRNA – Messenger ribonucleic acid

BV – Bone volume

TV – Tissue volume

TMD – Tissue mineral density

ER α – Estrogen receptor alpha

ER β – Estrogen receptor beta

BCL2 - B-cell lymphoma 2

CREB - Cyclic-adenosine monophosphate response element-binding protein

EDL – Extensor digitorum longus

TGF- β – Transforming growth factor beta

CM – Conditioned media

C2C12 – Refers to a myoblast cell line differentiated into myotubes

M1/M2 – Refers to sub-classification of macrophages (type 1 or 2)

MuRF-1 - E3 ubiquitin-protein ligase TRIM63

A β – Amyloid beta

mTOR – mammalian target of rapamycin

Akt – protein kinase B

5xFAD – 5x Familial Alzheimers Disease mouse model containing five familial variants

known to increase risk of developing Alzheimers Disease

4E-BP – eukaryotic initiation factor 4E – binding protein

ALS - Amyotrophic lateral sclerosis

TNF- α – Tumor Necrosis Factor alpha

HMGB1 – High mobility group box 1

SERM – Selective Estrogen Receptor Modulator

FasL – Fas cell surface death receptor ligand

PGC-1 α - Peroxisome Proliferator-Activated Receptor Gamma Coactivator 1 Alpha

CHAPTER ONE: Background

The proportion of the human population over the age of 65 is continuing to grow, mostly due to the aging baby boomer population born in the 1950's and 1960's but also compounded by the miracles of modern medicine continuing to extend life expectancy [1, 2]. However, as a person ages, their risk for developing diseases such as cancer, diabetes, or dementia increases. To continue making advances towards average life expectancy and quality of life in advanced age, we must find treatments for age-related diseases. This involves understanding not only the mechanisms of aging itself, but also how aging exacerbates other risk factors for development of these age-related diseases. In this context, understanding aging is not the primary goal, but rather understanding how aging works with other risk factors to influence disease. Herein, we will discuss aging as a context for studying a genetic risk factor for age-related disease, and how risk factors for a disease of the brain can also impact other tissues, notably bone and skeletal muscle.

Aging cannot be pinpointed to a singular process or event, biological or otherwise. Aging is an amalgamation of societal, environmental, physiological, and biological processes that change and progress across a person's lifetime. Biological aging is multifaceted, and includes molecular mechanisms of cellular aging, material and mechanical changes of tissues of the body, and the physiological or psychological consequences of these changes. Although aging itself is not necessarily a disease on its own, it is a risk factor contributing to the development of multiple diseases. This is due to age-related changes in processes such as cellular senescence, secretion of inflammatory cytokines, accumulation of genetic errors, and many other mechanisms that have been discussed elsewhere [3-6]. However, the biological process of aging in and of itself is not

the primary focus of this work. Instead, we will focus on the study of age-related disease, specifically Alzheimer's Disease (AD), a type of dementia. Age, due to the aforementioned effects on cellular processes, is the largest risk factor for the development of dementia [7, 8]. Dementia is a general term for neurodegenerative diseases that cause cognitive and behavioral impairments, and includes diseases such as frontal temporal dementia, Lewy body dementia, Parkinson's Disease, and Alzheimer's Disease [9].

Alzheimer's Disease is the most common type of dementia, and its incidence is projected to grow across the next few decades [10, 11]. AD initially presents as mild cognitive impairment (MCI) such as memory loss, and histopathology includes the presence of amyloid precursor protein (APP) and amyloid-beta ($A\beta$) plaques in the cerebral spinal fluid and brain respectively [9]. APP is found in other tissues both in AD and in a non-disease environment, but in AD is improperly folded and accumulates as what are called plaques [12-14]. Tau neurofibrillary tangles are a hallmark pathological feature of AD, microtubule-associated protein tau that have become hyper phosphorylated and contribute to dysregulated neuronal microtubule dynamics, synaptic dysfunction, and memory loss [15]. These pathologies are cited as critical components of the onset and degeneration of memory and cognitive function in AD. However, there are other cellular contributors to AD and neurodegeneration beyond these pathological proteins.

Neurodegeneration researchers have identified a critical role for microglia in the onset and pathogenesis of neurodegeneration and dementia. Microglia are myeloid cells of the brain which, at a young age, are involved in synaptic pruning and brain homeostasis [16]. The synaptic pruning process occurs most notably in development where the microglia prune, or remove, synapses from neurons to help the neural circuit develop and

become more efficient [17]. Although this synapse-microglia relationship and selection process is not entirely understood, it is thought that the disruption of this pruning can lead to schizophrenia, autism, and potentially epilepsy [18, 19]. In AD, microglia also prune what are referred to as dystrophic neurites, which are neurons that are rendered nonfunctional due to AD pathology. The phagocytosis of these neurons by microglia is disrupted in AD by dysfunctional complement and Triggering Receptor Expressed on Myeloid cells 2 (TREM2)-mediated signaling and phagocytosis [20, 21]. However, microglia have also been shown to contribute significantly to the pathogenesis and inflammation of dementia and AD [22]. As such, microglial biologists have studied the role of microglia in the brain and how AD causes microglia to change their cellular activity in a way that contributes to the pathogenesis and progression of neurodegenerative disease. Although many mechanisms of microglial function have been shown to contribute to AD, one key mechanism has been the role of TREM2. TREM2 has been shown to play a critical role in microglial response to AD pathology, potentially even being a receptor for the A β oligomers and dictating microglial response to plaque [23]. Interestingly, TREM2 activation does not seem to trigger phagocytosis, but rather causes the cell to spread out and cover the plaque in an attempt to prevent more oligomers from attaching and expanding the plaque [24-26].

Although the principle components of AD are in the brain, previous work has shown AD to also negatively impact other tissue systems beyond the brain. Loss of mobility is one of the most physically limiting aspects of dementia, contributing to an estimated \$221 billion in caregiver labor [27]. Further, limitation of physical function is one identified predictor of mortality in AD patients, suggesting that improving such defects

could improve longevity in AD patients [28]. Dementia patients are also more likely to suffer from fracture, and those who do fracture are less likely to regain mobility [29]. These observations suggest a connection between musculoskeletal health and AD, but how bone and skeletal muscle function, specifically the strength of these tissues, are impacted by AD remains unclear. There are two primary ideas as to how bone and skeletal muscle are impacted in AD: first, that the bone and muscle weakness is an effect of the central neuropathology, or the second idea is that the mechanisms contributing to the central neuropathology in AD are also active in bone and skeletal muscle and could be independent of the central neuropathology. This study explores the second idea, using a mouse model carrying a genetic variant known to increase the risk for developing AD in human patients [30].

GWAS studies have identified the R47H variant in TREM2 to confer a significantly increased risk of developing AD [31-33]. This variant has been primarily discussed in microglia and macrophages, as will be detailed in the Introduction, but no work has been done in other myeloid cells of the musculoskeletal system such as osteoclasts of the bone. Recent work by Dr. Oblak demonstrated that metabolically, behaviorally, and anatomically no effect is seen in male or female mice that are homozygous for the TREM2 R47H variant, and no plaque or tau tangle pathology is seen in the brains of these animals [34]. Interestingly, both male and female mice homozygous for the TREM2 R47H variant did have greater impairment in motor coordination at 24 months of age compared to 4 months of age and a decreased latency to fall by rotarod motor coordination assay. 24 month old male animals homozygous for the TREM2 R47H variant also had increased activity as measured by increased distance travelled in running wheel activity [34]. These data suggest

that the R47H variant likely has an effect on the musculoskeletal system through changes in the nervous system with aging, but skeletal muscle or bone strength were not evaluated. And in many studies of AD, bone and skeletal muscle are not directly assessed.

This leaves open the question of whether bone or skeletal muscle is negatively impacted beyond the central degeneration of AD, and whether mechanisms of AD active in cells of the brain are also active in other tissues serving as a potential shared therapeutic target. Herein, we will explore the TREM2 R47H variant's effect on bone and skeletal muscle size, shape, and function. These results will identify whether mechanisms known to be active in the brain during AD may also be active and deleterious in other tissues beyond the brain, and will be some of the first evidence to suggest TREM2 as the link between observed correlations in brain and bone. Further, these data will be some of the first to suggest a role for TREM2 in skeletal muscle.

CHAPTER TWO: Sex-dependent bone loss and weakness occur between 4 and 20 months of age in TREM2^{R47H/+} mice

Introduction

Bone is the calcified tissue that comprises the skeletal system, responsible for maintaining upright body posture and provides protection for vital internal organs such as the brain encapsulated by the skull and the heart, liver, and lungs encased by the rib cage. Bone is often referred to as a foundation, likely due to its hard calcified state upon which many other tissues and organ systems lay adjacent. Unlike a foundation, bone is not a vapid rock, but a cell-dense tissue system. This includes the plethora of cells contained in the bone marrow, chondrocytes of the cartilage, and fibroblasts of the tendons, all of which are critically important in their own way. Bone biology and the maintenance of bone integrity are facilitated by three primary bone cells: the osteoblast, osteocyte, and osteoclast. These primary bone cells are critical in maintaining the bone strength required for daily living activities and are also responsible for age-related bone loss. Bone loss and associated weakness is also known as osteoporosis. Osteoporosis is defined clinically as having a low bone mineral density (BMD) compared to healthy controls, and this measurement is established as a strong indicator of fragility and risk for fracture [35, 36]. Osteoporosis-related fractures are projected to affect 1 in 3 women and 1 in 5 men over the age of 50, and are known to significantly increase mortality [36-38]. Osteoporosis is not only a disease of age and can be caused by chronic glucocorticoid use, sex steroid deficiency, menopause, and spaceflight/unloading [39-42].

Although there are existing treatments that have been proven effective in increasing BMD and reducing fracture risk, they are not effective long term due to a variety of

concerns. For example, bisphosphonates such as zoledronic acid and alendronate are a class of drugs that target the bone exclusively and stop resorption by osteoclasts, but long-term side effect concerns include osteonecrosis of the jaw, atypical femoral fractures, kidney failure, and cardiac concerns [43-48]. Denosumab is another potent drug that stops osteoclasts from differentiating through blockade of potent osteoclastic activator Receptor Activated by NFkB Ligand (RANKL), but after treatment the rebound in bone loss happens rapidly after final treatment, problems of osteonecrosis of the jaw remain present even with Denosumab. This leaves many patients in need of more therapies [PTH ADD HERE] [49-51]. Therefore, continued understanding of the underlying cellular mechanisms of osteoporosis are needed, and of primary focus has been the osteocyte. Further, the intersection of AD and age-related bone loss remains unknown, and this limit in our knowledge limits our ability to find more targeted, effective therapeutics for bone loss.

Osteocytes are considered the master regulators of the bone, embedded in the calcified tissue and interconnected in a network that works to coordinate the maintenance of healthy, strong bone throughout life [52-54]. As aging occurs, osteocytes undergo apoptosis and are unable to communicate with each other or other bone cells [55, 56]. This lack of communication leads to unregulated, imbalanced bone remodeling where more bone is being resorbed by the osteoclast than can be made by the osteoblast. It has been shown that this osteocyte apoptosis not only occurs with aging, but contributes to the age-related bone loss [57, 58]. Although the osteocytes are embedded in the bone in their lacunae, when they undergo apoptosis they release a variety of cytokines and signaling factors. The profile of these factors is not completely defined, but data has demonstrated factors like RANKL, HMGB1, and exosomes are released by the apoptotic osteocyte and

enable the increased resorption-induced bone loss [58-60]. Although bisphosphonates have been shown to have some positive effect on the osteocyte, it remains unknown whether targeting osteocyte viability pharmacologically is a potential therapeutic mechanism in osteoporosis-related bone loss [61, 62].

A majority of the pharmaceutical and research focus to improve bone mass and strength is focused on limiting the function of the osteoclast thereby stopping bone resorption and limiting further loss. Whether through inhibition of RANKL-induced osteoclastogenesis (Denosumab) or by stopping degradation of bone via bisphosphonates stopping osteoclast activity through various mechanisms is the primary target of pharmacological intervention for bone loss with aging [63-66]. RANKL is known as the most potent osteoclastogenic factor, signaling for myeloid progenitor cells to differentiate into osteoclasts as well as contributing to pro-survival signals [67-70]. More recent work has suggested RANKL may also aid in osteoclast activity and the fusion/fission “recycling” process, although this is not well understood [71]. Other factors such as macrophage colony stimulating factor (mCSF) are also critical for osteoclast differentiation, and other factors are also known to stimulate osteoclastogenesis [72, 73]. For example, Tumor Necrosis Factor-alpha (TNF α) is known to induce osteoclast differentiation in the presence of RANKL [74, 75]. This focus is due to the fact that, with aging, one of the strongest drivers of bone loss is increases in osteoclast differentiation and activity.

This is partially due to previously mentioned mechanisms of osteocyte death and release of osteoclastogenic factors such as HMGB1 and other ligands for the receptor for advanced glycosylation end products (RAGE) [58, 76]. However, another strong contributor to age-related bone loss is the loss of estrogen signaling that occurs in women

with menopause [77, 78]. Menopause, age-associated loss of sex-hormones, particularly estrogen, contributes to the greater prevalence of osteoporosis among women compared to men. The loss of estrogen hormone due to menopause has a significant deleterious effect on bone [79-81]. Estrogen signaling in the osteoclast induces apoptosis in the osteoclast and inhibits the amount of bone that can be lost by resorption [82, 83]. This is due in part to estrogen signaling in the osteoclast, increasing the expression of FasL which induces cellular apoptosis [84-88]. Indeed, by selectively stimulating estrogen signaling in the bone through selective estrogen receptor modulators (SERMs), osteoclast activity can be reduced and bone mass preserved, although some evidence suggests this may also be due to positive effects on the osteoblast and osteocyte [89-93]. SERMs have served as a successful therapeutic strategy for inhibiting osteoclast-mediated bone resorption, but concerns remain over undesirable estrogen-like stimulation in other tissues such as breast tissue, limiting therapeutic effectiveness in some post-menopausal women [94, 95]. Although targeting osteoclast function has served as an effective therapeutic strategy there is focus on finding new targetable mechanisms that can not only stop the loss of bone but improve bone mass and, more importantly, bone strength.

Bone mechanical strength is commonly referred to as bone's resistance to fracture. Contributing factors to this strength include the volume and shape of the bone, as well as the material of the bone. Bone matrix is primarily made up of cross-linked collagen fibrils surrounded by mineral, organic matrix, and water [96]. Osteoblasts build bone by secreting collagen along with other organic matrix proteins that eventually becomes mineralized with a mix of hydroxyapatite [97, 98]. The process of resorbing bone and replacing it with new bone is a coordinated event where old bone is being replaced with new and is termed either

modeling or remodeling [99]. This coordinated cell function is orchestrated by the osteocyte, but these cells also communicate with each other through paracrine signaling to coordinate activity, movement, and location of these remodeling units of osteoclast and osteoblast activity [100, 101]. This coordinated effort among the bone cells maintain two key aspects of bone strength: the geometry of the bone and the material.

The geometry of the bone, specifically parameters of the cortical bone, determine the mechanical strength of the bone to resist displacement and fracture when tested by three point bending. Femoral three point bending places force perpendicularly on the mid-shaft of the femur and measures the mechanical strength of the bone, measuring the amount of displacement caused by increasing force to the point the bone permanently deforms, the yield point, and finally reaches a failure point and breaks. These assessments of mechanical strength, however, are primarily based on geometry and assume the material of the bone is similar between groups being tested. Bone material can vary between groups for a variety of reasons, such as improper collagen crosslinking or the accumulation of molecules like advanced glycosylation end products in the bone matrix with age resulting in reduced strength of the bone material [102-104]. Therefore, it is helpful to also assess the strength of the bone material. Material properties of the bone can be derived from the mechanical assessment if the cortical bone geometry is known, and stress-strain equations can be applied to get estimations of the material properties, or the intrinsic resistance of the bone material to deformation [105]. Changes to bone mechanical and material strength with age are known, it remains untested if AD-associated mutations also contributes or changes bone strength.

The economic and medical burden of age-related diseases continues to grow, and musculoskeletal disease including fractures continue to be among the most prevalent and costly age-related complications, highlighting the importance of identifying effective interventions to improve musculoskeletal strength and function [106-108]. One of the most widespread age-related diseases is dementia, which is associated with lack of independence and increased death. Dementia is a broad term used to describe neurodegenerative diseases that cause declines in cognitive functions such as memory, the most prevalent being AD. AD is a neurodegenerative disease with distinct pathology including neuroinflammation, accumulation of A β plaques, and tau neurofibrillary tangles [109]. Although AD is a disease of the brain, clinical evidence suggests that other tissues may be negatively impacted by AD, including bone and skeletal muscle. Skeletal muscle has also been shown to be negatively impacted by AD, based on evidence that female and male patients progressively lose skeletal muscle mass and strength as disease progression worsens compared to age and sex-matched controls, suggesting that AD may be exacerbating age-related loss of strength [110, 111].

In mouse models of neurodegenerative disease, mice with genetic variants that experience AD-like neuropathology, including the APP/PS1 model of plaque and the MAPT model of tau neurofibrillary tangles, exhibit less bone mineral density (BMD) compared to controls, suggesting a connection between brain and bone health [112, 113]. Low BMD is a prognostic indicator of a risk for fracture, and is used clinically to help decide when therapeutic interventions are necessary [114-116]. Interestingly, amyloid precursor protein (APP) has been shown to both stimulate and suppress osteoblast activity, making it unclear what contributions the osteoblasts make to the observed bone loss and

weakness in AD [117, 118]. Other work in the APP/PS1 mouse model has demonstrated decreased bone volume, although this was only quantified in the trabecular compartment, and the bone loss was only observed four months after peak plaque burden was observed and 10-11 months after plaque content began forming, suggesting central pathology may not be the only contributing factor to bone loss [119]. This relationship is not only found in animal models, but clinical studies in AD and dementia patients have demonstrated a correlation between brain and bone volume suggesting BMD may be an indicator of neurodegeneration [29, 120]. Clinical studies have even suggested that low BMD may serve as a predictive factor for the development of AD, suggesting the accelerated bone loss may precede onset and diagnosis of AD [121]. Further, work in Nasu-Hakola disease has demonstrated that although brains from patients with Nasu-Hakola disease have plaque in their brains, it is concluded to not contribute to overall clinical disease course, and since bone pathology is common in Nasu-Hakola disease patients, this suggests plaque alone may not be able to explain bone loss in AD patients [122].

Clinical studies have demonstrated a significant association with cognitive decline, bone loss, and fracture risk, [123] and a significant correlation between low bone mineral density (BMD) and lower brain volume suggesting that AD may increase the risk for developing bone weakness [29]. Further, retrospective studies have demonstrated that both low BMD and osteoporosis diagnosis were significant predictors of progression from mild cognitive impairment to diagnosed dementia, suggesting that bone loss may precede some of the clinical manifestations of AD [120, 121].

Previous work in mouse models of AD has shown bone loss in the distal femur measured by micro-computerized tomography (μ CT) in young but not in an aged mouse

model of plaque neuropathology, as well as increases in osteoclast differentiation of cells from young but not old mice that cannot be singularly explained by the presence of A β [124]. Further work has demonstrated age-dependent loss of femoral bone mass in a different mouse model of plaque neuropathology in AD [119]. However, these data are limited and suggest that there may be mechanisms of AD-related bone loss that are not only independent of the central neuropathology but may be a consequence of age. To date, no mechanistic links between bone loss and AD have been identified, and the interaction between age and AD-related bone loss has never been explored. AD patients are more susceptible to falls and fractures, which often result from reduced skeletal muscle and bone strength [125, 126]. Therefore, understanding the mechanisms underlying bone and muscle loss in AD will be critical for finding therapeutic targets that could effectively reduce falls and fractures by targeting both tissues. Further, defining a potential mechanism of bone and muscle loss independent of central neurodegeneration will improve the overall understanding of neurodegenerative effects on peripheral physiology.

Triggering Receptor Expressed on Myeloid Cells 2 (TREM2) is a phagocytic receptor expressed on cells of the myeloid lineage including microglia, macrophages, and osteoclasts [23]. TREM2 is used by microglia for synaptic pruning and in macrophages to aid in phagocytosis and inflammatory response [127-129]. Additionally, TREM2 has been shown to contribute to the neuroinflammation that occurs during AD by altering microglial function [130-132]. TREM2 has been shown to play a critical role in microglial response to AD pathology, being a receptor for the A β oligomers and dictating microglial response to plaque although not triggering phagocytosis of the plaque but forming a barrier to prevent further expansion of the plaque [23-25]. Previous studies on TREM2 signaling in

osteoclasts have identified β -catenin as being a critical downstream mediator of TREM2 signaling in osteoclasts, and TREM2 is known to contribute to osteoclast differentiation and resorption [133, 134]. Although the role of wild type TREM2 in osteoclasts is somewhat understood, whether TREM2 may also contribute to AD-related degeneration beyond the brain such as bone fragility remains unexplored. Previous work by Jay et al. have primarily used TREM2 knockout models that do not express any TREM2 receptor to understand TREM2 signaling and consequences [23, 26]. However, knockout models may not explain how amino acid variants that alter TREM2 signaling contribute to the observed increased risk for AD.

Genome wide associations studies (GWAS) have identified the R47H variant of the TREM2 gene to significantly increase the risk for developing AD [135]. The TREM2 R47H variant has previously been shown to have a phenotype in brain similar to that of a heterozygous knockout in a mouse model of AD, decreasing microglial response to plaque by reducing the plaque-barrier function of microglia [136]. However, the TREM2 R47H variant has also been shown to alter intracellular signaling, specifically phospho-Syk, without having an observable phenotype on macrophages differentiated from human induced-pluripotent stem cell macrophages [137]. Biochemical work has demonstrated that the R47H variant occurs in the ligand binding domain of the receptor, and these effects of the R47H variant in microglia and macrophages are likely due to changes in receptor binding to ligand [138]. Previous work in Nasu-Hakola neurodegenerative disease has identified variants in TREM2 that impact bone and brain simultaneously [139]. However, no such work has identified a similar effect of TREM2 variants on brain and bone that are associated with AD. Further, it remains unclear whether AD-associated bone loss is

secondary to the neurodegeneration or if mechanisms of bone loss occur independent of the neurodegeneration.

This work is the first to address whether a genetic variant in TREM2 known to contribute to high risk of developing AD could also be involved in bone loss independent of central neurodegeneration pathology. To do this, we utilized global TREM2^{R47H/+} mice and WT littermates to evaluate whether the AD-associated R47H variant in TREM2, identified in GWAS studies to increase risk for developing AD by three- to four-fold, could also contribute to the bone and muscle weakness seen clinically [32, 135]. These mice have no additional mutations that would be needed to cause AD pathology, and thorough characterization of mice homozygous for the R47H variant has shown that mice with this variant do not develop AD pathology [30, 34]. These results are the first to define a potential mechanism of AD-associated bone loss independent of neurodegeneration and suggest that TREM2 may be a common link between AD-related degeneration of brain and bone.

Methods

Mice

TREM2^{R47H/+} mutant mice were generated by Jackson Labs in collaboration with the Model-AD center using CRISPR-Cas9 genome editing as previously described [136]. Animals were maintained heterozygous for the global TREM2 R47H mutation (TREM2^{R47H/+}) and wild-type TREM2^{+/+} (WT) littermates were used as controls. SNP-based genotyping (Thermo Fisher) was used to identify carriers in subsequent crosses using the following: forward primer: 5'-ATGTA CTTATGACGCCTTGAAGCA, reverse primer: 5'-ACCCAGCTGCCGACAC, SNP reporter 1: 5'-CCTTGCGTCTCCC, SNP reporter 2: 5'-CCTTGTGTCTCCC. All mice presented C57BL/6J background, were fed a regular diet and water *ad libitum* and maintained on a 12h light/dark cycle. All animal studies were approved by the Institutional Animal Care and Use Committee of Indiana University School of Medicine.

qPCR

Total RNA from ex vivo isolated and differentiated osteoclasts, whole tibias, whole brain, and gastrocnemius muscles was isolated using TRIzol (Invitrogen, Grand Island, NY) [140]. Reverse transcription was performed using a high-capacity cDNA kit (Applied Biosystems, Foster City, CA). qPCR was performed using the Gene Expression Assay Mix TaqMan Universal Master Mix with the 7500 Real Time PCR/StepOne Plus system and software (Life Technologies). Gene expression was corrected by the levels of the house-keeping gene glyceraldehyde 3-phosphate dehydrogenase (GAPDH). Primers and probes were commercially available (Applied Biosystems, Foster City, CA) or were designed

using the Assay Design Center (Roche Applied Science, Indianapolis, IN). Relative expression was calculated using the ΔC_t method.

Body weight and bone mineral density (BMD)

BMD was measured regularly from 1 to 20 months of age by DXA/PIXImus (G.E. Medical Systems, Lunar Division, Madison, WI) [140]. Body weight was measured at the time of the DXA scan. BMD measurements included total (whole body excluding the head and tail), femur and spine (L1-L6). Calibration was performed using a standard control phantom before scanning, as recommended by the manufacturer.

Micro Computed Tomography (μ CT) Analysis of Femurs Bone Morphometry

μ CT scanning was performed to measure morphological and bone mass indices of femoral bone [141, 142]. After euthanasia, the left femurs were wrapped in saline-soaked gauze and frozen at -20°C until imaging. Bone samples were rotated around their long axes and images were acquired using a Bruker Skyscan 1176 (Bruker, Kontich, Belgium) with the following parameters: pixel size = $9\ \mu\text{m}^3$; peak tube potential = 65 kV; X-ray intensity = 300 μA ; 0.7° rotation step. Calibration of the grayscale levels was performed using hydroxyapatite phantoms (0.25 and 0.75 g/cm^3 Ca-HA). Based on this calibration and the corresponding standard curve generated, the equivalent minimum calcium hydroxyapatite level was $0.42\ \text{g}/\text{cm}^3$. Raw images were reconstructed using the SkyScan reconstruction software (NRecon; Bruker, Kontich, Belgium) to 3-dimensional cross-sectional image data sets using a 3-dimensional cone beam algorithm. Structural indices of the trabecular bone were calculated on reconstructed images using the Skyscan CT Analyzer software (CTAn; Bruker, Kontich, Belgium). Cortical bone was analyzed by threshold of 80–255 in a 100-

slice selection of the femoral mid-shaft using code as described previously [141]. Cortical bone parameters included periosteal bone surface (Ps.BS), endocortical bone surface (Ec. BS), bone area/tissue area (BA/TA or Ct. Ar / Tt. Ar), cross-sectional tissue (bone + bone marrow) area (Tt. Ar or Total CSA), marrow area, cortical bone area (Ct. Ar), cortical thickness (Ct.Th), and Moment of Inertia. Trabecular bone was analyzed between 0.5 and 1.0 mm above the femoral distal growth plate using a threshold of 80–255 at 4 and 13 months and 50-255 at 20 months. Trabecular parameters included bone volume fraction (BV/TV), number (Tb.N), thickness (Tb.Th), and separation (Tb.Sp).

Three-point bending

Following μ CT, left femora were thawed and mechanically tested using a three-point monotonic test to failure [141]. Femora were loaded with the anterior surface in tension at a rate of 0.025 mm/s and a lower support span of 8 mm. Sample hydration was maintained with PBS throughout testing. The values of c-anterior extreme fiber length, the furthest distance from the bone centroid to the surface in tension, and I_{ML} , the moment of inertia about the medial-lateral axis, obtained from μ CT of the mid-diaphysis were then used to normalize force-displacement data into stress-strain data and calculate estimated material level properties [143], using standard beam bending equations, as described previously [141].

Bone histomorphometry

Femur harvested from 13-month-old female mice were fixed in 10% neutral buffered formalin, cut, and embedded in plastic and paraffin using previously established methods at the Indiana Center for Musculoskeletal Health Histology and Histomorphometry Core

[57]. To allow for dynamic histomorphometric analysis, mice were injected intraperitoneally with calcein (30 mg/kg; Sigma) and alizarin red (50 mg/kg; Sigma) 7 and 2 days prior to euthanasia. Dynamic histomorphometry was performed on unstained, undemineralized methyl methacrylate-embedded distal femur cross-sections using an epifluorescence microscope. Osteoclasts were quantified in demineralized, paraffin-embedded femoral bone mid-diaphysis cross-sections stained for TRAP/Toluidine blue. Histomorphometric analyses were performed using OsteoMeasure high resolution digital video system (OsteoMetrics Inc., Decatur, GA, USA). The terminology and units used are those recommended by the ASBMR Histomorphometry Nomenclature Committee [144].

Osteoclast assays

Bone marrow cells (BMCs) were isolated from 4 month old female and male WT and TREM2^{R47H/+} C57BL/6J mice by flushing the bone marrow out with 10% FBS and 1% P/S- α -MEM and cultured for 48h [140, 145]. Non-adherent cells were then collected and 2×10^4 cells/cm² were seeded on 96-well plates. RANKL (80ng/ml) and M-CSF (20ng/ml) were added to induce osteoclast differentiation and media was changed every 2-3 days for 2, 5, or 7 days. Cells were stained using a TRAPase kit (Sigma-Aldrich) and mature osteoclasts that stained TRAP positive and exhibiting 3 or more nuclei were quantified.

Multiplex cell-signaling assays

Kinase activation was measured in osteoclast protein lysates made from *ex vivo* bone marrow cells from WT and TREM2^{R47H/+} animals after seven days of differentiation as described above using the Bioplex protein array system at the Multiplex Analysis Core

(MAC) at IUSM. Premixed magnetic beads of the Milliplex multi-pathway 9-plex phospho- and total protein kits were used (Milliplex, Burlington, MA).

Statistics

All statistical analyses were performed using GraphPad Prism 9.0.0 (GraphPad Software, San Diego, CA, USA). In general, Student's t-tests were performed to determine significant differences between TREM2^{R47H/+} and WT groups for each sex, comparisons were not made between sexes. For data that failed either the D'Agostino & Pearson test or Shapiro-Wilk test for normality, analysis was performed using the Mann-Whitney test, and for data with unequal variance, the Welch's t-test was used as indicated in the corresponding figure legends. For longitudinal data taken across 20 months, multiple frequencies, or contractions, a 2-way analysis of variance (ANOVA) was performed, followed by post-hoc comparisons for each time point. Post-hoc tests used is specified in the figure legends and vary depending on the comparison being made. All results of the ANOVA tests are included in the Supplementary Tables. Statistical significance was set at $P \leq 0.05$, and the data are presented as box plots where the horizontal line represents the median, the box outlines the interquartile range, and the bars represent maximum and minimum, whereas each dot corresponds to an individual animal. For longitudinal data, the symbol represents the median and bars represent the interquartile range. Sample sizes vary due to variability in genotypes generated as data was collected, and samples were excluded if damaged during collection or analysis (ex. Femurs broken excluded from microCT analysis).

Results

The TREM2 R47H variant has been shown to impact mRNA splicing of the TREM2 transcript in cortical brain and microglia lysates, producing a protein expression knockdown similar to that of a heterozygous knockout, evident by decreases in mRNA expression measured by qPCR of the TREM2 gene [136, 146]. However, qPCR analysis of both whole bone and ex vivo osteoclast cultures, comparable to cortical brain and microglia respectively, from female and male WT and TREM2^{R47H/+} bone marrow cells demonstrates that expression of the TREM2 R47H variant does not result in a different splicing variant in these tissues (**Figure 1-1**). This evidence suggests that the TREM2 gene is spliced differently in bone versus brain, and that the consequences of TREM2 R47H expression in bone are not due to reduced expression levels.

Ex vivo μ CT analyses showed no differences in trabecular (**Figure 1-2A**) or cortical (**Figure 1-2B**) bone geometry in male or female TREM2^{R47H/+} animals compared to WT littermates at 4 months of age. On the other hand, three-point bending analysis demonstrated that the pre-yield displacement was decreased in female TREM2^{R47H/+} animals compared to WT littermates (**Figure 1-3**). These data demonstrate that by skeletal maturity, the TREM2 R47H variant has no effect on bone geometry and only a mild effect on mechanical integrity noted in the pre-yield displacement, and only in female animals. However, bone mineral density gain between 1 and 12 months of age was significantly lower in the femur, but not spine or total BMD, in female TREM2^{R47H/+} mice, compared to WT littermates (**Figure 1-4**). On the other hand, no differences in BMD at each age or in bone gain were detected in males up to 20 months.

Based on the differences in BMD accrual, we analyzed bone mass and strength in femoral bones of female WT and TREM2^{R47H/+} mice at 13 months of age. TREM2^{R47H/+} female animals had decreased trabecular bone volume in the distal femur compared to WT, indicated by lower bone volume/tissue volume, trabecular thickness, a larger trabecular separation, and a lower trabecular number (**Figure 1-5A**). Additionally, TREM2^{R47H/+} female mice had significantly increased marrow area, smaller cortical thickness and bone area/tissue area, an increased cross-sectional area, and increased endocortical bone surface compared to WT littermates (**Figure 1-5B**). These data demonstrate that the TREM2^{R47H/+} bone is thinner but wider, suggesting the TREM2^{R47H} variant may be accelerating age-related bone loss patterns of endosteal resorption sometime between 4 and 13 months of age. *Ex vivo* three-point bending analysis demonstrated that TREM2^{R47H/+} female femurs are weaker than WT, indicated by lower mechanical properties of the bone such as yield force and work to yield, as demonstrated in the force-displacement graph (**Figure 1-6**). Estimations of the material properties of the female TREM2^{R47H/+} femurs were also decreased compared to WT as exemplified in the representative stress-strain graph, including a decreased yield stress, resilience, ultimate stress, and modulus compared to WT littermate controls (**Figure 1-6**). These data suggest that the TREM2^{R47H/+} variant has a deleterious effect on bone geometry as well as bone mechanical and material properties in female animals at 13 months of age.

At 20 months of age, *ex vivo* μ CT analysis of TREM2^{R47H/+} animals did not show differences in cancellous bone volume of the distal femur of female compared to WT mice (**Figure 1-7A**). However, analysis at the femoral mid-diaphysis shows that female TREM2^{R47H/+} mice have decreased cortical area and periosteal bone surface, as well as a

smaller cross-sectional area compared to WT littermates at 20 months (**Figure 1-7B**). Female $TREM2^{R47H/+}$ femurs also have a decreased moment of inertia compared to WT littermates (**Figure 1-7B**). Female $TREM2^{R47H/+}$ femurs also showed a decreased tissue mineral density (TMD) of the cortical bone compared to WT, but have similar mechanical and material properties of the femur at 20 months of age by three-point bending compared to WT (**Figure 1-8**). These data suggest that the bone deterioration present in 13-month $TREM2^{R47H/+}$ female mice is not continually exacerbated through 20 months of age. Further, our evidence is consistent with an accelerated skeletal aging in $TREM2^{R47H/+}$ females up to 13 months, a process that stalls out allowing for the aging WT mice to catch up, resulting in comparable bone mass and strength in $TREM2^{R47H/+}$ and WT mice at 20 months of age.

Male $TREM2^{R47H/+}$ animals did have decreases in cancellous bone volume/tissue volume, trabecular number, and increased trabecular spacing in the distal femur compared to WT littermates (**Figure 1-7A**). However, even with the added impact of aging, male $TREM2^{R47H/+}$ animals had no differences in the cortical bone geometry at the femoral mid-diaphysis compared to WT (**Figure 1-7B**). Interestingly, three-point bending shows that male $TREM2^{R47H/+}$ femurs have mild increases in the ultimate strain and failure force mechanical properties, but no difference in TMD or any other strength properties compared to WT (**Figure 1-8**). Together, these data indicate that male $TREM2^{R47H/+}$ may be impacted by the $TREM2$ R47H variant, but only at an aged time point, whereas female animals are most strongly impacted at an intermediate aged time point (13 months). Further, there is a disparate effect of the variant in male mice at 20 months of age, with reduced cancellous

bone mass and increased cortical bone strength. These data demonstrate that the TREM2 R47H variant has a sex- and age-dependent effect on both bone geometry and strength.

Because TREM2 is primarily expressed on cells of the myeloid lineage, we investigated whether this TREM2 R47H variant increased osteoclast differentiation similar to what has been previously reported in TREM2 null osteoclasts [134]. Although decreases in cortical and cancellous bone volume were found in 13-month-old female TREM2^{R47H/+} femurs compared to WT, there were no changes in osteoclast number, osteoclast surface, or eroded surface on the femoral endocortical surface, as measured by histomorphometry (**Figure 1-9**). Dynamic histomorphometry of the femoral mid-diaphysis showed no significant difference in any of the periosteal parameters scored, but there was a slight increase in the endocortical mineral apposition rate of female TREM2^{R47H/+} mice compared to WT (**Figure 1-10**). Since these data demonstrated a clear impact of the TREM2 R47H variant on bone, and TREM2 is known to be expressed in the osteoclast, we decided to further investigate the effect of the TREM2 R47H variant on osteoclasts.

To better understand the effect of the TREM2 R47H variant on osteoclast ability to differentiate, non-adherent bone marrow cells isolated from 4-month-old TREM2^{R47H/+} long bones were exposed to RANKL/M-CSF for 2, 5, and 7 days (D2, D5, D7), and number of TRAP⁺ osteoclasts with ≥ 3 nuclei was quantified. More osteoclasts differentiated from male TREM2^{R47H/+} cells after seven days of differentiation compared to WT, while no difference was found in the number of female TREM2^{R47H/+} osteoclasts (**Figure 1-11A**). However, follow-up gene expression analysis demonstrated that both female and male TREM2^{R47H/+} osteoclasts express significantly higher levels of estrogen receptor (ER) α mRNA compared to WT cells (**Figure 1-11B**), while neither male nor female TREM2^{R47H/+}

cells expressed different levels of the sex hormone receptors ER β or androgen receptor (**Figure 1-11B**). To assess whether increased ER α expression might also increase the expression of ER α target genes, we evaluated gene expression of ER α target gene complement 3 (C3) and found that female TREM2^{R47H/+} osteoclasts had decreased mRNA levels of C3 expression (**Figure 1-12A**). Female TREM2^{R47H/+} osteoclasts also had increased mRNA levels of pro-survival gene BCL2, which suggests the pro-apoptotic effect of estrogen on osteoclasts may be impaired by TREM2 R47H expression in female cells (**Figure 1-12A**).

Previous studies have also demonstrated a potential interaction of β -catenin in TREM2 signaling [133]. Female TREM2^{R47H/+} osteoclasts express decreased mRNA levels of Wnt/ β -catenin target gene cyclin D1 compared to WT, suggesting the TREM2 R47H variant may also interact with β -catenin (**Figure 1-12A**). No differences in C3, BCL2, or Cyclin D1 were detected in male TREM2^{R47H/+} osteoclasts compared to WT (**Figure 1-12A**). Together, these data suggest that female TREM2^{R47H/+} osteoclasts exhibit decreased sensitivity to estrogen signaling.

In addition to inducing changes in gene expression, activation of the estrogen receptors can lead to kinase activation, the so-called non-genotropic effects of the ligand. To test the possibility that the TREM2 R47H variant would affect intracellular kinase activation, multiplex analysis of protein lysates was performed. We found increased phosphorylated Akt in female but not male TREM2^{R47H/+} osteoclasts compared to WT cells (**Figure 1-12B**). However, male but not female TREM2^{R47H/+} osteoclasts had increased protein levels of phosphorylated CREB compared to WT cells (**Figure 1-12B**). Taken together, these data suggest that TREM2^{R47H/+} variant alters intracellular osteoclast

signaling in a sex-dimorphic manner, but only male TREM2^{R47H/+} osteoclast precursors have a cell-autonomous increase in differentiation.

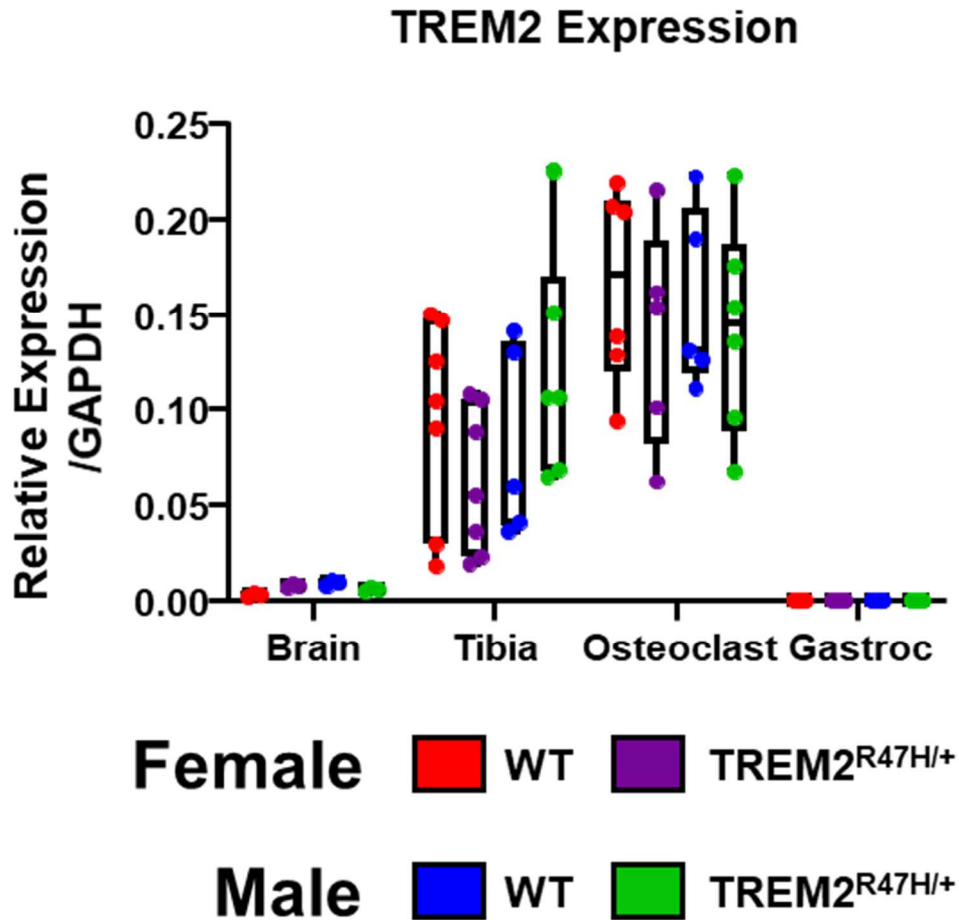


Figure 1-1: TREM2 mRNA expression is not altered in brain, marrow-flushed tibias, ex vivo differentiated osteoclast cultures, or whole gastrocnemius muscle lysates from male or female TREM2^{R47H/+} mice compared to WT.

mRNA expression of TREM2 from lysates of whole brain (N= 3), whole bone (N= 5-7), ex vivo osteoclasts differentiated for seven days (N= 5-6), and gastrocnemius muscle (N= 7-8) of male and female TREM2^{R47H/+} and WT mice 4 months of age.

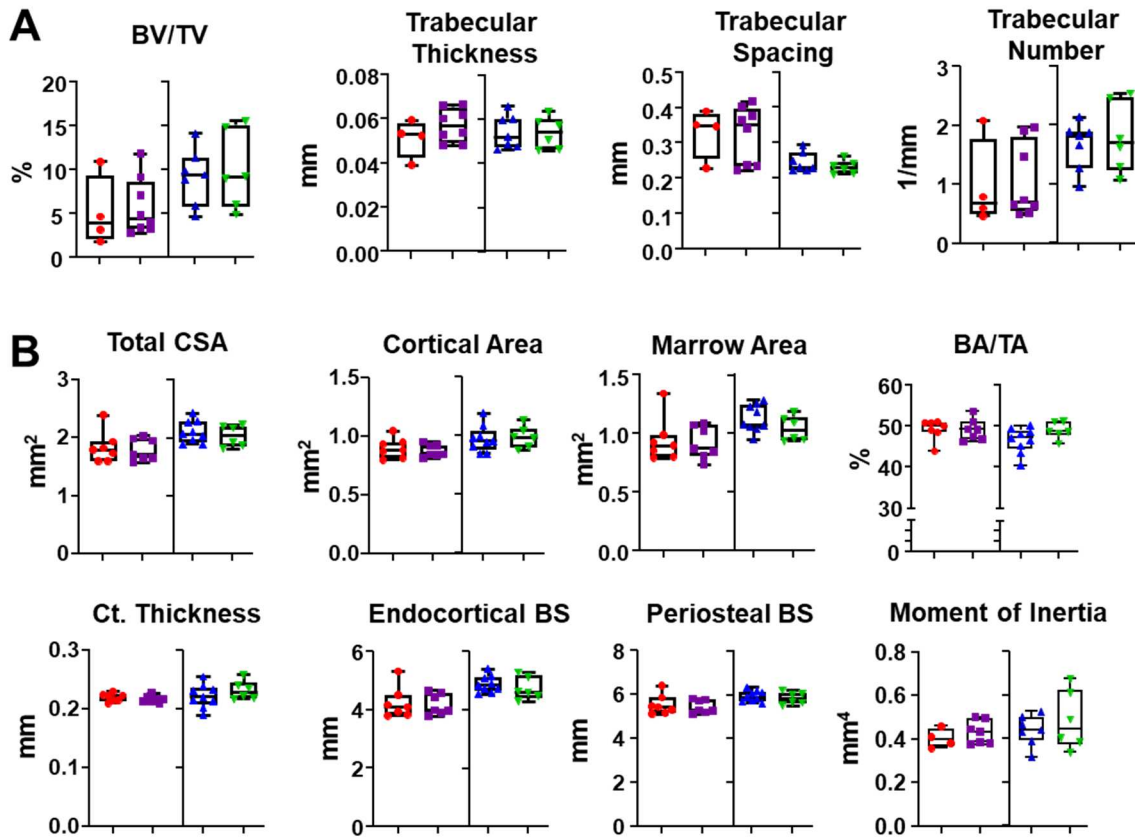


Figure 1-2: $TREM2^{R47H/+}$ has no effect on cortical or trabecular bone volume in male or female mice at 4 months of age.

μ CT analysis of cortical bone of the cancellous bone of the distal femur (N = 4-8/group) (A), and femoral mid-diaphysis (N=6-9/group) (B).

4 months of age

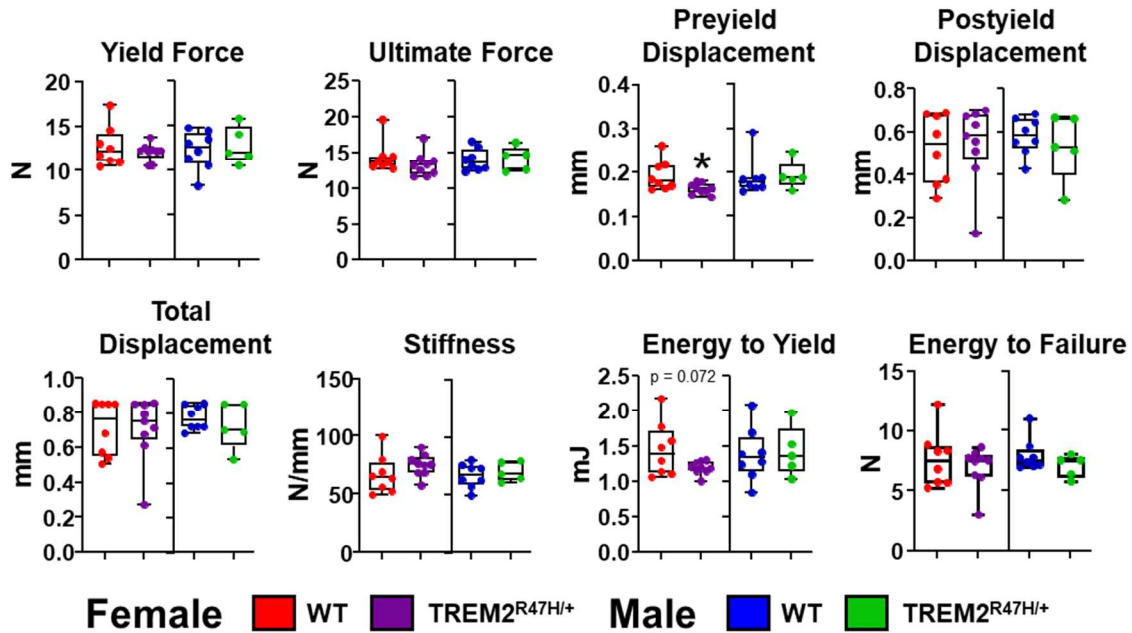


Figure 1-3: TREM2^{R47H/+} has minimal effect on femoral bone strength in female but not male mice as assessed by three-point bending.

Mechanical and derived material properties of the femur as assessed by three-point bending mechanical testing (N = 5-9/group) in 4-month-old male and female TREM2^{R47H/+} and WT mice. Comparisons are sex-matched between TREM2^{R47H/+} vs. WT using Welch's t-test: Female Pre-yield Displacement p = 0.042, Energy to Yield p = 0.072.

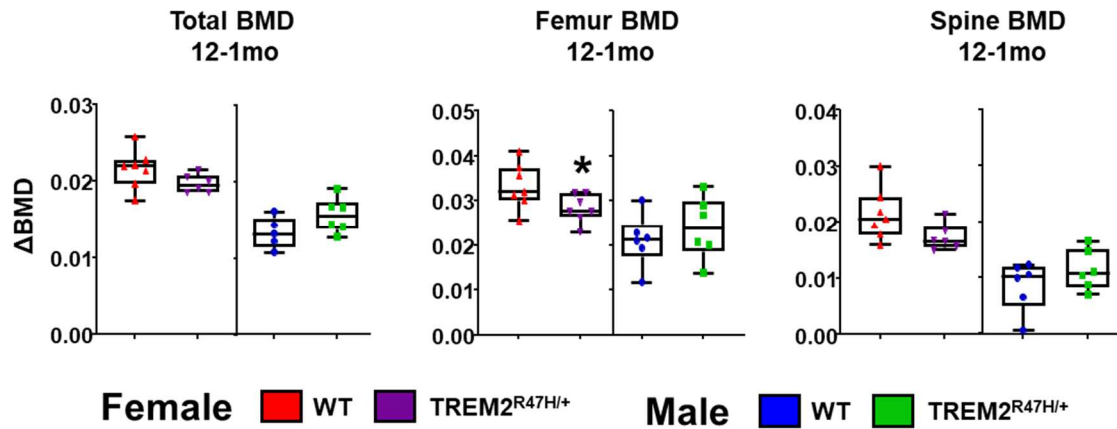


Figure 1-4: BMD accrual is reduced in female but not male TREM2^{R47H/+} animals.

BMD accrual between 12 and 1 month of age in the total body, femur, and spine of male and female TREM2^{R47H/+} and WT mice. Sex-matched comparisons made between TREM2^{R47H/+} and WT by Student's t-test: Female Femur BMD $p = 0.0476$, Female Spine BMD $p = 0.075$.

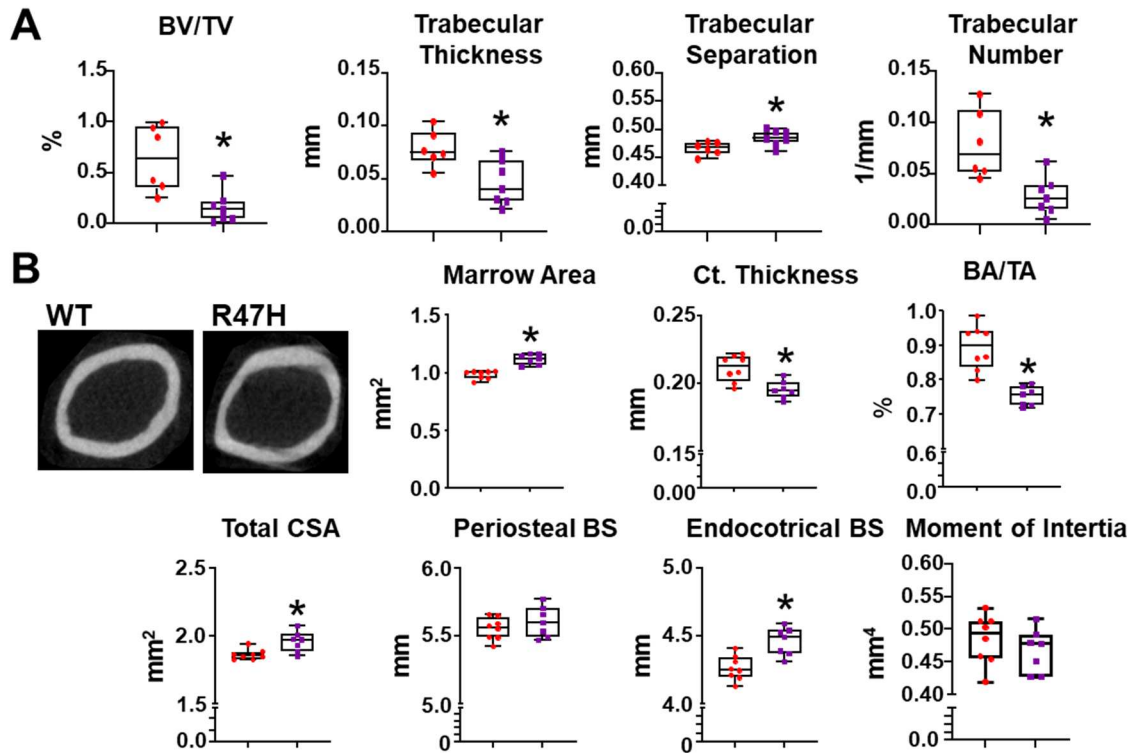


Figure 1-5: Female $TREM2^{R47H/+}$ mice have cortical and trabecular bone loss at 13 months of age.

μ CT analysis of cancellous bone of the femoral mid-diaphysis (N=7-8/group) (**A**), cortical bone of the distal femur (N = 7/group) (**B**). Representative images of female WT and $TREM2^{R47H/+}$ cortical bone images oriented with the medial-lateral angled on the X-axis.

Comparisons between female $TREM2^{R47H/+}$ vs. WT using Student's t-test: (**A**) Marrow Area p = 0.00002, Ct. Thickness p = 0.003, BA/TA p = 0.00008, Total CSA p = 0.007, Ec. BS p = 0.0017. (**B**) BV/TV p = 0.0027, Trabecular Thickness p = 0.009, Trabecular Separation p = 0.015, Trabecular Number p = 0.002.

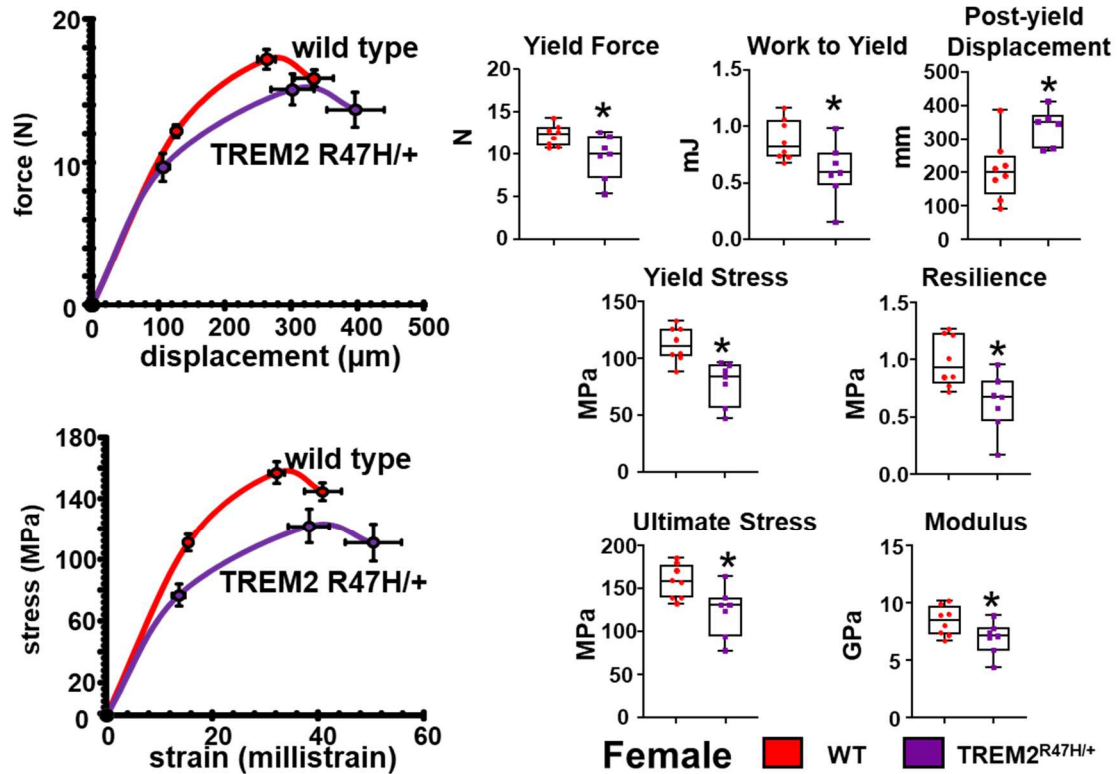


Figure 1-6: Female TREM2^{R47H/+} mice have less mechanical and material strength compared to WT littermates at 13 months of age.

Three-point bending mechanical testing (N = 7/group) in 13-month-old female TREM2^{R47H/+} and WT mice. Representative force-displacement and stress-strain graphs are shown. Comparisons between female TREM2^{R47H/+} vs. WT using Student's t-test: Yield Force p = 0.029, Work to Yield p = 0.031, Post-yield Displacement p = 0.011, Yield Stress p = 0.0019, Resilience p = 0.01, Ultimate Stress p = 0.015, Modulus p = 0.048.

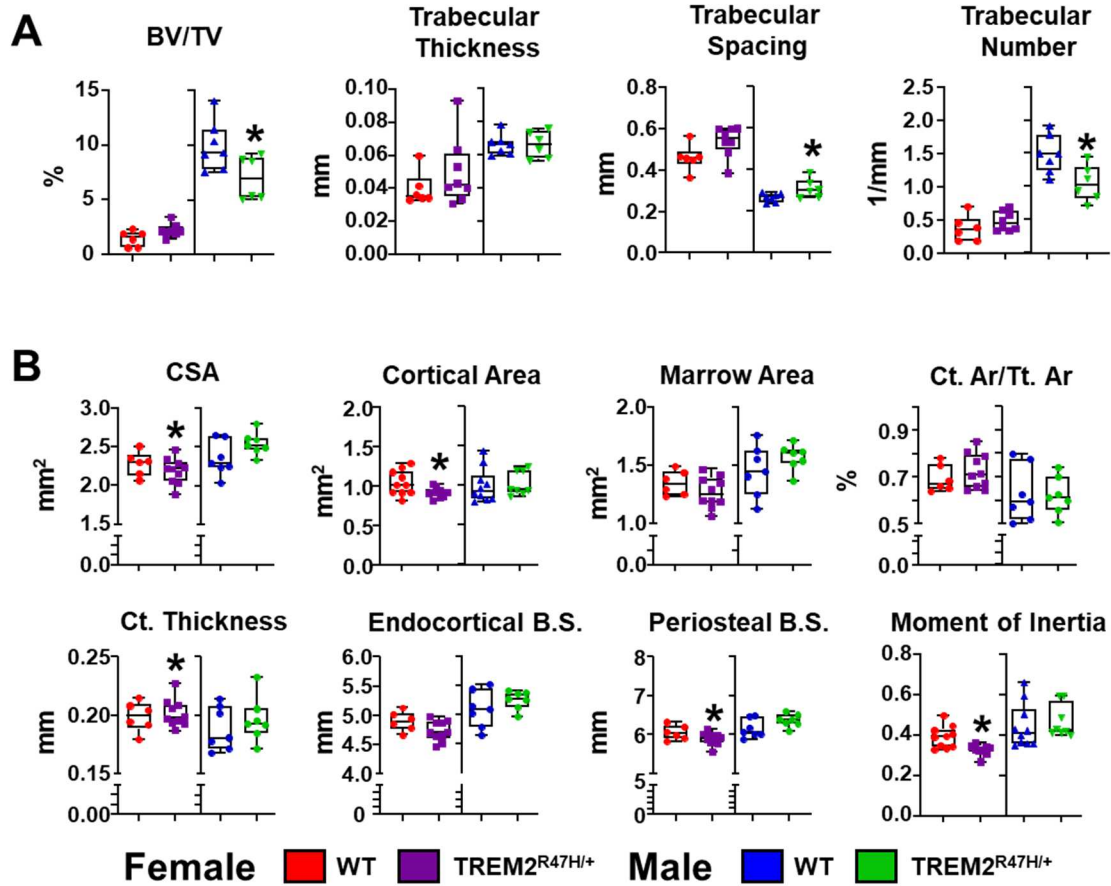


Figure 1-7: Age-induced bone loss in male and female TREM2^{R47H/+} animals at 20 months of age.

μ CT analysis of cancellous bone of the femoral mid-diaphysis (N=5-8/group) (**A**), cortical bone of the distal femur (N = 6-10/group) (**B**), in 20-month-old male and female TREM2^{R47H/+} and WT mice. Comparisons are sex-matched, TREM2^{R47H/+} vs. WT using Student's t-test: (**A**) Male BV/TV p = 0.0513, Male Trabecular Separation p = 0.047, Male Trabecular Number p = 0.016. (**B**) Female Cortical Area p = 0.03, Female Periosteal BS p = 0.011, Female Moment of Inertia p = 0.005. Comparisons are sex-matched, TREM2^{R47H/+} vs. WT using one-tailed, equal variance t-test: (**A**) Female Total CSA p = 0.032, male Cortical Thickness p = 0.037.

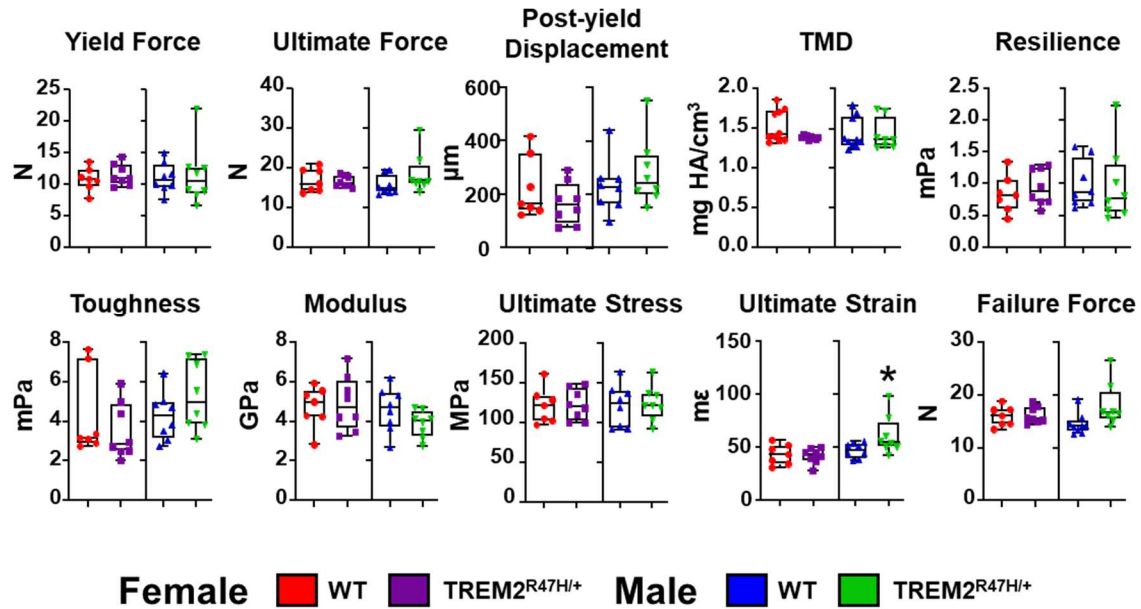


Figure 1-8: Mechanical and material strength of bone from $TREM2^{R47H/+}$ animals at 20 months of age.

Three-point bending mechanical testing (N = 7-10/group) in 20-month-old male and female $TREM2^{R47H/+}$ and WT mice. Comparisons are sex-matched, $TREM2^{R47H/+}$ vs. WT using Student's t-test: Tissue Mineral Density (TMD) $p = 0.041$, Failure Force $p = 0.038$. Comparisons are sex-matched, $TREM2^{R47H/+}$ vs. WT using Mann-Whitney test: Male Failure Force $p = 0.015$. Comparisons are sex-matched, $TREM2^{R47H/+}$ vs. WT using Welch's one-tailed t-test Male Ultimate Strain $p = 0.039$.

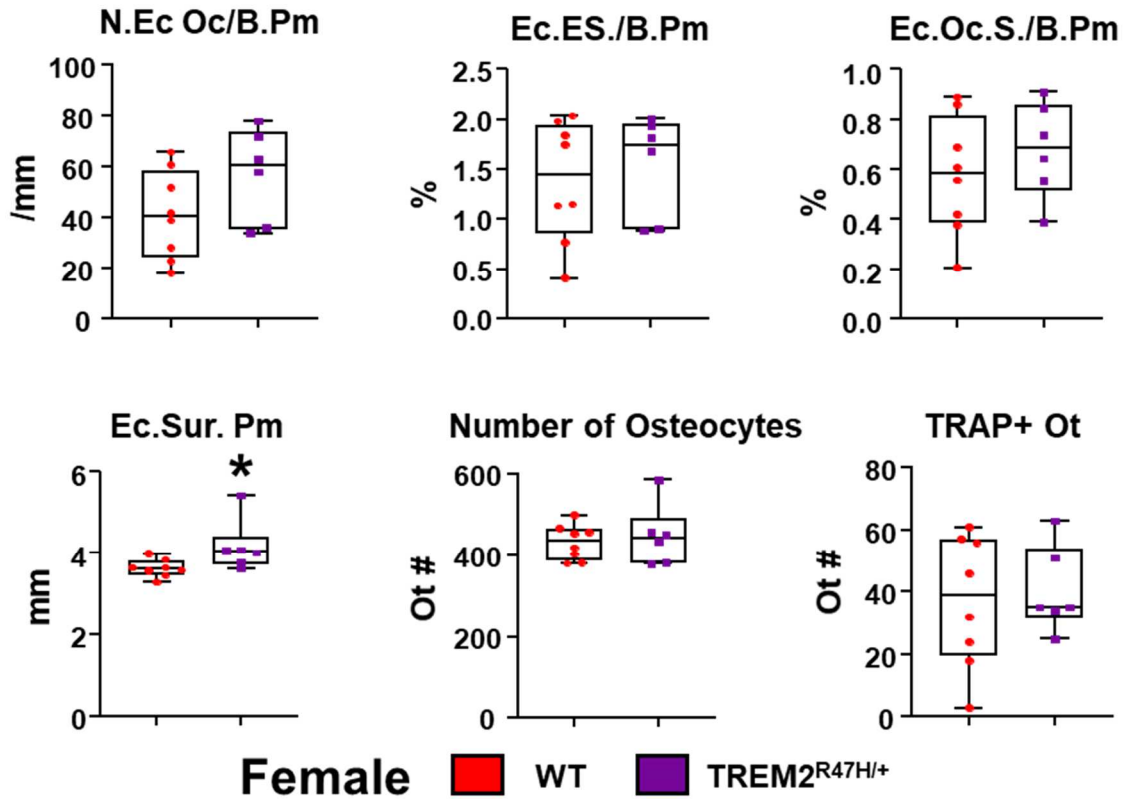


Figure 1-9: TRAP-stained scoring of cortical bone from female TREM2^{R47H/+} and WT femurs.

Scoring of osteoclasts in TRAP-stained cortical sections of bone from 13-month-old female TREM2^{R47H/+} and WT bones. *: p<0.05 vs. WT by Student's t-test. Ec: endocortical, Pm: perimeter, N: Number, Oc: Osteoclast, B: Bone, Sur: Surface, BS: Bone Surface, Ot: Osteocyte, Ps: Periosteal. Comparisons made between TREM2^{R47H/+} and WT by Student's t-test. (A) N. Ec Oc/ Bone PM p = 0.065, Ec.Sur. Pm p = 0.0252

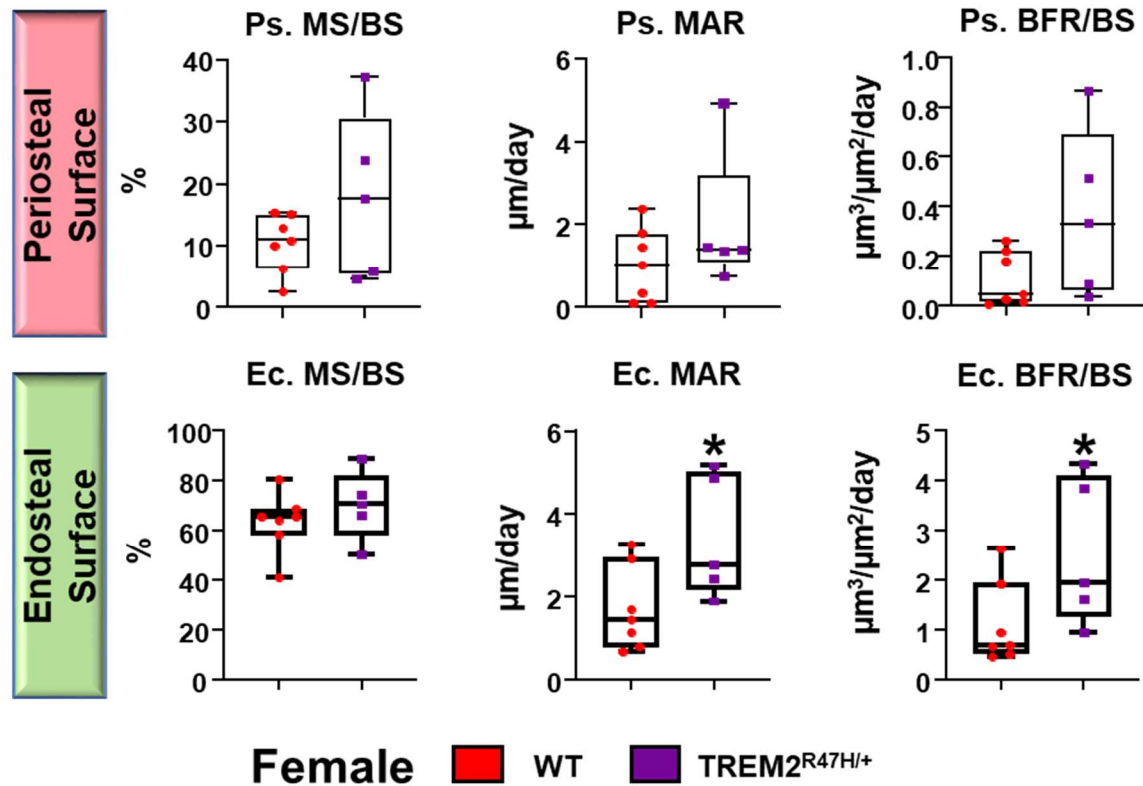


Figure 1-10: Dynamic histomorphometry analysis of cortical bone from female $TREM2^{R47H/+}$ femurs.

Dynamic histomorphometric parameters in cortical sections of bone taken from the femoral mid-diaphysis of 13-month-old female $TREM2^{R47H/+}$ and WT mice. *: $p < 0.05$ vs. WT by Student's t-test. Ec: endocortical, Pm: perimeter, N: Number, Oc: Osteoclast, B: Bone, Sur: Surface, BS: Bone Surface, Ot: Osteocyte, Ps: Periosteal, MS: Mineralizing Surface, MAR: Mineral Apposition Rate, BFR: Bone Formation Rate. . Comparisons made between $TREM2^{R47H/+}$ and WT by Student's t-test: Ec. MAR $p = 0.038$. Comparisons made between $TREM2^{R47H/+}$ and WT by Man-Whitney test: Ps. BFR/ BS $p = 0.165$, Ec. BFR/ BS $p = 0.048$.

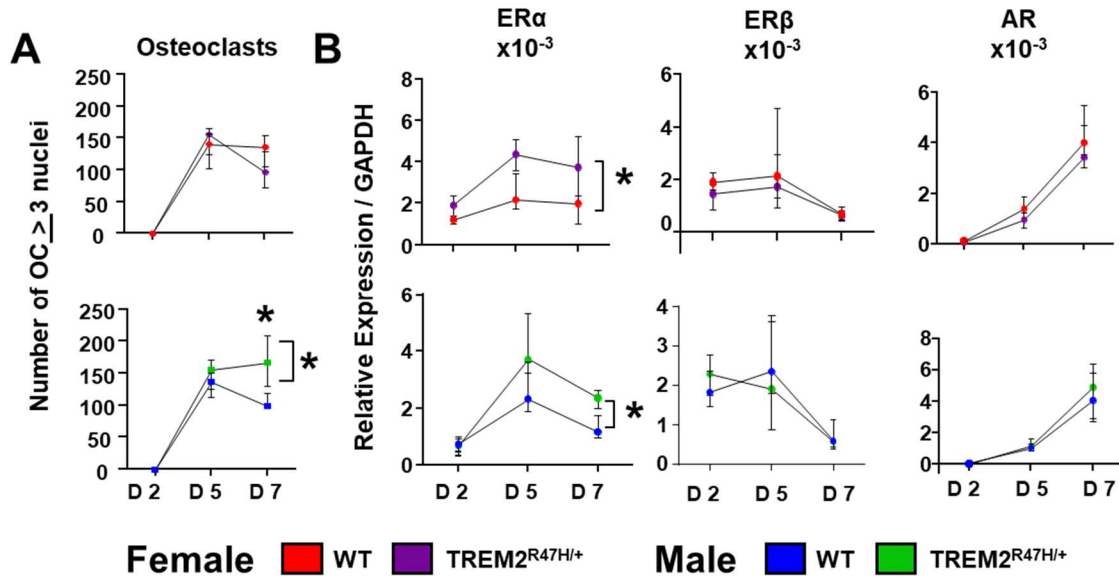


Figure 1-11: Sex-dependent alterations in osteoclast differentiation and sex-hormone receptor expression in TREM2^{R47H/+} osteoclasts.

Osteoclast differentiation from male and female, TREM2^{R47H/+} and WT non-adherent bone marrow cells. Cells were differentiated for 2, 5, and 7 days, and the number of TRAP⁺, ≥ 3 nuclei was assessed (N=4/5 wells counted/group) **(A)**, mRNA levels of Estrogen Receptor alpha (ER α), Estrogen Receptor beta (ER β), and Androgen Receptor (AR) normalized to GAPDH in male and female TREM2^{R47H/+} and WT osteoclasts (N = 5-6/group) **(B)**, Comparisons are sex-matched, TREM2^{R47H/+} vs. WT using Two-way ANOVA with mixed effects and Sidak's multiple comparisons test: **(A)** Genotype x Time interaction in Male OC differentiation p = 0.007, Male TREM2^{R47H/+} vs. WT multiple comparison test at D7 p = 0.0017. **(B)** Female ER α expression at D5 p = 0.024, D7 p = 0.018, Male ER α Expression at D5 p = 0.004. See Table 1 for details on the ANOVA analysis.

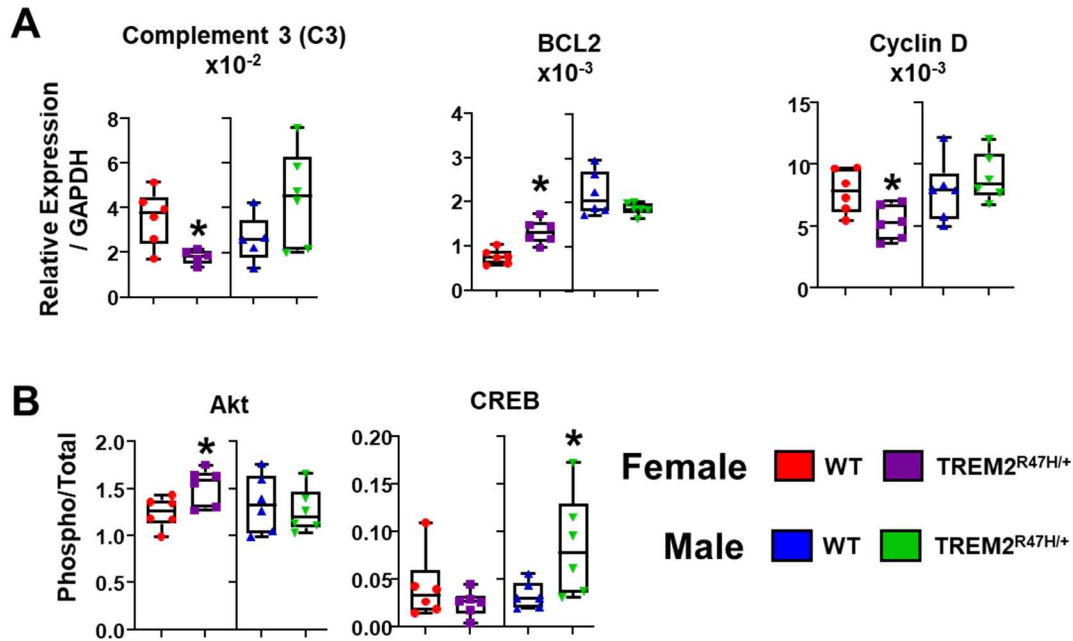


Figure 1-12: Sex-dependent alterations in intracellular signaling in TREM2^{R47H/+} osteoclasts.

mRNA levels of Complement 3 (C3), BCL2, and Cyclin D normalized to GAPDH from male and female TREM2^{R47H/+} and WT osteoclasts after 7 days of differentiation (N = 5-6/group) **(A)**, protein multiplex of bone lysates from male and female TREM2^{R47H/+} osteoclasts after 7 days of differentiation **(B)**. Comparisons are sex-matched, TREM2^{R47H/+} vs. WT using Student's t-test: **(C)** BCL2 p = 0.0015, Cyclin D p = 0.02. **(A)** Female Akt p = 0.0227. Comparisons are sex-matched, TREM2^{R47H/+} vs. WT using Welch's t-test: **(A)** C3 p = 0.016. **(B)** Male CREB p = 0.0627.

	Mixed Effect Two-Way ANOVA Source of Variation (p value)		
	Time x Genotype	Time	Genotype
Female OC Differentiation	0.207	< 0.0001 *	0.404
Male OC Differentiation	< 0.0227 *	< 0.0001 *	0.0033 *
Female OC Er α	0.0004 *	0.006 *	0.274
Male OC Er α	0.0727	< 0.0001 *	0.0019 *
Female OC Er β	0.626	0.023 *	0.263
Male OC Er β	0.584	0.0027 *	0.831
Female OC AR	0.592	< 0.0001 *	0.4397
Male OC AR	0.873	< 0.0001 *	0.541

Table 1: ANOVA analysis from Figure 1-11.

CHAPTER THREE: Sex-dependent increase in skeletal muscle strength with TREM2

R47H variant

Introduction

Skeletal muscle constitutes a majority of a person's body weight (approximately 40%), and as such its mass and function can significantly impact overall physical function [147, 148]. Although the amount of skeletal muscle and size of skeletal muscle is an important measurement and indicator, arguably the most physiological measure of skeletal muscle is function. There is a large body of research demonstrating that one of, if not the most effective way to preserve skeletal muscle strength with aging is through exercise, and exercise has especially been shown to improve skeletal muscle function with aging [149-152]. However, it remains unknown how aging and AD interact to influence skeletal muscle mass and function. Whether the effect of AD on skeletal muscle are due to changes in the central nervous system or intrinsic to the tissue itself remains unclear.

Loss of skeletal muscle mass and strength with age is known as sarcopenia, and severely limits physical function due to loss of ability to perform daily tasks [153]. Additionally, sarcopenia is associated with an increased risk of falls, which by proxy increases risk of bone fracture [154, 155]. It is for this reason why skeletal muscle and bone with age are commonly studied together. Concurrent loss of bone and skeletal muscle results in an increased risk for falls and fractures, and is referred to as osteosarcopenia [156]. The underlying cellular and molecular mechanisms driving this deterioration of skeletal muscle mass and function is not completely understood. In mouse models of aging, it has been shown that skeletal muscle atrophy and functional loss primarily driven by

atrophy due to increases in dysregulated protein synthesis vs. degradation, metabolic shifts, and changes in fiber-type.

Loss of skeletal muscle mass and strength with age is known as sarcopenia, and severely limits physical function due to loss of ability to perform daily tasks [153]. Additionally, sarcopenia is associated with an increased risk of falls, which by proxy increases risk of bone fracture [154, 155]. It is for this reason skeletal muscle and bone with age are commonly studied together. Concurrent loss of bone and skeletal muscle with age is termed osteosarcopenia [156]. The underlying cellular and molecular mechanisms driving this deterioration of skeletal muscle mass and function is not completely understood. In mouse models of aging, it has been shown that contributors to skeletal muscle atrophy and functional loss include dysregulated protein synthesis vs. degradation, metabolic shifts, and changes in fiber-type driven by denervation re-innervation.

Skeletal muscle size is primarily driven by the balance of protein synthesis and protein degradation, also referred to as anabolism and catabolism, respectively. This balance of making and breaking down protein is normal and occurs to maintain cell viability, but with skeletal muscle atrophy this becomes imbalanced and more protein is broken down than is synthesized. This is accompanied by increases in the expression and activity of E3-ubiquitin ligases such as MUSA, MuRF-1, Atrogin-1 [157]. These ubiquitin ligases tag proteins to be degraded by the proteasome where the protein is broken down and recycled in the cell. Muscle atrophy also leads to decreases in strength, as many of the proteins tagged for destruction by the ubiquitin ligases are used in the cellular machinery used for contraction and movement. For example, it has been shown in a mouse model of denervation that MuRF-1 targets myosin heavy and light chains for destruction [158].

However, it remains unclear whether these ubiquitin ligases are increased in activity of amount with age [159, 160]. One study found that MURF-1 protein levels were increased in aged rats compared to young, but Atrogin-1 was decreased [161]. Our group found an increase in ubiquitin-tagged proteins in aged compared to young muscle samples with increased ubiquitin ligase expression [162]. However, aged rats fed a calorie restrictive diet has increased lean mass compared to normal diet controls, but increased levels of MURF-1 and Atrogin-1, suggesting age-related changes to skeletal muscle mass and function cannot be completely dependent on increases in protein degradation [160]. Rather, protein synthesis pathways are also significantly decreased in aged skeletal muscle.

Protein synthesis is a tightly controlled process made even more interesting when you consider skeletal muscle coordinates mRNA transcription and translation across multiple nuclei in the long single cell [163]. One of the strongest known regulators of anabolism, in skeletal muscle is the Akt/mTOR signaling pathway [164]. This is due in part due to Akt-mediated inhibition of FOXO-mediated transcription of atrophy-related ubiquitin ligases such as Atrogin-1 and MuRF-1 which increases the ratio of synthesis to catabolism of proteins [165]. However, mTOR (mammalian target of rapamycin) activity is known to be one of the most potent regulatory of protein synthesis in skeletal muscle and is responsive to a number of stimuli including exercise, nutrition, and aging [166-168]. This is partially due to the direct phosphorylation and activation of translation machinery 4E-BP (eukaryotic initiation factor4E- binding protein) which increases RNA synthesis and can be stimulated by exercise or nutritional supplement [169, 170]. However, previous studies on skeletal muscle anabolic and catabolic potential reveal little to no difference between young and old skeletal muscle, suggesting that the potential for skeletal muscle to

build protein is not impaired with age, but the skeletal muscle response to anabolic signals may be diminished with age [171]. For example, aged patients do not have the same anabolic signaling in the skeletal muscle post exercise as young patients, rather the data suggests the anabolic signal is significantly delayed but the potential is similar [172, 173]. This may be, in part, due to the impaired ability of contraction to activate mTOR signaling in aged skeletal muscle [174]. Providing high-protein supplement, specifically essential amino acids, has been shown to improve skeletal muscle protein synthesis and prevent some skeletal muscle atrophy but whether this translated to measurable benefit in sarcopenia patients remains unclear and may depend on addition of resistance exercise [175-179]. In addition to decreased responsiveness to nutritional and exercise anabolic stimuli, aged skeletal muscle is less responsive to insulin.

Insulin resistance and decreased responsiveness to insulin sensitivity is known to occur across whole-body metabolism with aging, but also occurs in the skeletal muscle [180]. Compared to young, aged skeletal muscle does not experience the insulin-stimulated increase in blood flow via vasodilation, which has been shown to contribute to skeletal muscle glucose uptake [181, 182]. Aged skeletal muscle is also less responsive to insulin-related signaling, such as impaired Akt activation [183]. However, due to the fact that a large percentage of a person's body mass is comprised of skeletal muscle, perhaps one of the most important and impactful effects of insulin resistance on skeletal muscle is impaired glucose uptake [184]. Impaired Akt activity can reduce the translocation of glucose transporters to the cell surface, contributing to the impaired glucose uptake, but there are many other regulators of glucose transporter translocation in skeletal muscle [185, 186]. These data suggest that increasing glucose uptake may improve skeletal muscle

function. Indeed, treatment with metformin improves skeletal muscle function, primarily in type 2 diabetic patients, via enhanced glucose uptake and upregulation of mitochondrial function and AMPK signaling [187-189]. Although there are clear cellular changes in the skeletal muscle that contribute to age-related declines in mass and strength, these changes are not homogenous across the tissue. Skeletal muscle as a tissue is composed of bundles of individual skeletal muscle fibers that run along the length of the tissue. These individual fibers within a single muscle are not molecularly identical, there are different types of fibers within the skeletal muscle, referred to as fiber types. Each muscle has a different ratio of these fiber types and this confers certain characteristics to the muscle such as metabolism, molecular, force production and endurance.

It is well documented that aging skeletal muscle undergoes a shift in the fiber type of the skeletal muscle fibers, preferentially losing fast-twitch type 2 fibers with minimal effect on the number or size of the slow-twitch type 1 fibers [190]. This preferential loss of fast-twitch fibers results in a lower force production of the skeletal muscle, or muscle weakness, seen with aging [191, 192]. Although the differences between the skeletal muscle fiber types are not completely understood, it is established that fast-twitch Type 2 fibers are more likely to be glycolytic, consuming glucose as their main source of energy, while slow-twitch Type 1 fibers are considered oxidative and rely primarily on oxidative phosphorylation to produce their energy [193]. Human data suggest that the mitochondrial organization is related to the metabolic preference in the skeletal muscle fibers, indicating that mitochondrial organization may also be influenced with different fiber types [194]. It has been suggested that Peroxisome proliferator-activated receptor-gamma coactivator (PGC-1 α) may be a regulator of this fiber-type differentiation. PGC-1 α is a transcriptional

coactivator which facilitates cellular use of oxidative phosphorylation, a metabolic process which uses fatty acids to generate energy. It is known to be cold-responsive and aids in thermogenesis in adipose tissue, but is also known to strongly impact skeletal muscle [195]. PGC-1 α is known to be more prevalent in slow-twitch oxidative Type 1 fibers, prominent in the soleus muscle for example [196, 197]. Indeed, PGC-1 α overexpression in aged animals rescues skeletal muscle fiber size and improves fatigability and oxidative capacity in the EDL, a skeletal muscle that is typically glycolytic, fast twitch [198, 199]. Glycolytic fibers are also likely more susceptible to age-induced atrophy due to decreases in insulin sensitivity, decreasing the uptake of glucose through glucose transporters as has been seen in diabetes-induced insulin resistance [200-202].

However, metabolic changes with aging are not the only contributing factor to fiber type-specific changes to skeletal muscle with aging. Innervation of the skeletal muscle also determines the fiber type and are a critical component of age-related skeletal muscle atrophy. Motor neurons innervate bundles of skeletal muscle fibers, referred to as a motor units, which are generally called “fast” and “slow” similar to the fiber types [203]. These motor units go through cycles of denervation and reinnervation normally, but with aging the reinnervation becomes less successful and nerves fail to reconnect, resulting in lack of neural input and skeletal muscle atrophy [204]. This cyclic denervation-reinnervation process is also different between fast and slow motor units, contributing to the resistance of age-related atrophy in slow twitch fibers [205]. In mouse models of nerve injury, significant loss of skeletal muscle mass and function is observed [206, 207]. However, little is known about whether this skeletal muscle innervation is changed with AD, or if changes in the central nervous system go on to impact skeletal muscle function directly.

It has been shown clinically that patients with AD are more likely to fall, and as cognitive impairment worsens in patients with AD skeletal muscle mass and function declines worsen, suggesting AD worsens skeletal muscle function [110, 208, 209]. However, it remains unclear if this decline in skeletal muscle function is intrinsic to the skeletal muscle or is a result of changes in motor coordination following neurodegeneration. In a mouse model containing 5 familial variants in the amyloid precursor protein gene (5xFAD), gait or walking pace of female animals 11-13 months old were significantly slower and described as “shuffling”, and their swim time was significantly shorter even though their peripheral nerve input was unaltered compared to WT littermates [210]. However, other work done in a 5xFAD model showed an increase in voluntary wheel running distance in both male and female animals at 6 and 12 months of age compared to WT [211]. In a mouse model of tau neurofibrillary tangle pathology of AD, mice had significantly decreased motor coordination as expressed by a decrease in rotarod assay coordination and decreases in muscle strength as shown in decreased hang time [212]. These data suggest that skeletal muscle is negatively affected by AD by changes in the brain, specifically the motor cortex, that go on to have a negative effect on muscle function. However, it remains unclear whether there may be other mechanisms contributing to skeletal muscle weakness with AD. Metformin has been shown to decrease plaque burden and improve microglial function in a mouse model of AD, suggesting it may serve as a potential therapeutic option for both skeletal muscle and AD [213, 214]. Additionally, metformin has previously been shown to reduce risk for developing AD and frailty related disease which includes osteoporosis and sarcopenia [215]. These data suggest that

improving skeletal muscle function may improve outcomes in this patient population, making it critical for us to understand this relationship.

As previously described, we will use the TREM2 R47H variant as a model to assess whether mechanisms active in the brain during neurodegeneration may also be active and contributing to clinically observed atrophy and functional loss of the skeletal muscle. The role of TREM2 in skeletal muscle has not been previously defined, making this some of the first work to evaluate whether TREM2 has any effect on skeletal muscle.

Methods

Mice

TREM2^{R47H/+} mutant mice were generated by Jackson Labs in collaboration with the Model-AD center using CRISPR-Cas9 genome editing as previously described [136]. Animals were maintained heterozygous for the global TREM2 R47H mutation (TREM2^{R47H/+}) and wild-type TREM2^{+/+} (WT) littermates were used as controls. SNP-based genotyping (Thermo Fisher) was used to identify carriers in subsequent crosses using the following: forward primer: 5'-ATGTA CTTATGACGCCTTGAAGCA, reverse primer: 5'-ACCCAGCTGCCGACAC, SNP reporter 1: 5'-CCTTGCGTCTCCC, SNP reporter 2: 5'-CCTTGTGTCTCCC. All mice presented C57BL/6J background, were fed a regular diet and water *ad libitum* and maintained on a 12h light/dark cycle. All animal studies were approved by the Institutional Animal Care and Use Committee of Indiana University School of Medicine.

Body Composition Assessment

Lean (muscle) and fat (adipose) mass was assessed at baseline and the day before sacrifice in physically restrained mice, by means of an EchoMRI-100 (EchoMRI, Houston, USA), as previously published [216].

Grip Strength Measurement

Forelimb strength was assessed using a commercially available grip strength meter (Columbus Instruments, Columbus, OH, USA), as previously described [217]. The absolute force (expressed in grams) and the normalized force (expressed as grams of force/body weight) were recorded. To reduce procedure-related variability, the same operator analyzed an average from several repeated peak force measurements in the same animal in a blind manner. For this assay, five measurements were performed, and the top three measurements were used for the analysis. Moreover, to avoid bias of habituation, the animals were tested every month during development (1-4 months of age) and every 2-5 months as the animals aged.

In vivo Muscle Contractility

Female and male WT and TREM2^{R47H/+} mice at 12 months of age were tested for muscle force by *in vivo* plantarflexion 2 days prior to euthanasia (Aurora Scientific, Aurora, ON, Canada), as performed previously [218, 219]. Briefly, the left hind foot was taped to the force transducer and positioned to where the foot and tibia were aligned at 90°. The knee was then clamped at the femoral condyles, avoiding compression of the fibular nerve. Two disposable monopolar electrodes (Natus Neurology, Middleton, WI, USA) were placed subcutaneously posterior/medial to the knee in order to stimulate the tibial nerve. Peak

twitch torque was first established in order to determine maximal stimulus intensity. Following determination of stimulus intensity, mice were subjected to an incremental frequency stimulation protocol to assess force–frequency relationships. The protocol utilized 0.2 ms pulses at 10, 25, 40, 60, 80, 100, 125, and 150 Hz with 1 min in between stimulations.

In vivo Electrophysiology

Triceps surae muscles of female and male WT and TREM2^{R47H/+} mice 12 months of age were subjected to electrophysiological functional assessment using the Sierra Summit 3-12 Channel EMG (Cadwell Laboratories Incorporated, Kennewick, WA, USA), as performed previously [220]. Two 28-gauge stimulating needle electrodes (Natus Neurology, Middleton, WI, USA) were used to stimulate the sciatic nerve of the left hindlimb, a duo shielded ring electrode (Natus Neurology, Middleton, WI, USA) was used for recording, and a ground electrode was placed over the animal's tail. Baseline-to-peak and peak-to-peak compound muscle action potential (CMAP) responses were recorded utilizing supramaximal stimulations (constant current intensity: < 10 mA; pulse duration: 0.1 ms) as previously described [219-221].

Ex vivo Contractility

The whole muscle contractility of the extensor digitorum longus (EDL) and soleus muscles was determined as previously described [218]. EDL and soleus muscles were dissected from hind limbs, the tendons were tied to stainless steel hooks using 4–0 silk sutures, and the muscles were mounted between a force transducer (Aurora Scientific, Aurora, ON, Canada). The muscles were then immersed in a stimulation bath with O₂/CO₂ (95/5%) and

Tyrode solution (121 mM NaCl, 5.0 mM KCl, 1.8 mM CaCl₂, 0.5 mM MgCl₂, 0.4 mM NaH₂PO₄, 24 mM NaHCO₃, 0.1 mM EDTA, and 5.5 mM glucose). The muscles were stimulated to contract using supramaximal stimuli between two platinum electrodes. Data were collected via the Dynamic Muscle Control/Data Acquisition (DMC) and Dynamic Muscle Control Data Analysis (DMA) programs (Aurora Scientific). Prior to each contraction bout, the muscle was lengthened to yield the maximum force (L₀). The force–frequency relationships were determined via an incremental stimulation frequency protocol (0.5 ms pulses at 10, 25, 40, 60, 80, 100, 125 and 150 Hz for 350 ms (EDL) or 600 ms (Soleus) at the supramaximal voltage) with 1 min rest periods between contractions. Following force frequency assessment, muscles rested for five minutes and then underwent a 60 (EDL) or 100 (Soleus)-contraction fatiguing protocol at 60Hz (every 3 seconds). The muscle weight and L₀ were used to determine the specific force.

Activity Monitoring

Female and male WT and TREM2^{R47H/+} mice at 12 months of age were placed one at a time in an Opto-Varimex Auto Track System (Columbus Instruments, Columbus, OH, USA), where activity was tracked and categorized across 2 minutes.

C2C12 Myotube differentiation

Murine C2C12 skeletal myoblasts (ATCC, Manassas, VA) were grown in high glucose DMEM supplemented with 10% FBS, 100 U/ml penicillin, 100 mg/ml streptomycin, 2 mM L-glutamine, and maintained at 37°C in 5% CO₂, as previously published [222]. Myotubes were generated by exposing the myoblasts to DMEM containing 2% horse serum (i.e. differentiation medium, DM), and replacing the medium every other day for 3 days. In

order to determine the dependence of myotube size on bone-derived factors, myotubes were exposed to 5% bone conditioned medium (CM) for 48 hours. Cells were fixed and stained as previously described [216].

Generation of bone-derived conditioned medium (CM)

Right femur and tibiae from 4 month old female and male WT and TREM2^{R47H/+} mice were carefully cleaned of muscle and fibrous tissues, epiphyses cut, and then marrow-flushed multiple times with α MEM. These long bones cortical preparations were then cultured *ex vivo* in 10% FBS and 1% penicillin/streptomycin (P/S)- α MEM for 48h. CM was collected and stored at -20°C prior to C2C12 exposure.

Assessment of Myotube Size

Cell layers were fixed in ice-cold acetone-methanol (50:50) and incubated with an anti-Myosin Heavy Chain antibody (MF20, 1:200, Developmental Studies Hybridoma Bank, Iowa City IA) and an AlexaFluor 488-labeled secondary antibody (Invitrogen, Grand Island NY) as described previously [216]. Analysis of myotube size was performed by measuring the average diameter of long, multinucleate fibers avoiding regions of clustered nuclei on a calibrated tissue image using the Image J 1.43 software [223].

Statistics

All statistical analyses were performed using GraphPad Prism 9.0.0 (GraphPad Software, San Diego, CA, USA). In general, Student's t-tests were performed to determine significant differences between TREM2^{R47H/+} and WT groups for each sex, comparisons were not made between sexes. For data that failed either the D'Agostino & Pearson test or Shapiro-Wilk test for normality, analysis was performed using the Mann-Whitney test, and for data

with unequal variance, the Welch's t-test was used as indicated in the corresponding figure legends. For longitudinal data taken across 20 months, multiple frequencies, or contractions, a 2-way analysis of variance (ANOVA) was performed, followed by post-hoc comparisons for each time point. Post-hoc tests used is specified in the figure legends and vary depending on the comparison being made. All results of the ANOVA tests are included in the Supplementary table 1. Statistical significance was set at $P \leq 0.05$, and the data are presented as box plots where the horizontal line represents the median, the box outlines the interquartile range, and the bars represent maximum and minimum, whereas each dot corresponds to an individual animal. For longitudinal data, the symbol represents the median and bars represent the interquartile range. Sample sizes vary due to variability in genotypes generated as data was collected, and samples were excluded if damaged during collection or analysis (ex. Femurs broken excluded from microCT analysis).

Results

Beyond bone fragility, reduced skeletal muscle strength significantly contributes to risk for falls, thereby increasing fracture risk that limit mobility and negatively impact patient quality of life [155]. Skeletal muscle mass and size has been shown to decline with AD progression [110]. However, no mechanisms for this loss of skeletal muscle mass and strength have been explored. Therefore, we also assessed the skeletal muscle phenotype of female and male TREM2^{R47H/+} mice. Female TREM2^{R47H/+} animals gain body weight differently across 20 months of age, as evaluated by repeated-measures Two-Way ANOVA (**Figure 2-1A**). This difference seems to be associated with decreases in fat mass percentage and lack of fat mass accrual in female TREM2^{R47H/+} animals, which is not seen in male animals (**Figure 2-1B**). However, there are only mild increases in lean mass percentage in female TREM2^{R47H/+} animals at 6 months of age, but no differences in lean mass between male TREM2^{R47H/+} animals compared to WT (**Figure 2-1C**). Surprisingly, grip strength was significantly increased in female TREM2^{R47H/+} animals at 8 months of age and changed differently compared to WT across 20 months of age, whereas male TREM2^{R47H/+} animals had an increased grip strength only at 8 months of age (**Figure 2-1D**). Activity monitoring of 12-month-old mice showed that female TREM2^{R47H/+} animals spent more time ambulatory, walking around, and less time performing stereotypic movements such as face touching compared to WT, with no differences detected in males (**Figure 2-2**). Lean mass and strength are altered in female but not male TREM2^{R47H/+} animals with age, and this may be explained by the increases in activity.

To further assess whether the TREM2^{R47H/+} variant alters skeletal muscle strength in a sex-dependent manner, *in vivo* plantar flexion was performed on anesthetized 12-

month-old female and male animals. Female TREM2^{R47H/+} animals had increased force across 60 – 150Hz of stimulation, as well as increased maximal twitch force and force produced at 100 Hz compared to WT littermates, whereas no effect was seen in force production in males (**Figure 2-3**). Compound muscle action potential (CMAP) stimulation of the sciatic nerve in the same animals demonstrated no differences, suggesting the effect of the TREM2 R47H variant on skeletal muscle strength are not likely due to changes in the peripheral nerve excitability (**Figure 2-4A**). These data suggest that the changes in skeletal muscle strength are not likely due to changes in nervous input to the skeletal muscle. *Ex vivo* skeletal muscle testing of the soleus muscle at the beginning of the fatigue assay showed increases in the twitch force of soleus muscles isolated from 13-month-old female TREM2^{R47H/+} animals compared to WT, but these muscles were also more fatigable (**Figure 2-5A**). Across 40-150 Hz of stimulation the 13-month female TREM2^{R47H/+} soleus muscle produced more force than WT (**Figure 2-5B**). However, *ex vivo* testing of the EDL showed no differences in force production or fatigue (**Figure 2-4B**). The soleus is primarily comprised of oxidative Type 1 fibers whereas the EDL is primarily comprised of Type 2B glycolytic fibers, suggesting that the effect of the TREM2 R47H variant on muscle strength but not total lean body mass percentage is due to sex-dependent, fiber-type specific changes [224].

Previous work has demonstrated the importance of bone-muscle crosstalk in disease states, including cancer and burn injury, and with exercise, therefore we assessed whether known bone-muscle crosstalk mediator TGF- β known to be released from the bone matrix during osteoclastic resorption [225, 226], could be involved in this phenotype. Unexpectedly, however, serum levels of TGF- β are decreased in both female and male

TREM2^{R47H/+} animals aged to 19-20 months, but not at 4 months (**Figure 2-6**). Further, C2C12 myotubes after 3 days of differentiation exposed to 10% conditioned media (CM) for 48 hours from male (but not female) TREM2^{R47H/+} marrow-flushed long bones were slightly smaller in the average diameter, but frequency distributions demonstrate no differences in the distribution of myotube diameters exposed to either male or female TREM2^{R47H/+} compared to WT bone CM (**Figure 2-7**). These data suggest that the changes in skeletal muscle phenotype seen in TREM2^{R47H/+} animals are likely not associated with alterations of the bone-muscle crosstalk, and may be due to other mechanisms.

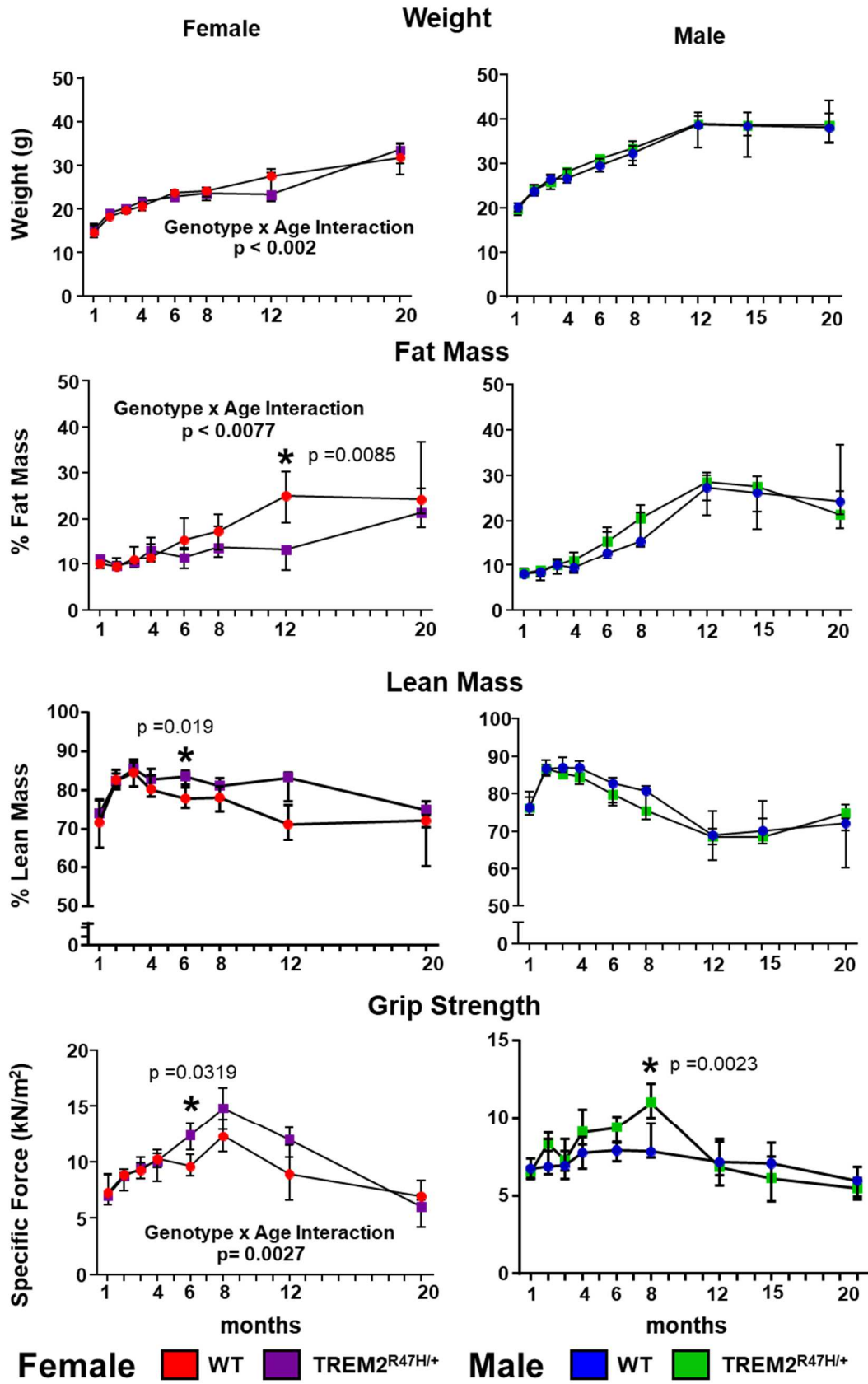


Figure 2-1: Body composition and strength are altered in female, but not male TREM2^{R47H/+} animals.

Body weight (**A**), fat mass percentage (**B**), lean mass percentage (**C**), and grip strength (**D**) of male and female TREM2^{R47H/+} animals compared to WT. N = 5-8/group. Comparisons are sex- and time-matched, TREM2^{R47H/+} vs. WT via RM Two-Way ANOVA mixed-effect model with Sidak's multiple comparisons test: (**B**) Female Fat mass at 12 months p = 0.0085. (**C**) Female Lean Mass 6 at months p = 0.0319. (**D**) Female Grip Strength at 6 months p = 0.0027, Male Grip Strength at 8 months p = 0.0023. See Table 2 for details on the ANOVA analysis

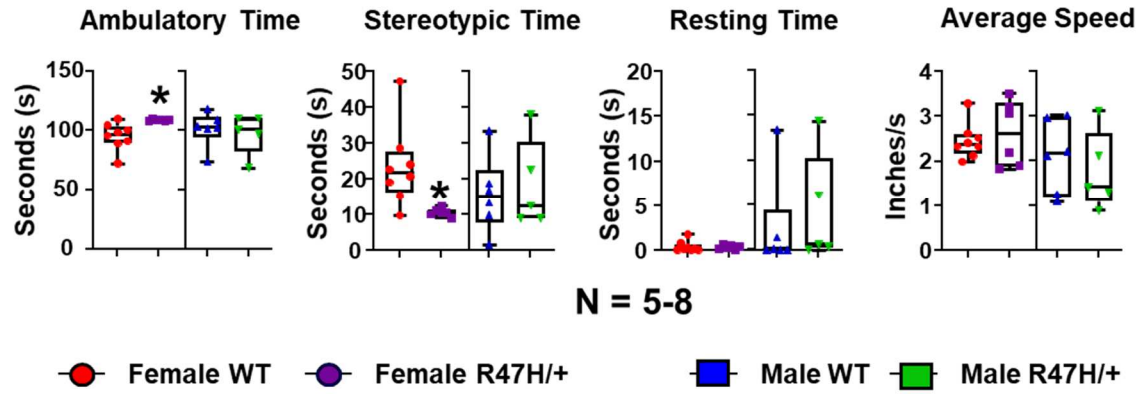


Figure 2-2: Activity monitoring of male and female TREM2^{R47H/+} animals at 12 months of age.

Various aspects of animal activity measured across two minutes. Comparisons are sex-matched between TREM2^{R47H/+} vs. WT assessed via Student's t-test: Ambulatory Time $p = 0.013$, Stereotypic Time $p = 0.016$.

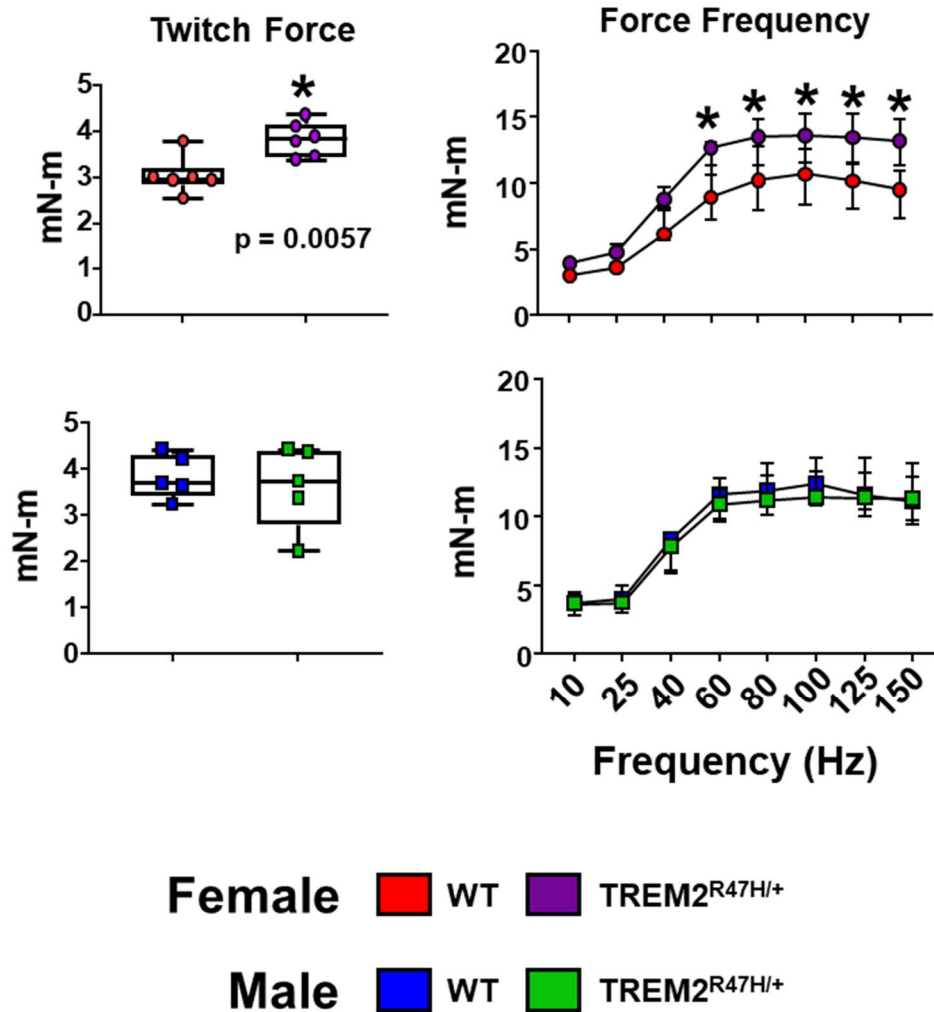


Figure 2-3: Increased *in vivo* plantar flexion in female and male TREM2^{R47H/+} animals at 12 months of age.

In vivo plantar flexion of 12-month-old male and female TREM2^{R47H/+} and WT animals demonstrating both maximal twitch force and force production across 150 Hz of stimulation (N = 5-6). Force Frequency comparison of female TREM2^{R47H/+} to WT using Two-way ANOVA and Bonferroni's multiple comparisons: 60Hz p = 0.024, 80Hz p = 0.023, 100Hz p = 0.016, 125Hz p = 0.0029, 150Hz p = 0.0006. See Table 3 for details on the ANOVA analysis.

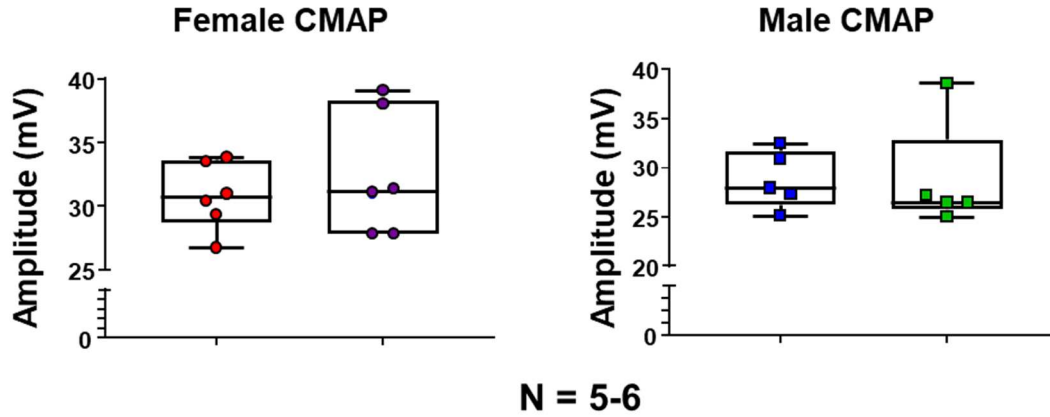
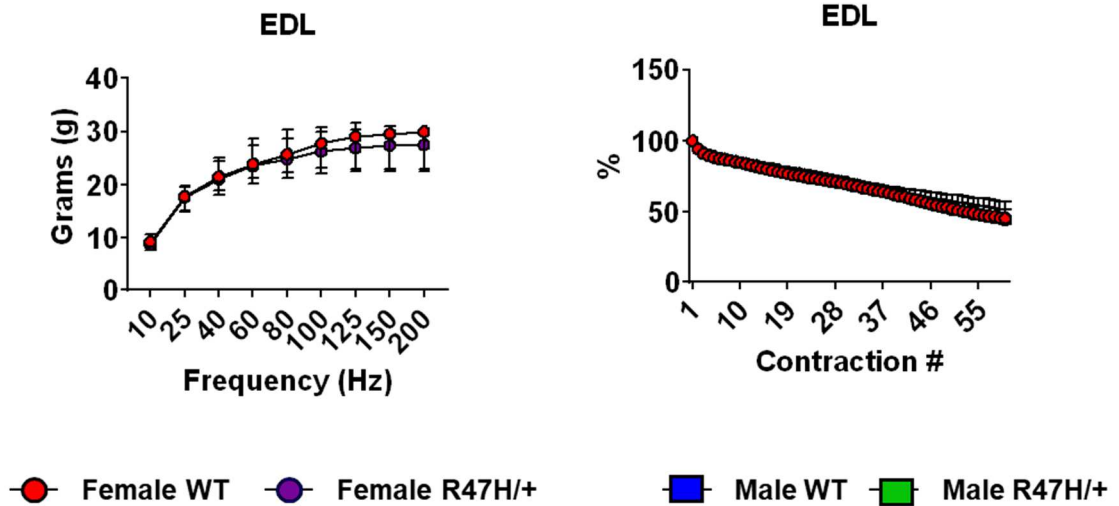
A**B**

Figure 2-4: Nerve input does not contribute to changes in muscle strength, and EDL muscle is unaffected by TREM2 R47H variant in female animals at 13 months of age.

In vivo CMAP measurements of the sciatic nerve from male and female TREM2^{R47H/+} and WT animals at 12 months of age (A), *ex vivo* contractility testing of the EDL from 13-month-old female TREM2^{R47H/+} and WT animals (B). See Table 4 for details on the ANOVA analysis.

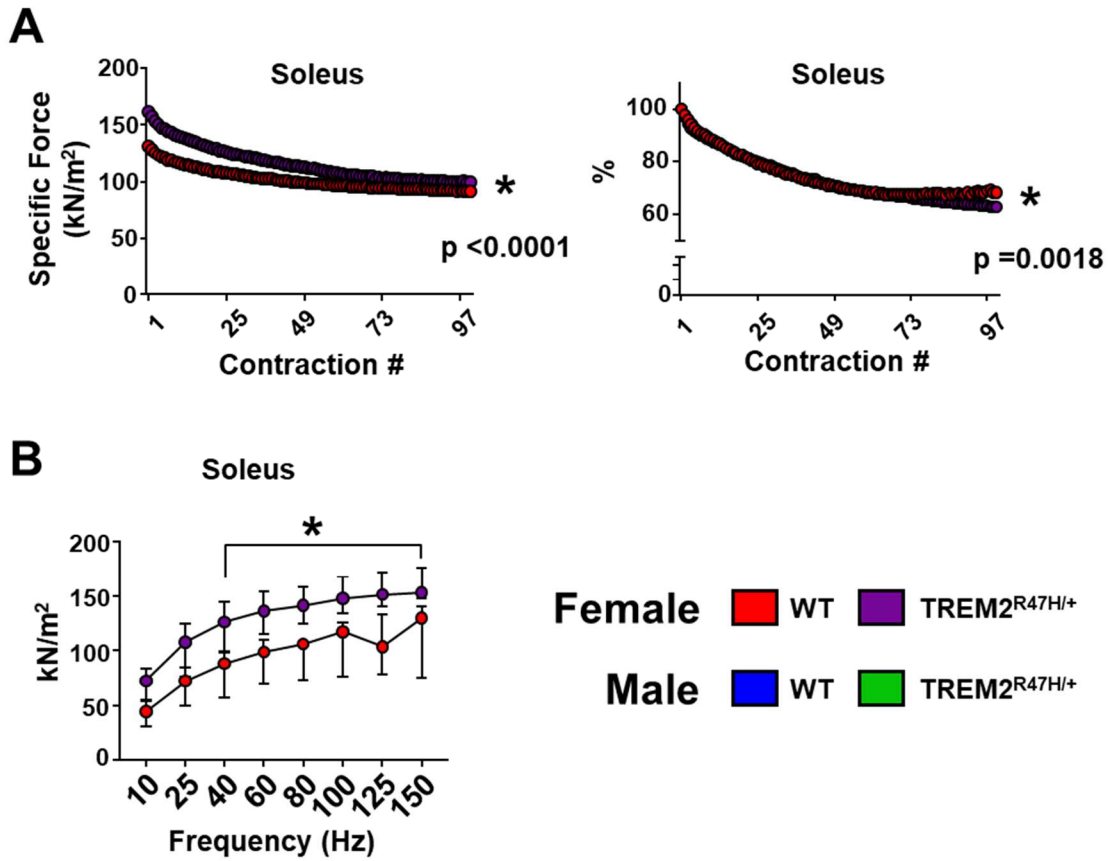


Figure 2-5: Increased *ex vivo* soleus contractility muscle strength in female $TREM2^{R47H/+}$ animals at 12 months of age.

Ex vivo contractility assessment of force production and fatigue of female $TREM2^{R47H/+}$ and WT soleus muscles across 97 contractions (**A**), as well as force frequency and force at 100 Hz of stimulation (**B**). Force Frequency comparison of female $TREM2^{R47H/+}$ to WT using Two-way ANOVA and Bonferroni's multiple comparisons: (**B**) 40Hz $p = 0.0127$, 60Hz $p = 0.0081$, 80Hz $p = 0.0031$, 100Hz $p = 0.0048$, 125Hz $p = 0.0027$, 150Hz $p = 0.0029$. Sex-matched comparisons of female and male $TREM2^{R47H/+}$ to WT using Student's t-test: (**B**) Force @ 150Hz $p = 0.0171$. See Table 5 for details on the ANOVA analysis.

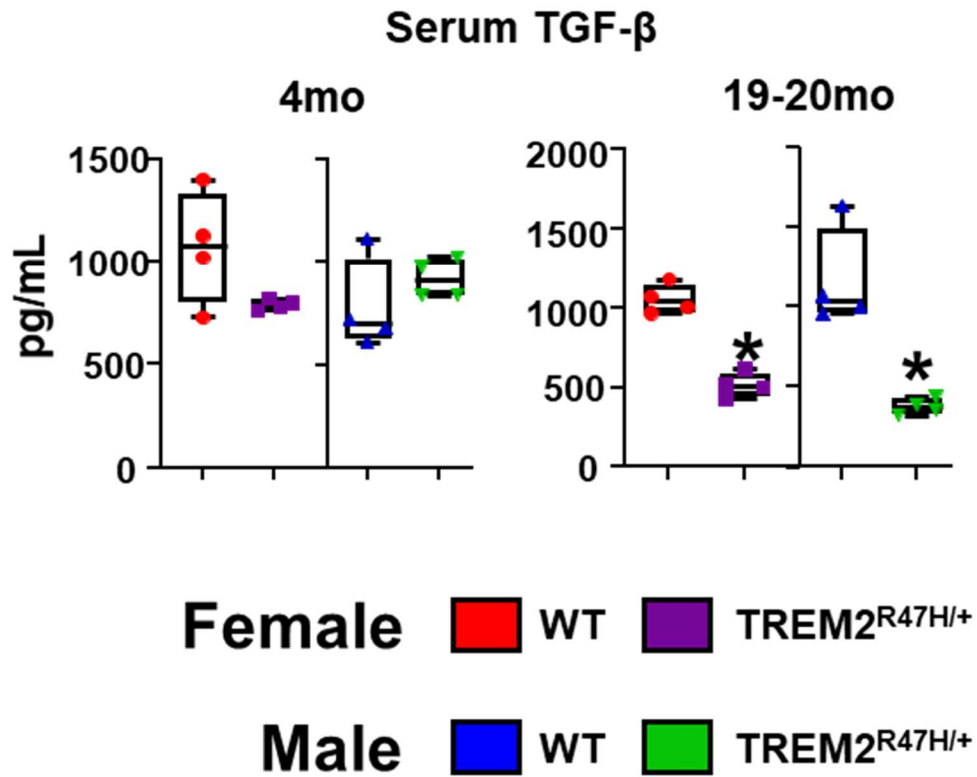


Figure 2-6: Serum TGF- β levels decreased in aged but not young male and female TREM2^{R47H/+} mice compared to WT littermates.

Serum TGF- β levels from 4- and 19-20- month-old male and female TREM2^{R47H/+} and WT animals. Sex-matched comparisons of female and male TREM2^{R47H/+} to WT using Student's t-test: 19-20 months Female p = 0.0001, Male p = 0.0026.

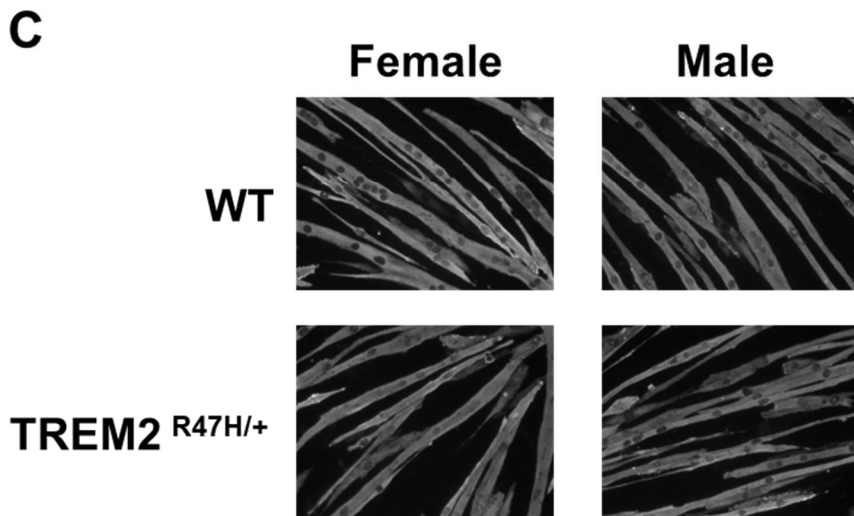
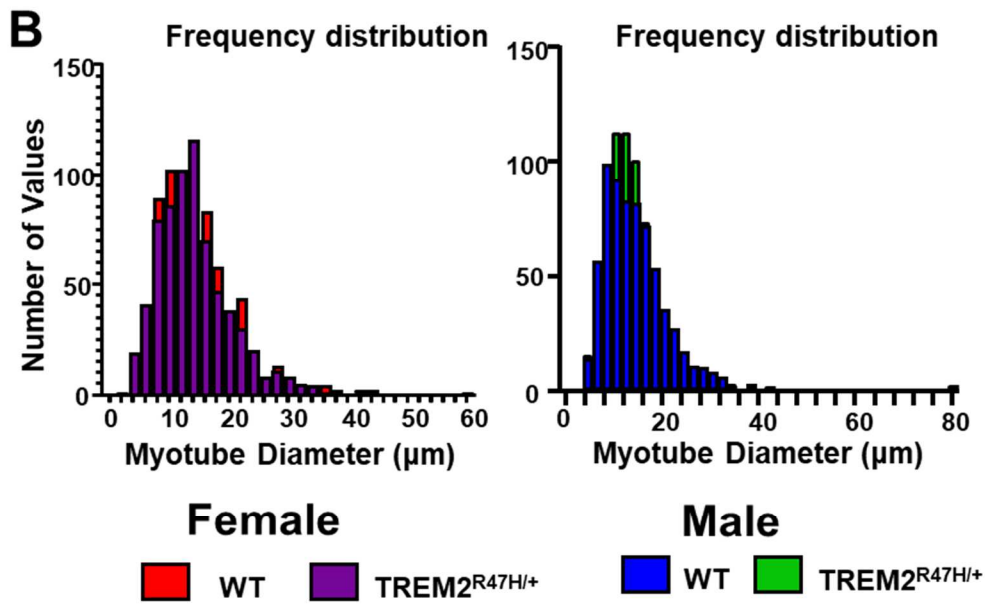
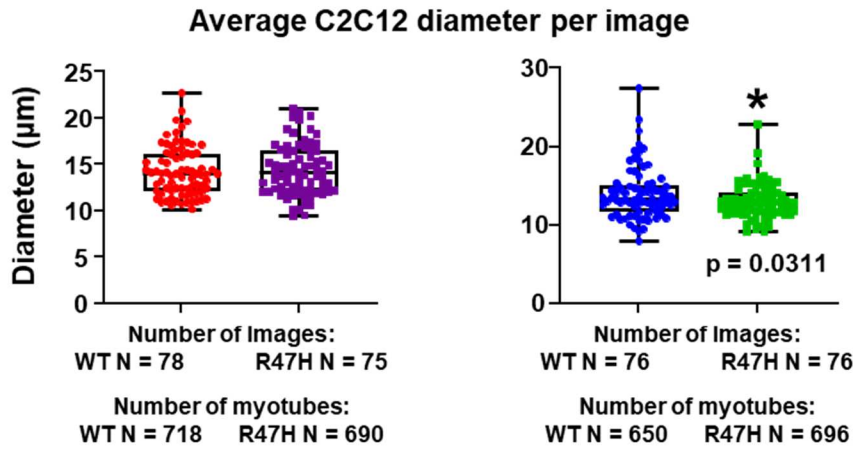


Figure 2-7: C2C12 myotubes exposed to conditioned media from marrow-flushed TREM2^{R47H/+} and WT bones.

C2C12 myoblasts differentiated into myotubes and exposed to CM from male and female TREM2^{R47H/+} and WT marrow-flushed bones, the average diameter (**A**), frequency distribution of myotube diameter (**B**), and representative images (**C**). Sex-matched comparisons made between TREM2^{R47H/+} and WT by Student's t-test. No statistical analysis was performed on the frequency distributions.

Mixed Effect Two-Way ANOVA Source of Variation (p value)			
	Time x Genotype	Time	Genotype
Female Weight	0.002 *	< 0.0001 *	0.953
Male Weight	0.732	< 0.0001 *	0.457
Female Lean Mass	0.073	< 0.0001 *	0.0045 *
Male Lean Mass	0.547	< 0.0001 *	0.339
Female Fat Mass	0.008 *	< 0.0001 *	< 0.0001 *
Male Fat Mass	0.336	< 0.0001 *	0.477
Female Grip Strength	0.0027 *	< 0.0001 *	0.0123 *
Male Grip Strength	0.0938	< 0.0001 *	0.0016 *

Table 2: ANOVA analysis from Figure 2-1.

		RM Two-Way ANOVA Source of Variation (p value)			
		Frequency x Genotype	Frequency	Genotype	Subject (F-value)
Figure 2-3	Female Plantar Flexion force Frequency	0.0098 *	< 0.0001 *	0.0061 *	< 0.0001 *
	Male Plantar Flexion Force Frequency	0.9453	< 0.0001 *	0.8779	< 0.0001 *

Table 3: ANOVA analysis from Figure 2-3.

		RM Two-Way ANOVA Source of Variation (p value)			
		Time x Genotype	Time	Genotype	Subject (F-value)
Figure 2-4	EDL Force Frequency	0.9961	<0.0001 *	0.7566	<0.0001 *
	EDL Fatigue	>0.9999	<0.0001 *	0.5929	<0.0001 *

Table 4: ANOVA analysis from Figure 2-4.

		RM Two-Way ANOVA Source of Variation (p value)			
		Frequency x Genotype	Frequency	Genotype	Subject (F-value)
Figure 2-5A	Female Soleus <i>Ex vivo</i> Contractility	0.9969	< 0.0001 *	0.637	< 0.0001 *
	Female Soleus <i>Ex vivo</i> Fatigue	0.0005 *	< 0.0001 *	0.5232	< 0.0001 *
Figure 2-5B	Female Soleus <i>Ex vivo</i> Specific Force	0.0037 *	< 0.0001 *	0.0082 *	< 0.0001 *

Table 5: ANOVA analysis from Figure 2-5.

CHAPTER FOUR: Discussion

AD is the most common form of dementia worldwide, and disease prevalence is projected to grow over the next 30 years [27]. AD is most prominently known for impacting memory, but AD patients also exhibit decreases in BMD and skeletal muscle function [29, 110, 227, 228]. Thus, the impact of AD goes beyond the brain. Nevertheless, there is limited understanding of the mechanisms that contribute to bone fragility and muscle weakness in AD patients. Preclinical studies using mouse models of AD have not conclusively demonstrated that bone fragility and skeletal muscle weakness seen clinically can be explained by the central neurodegeneration of the brain. Neuroinflammation and myeloid cells of the brain have been shown to contribute to AD pathogenesis, and many of these pathways and mechanisms are also present in cells of the bone and skeletal muscle. But whether these mechanisms also contribute to the bone and muscle loss seen clinically independent of the pathology in the brain has been unexplored.

This study focused on the musculoskeletal abnormalities associated with a TREM2 variant, known to contribute to neuroinflammation and central pathology in AD via functional changes in microglia, myeloid cells of the brain [229]. Previous studies of Nasu-Hakola disease, which is a neurodegenerative disease that also presents with bone cysts, have demonstrated that amino acid substitutions in the TREM2 receptor can cause brain and bone disease simultaneously [230]. However, no AD-associated mutations in TREM2 known to contribute to central neurodegeneration have been shown to influence bone or muscle. TREM2 expression inhibits osteoclast differentiation and resorption [231], but it remains unclear whether amino acid variants known to alter TREM2 signaling associated

with AD may also alter osteoclast function. Further, there is no existing literature on the role of TREM2 in skeletal muscle aging.

In the present study, we used a mouse model of a genetic risk factor for AD carrying the TREM2 R47H variant, which lacks the ability to develop central neurodegeneration in the absence of additional mutations as shown in previous work [30, 34, 232]. Our data using this model of AD risk factor has identified a potential mechanism by which bone loss, but not muscle loss, may be explained in AD patients preceding neurodegeneration diagnosis. Global heterozygous expression of the R47H variant used in this study mimics what is seen clinically and allows to better translate the potential effect size of the TREM2 R47H variant on bone and muscle. Our data demonstrates this variant only causes bone loss after 13- and 20- months of age in female and male animals, respectively, with a minimum effect in females at 4 months, suggesting the effect of the variant on bone volume is age-dependent and is not involved in skeletal development or maturation.

Late-Onset Alzheimer's disease (LOAD), which the TREM2 R47H variant is associated with, is typically found in patients 65 years of age or older [135]. This suggests that age-related changes (*e.g.*, cellular senescence/senescence-associated secreted proteins, increased inflammation) that may contribute to TREM2-mediated risk for AD in the brain may also be active in contributing to bone loss and fragility.

Our study identified a poignant sex-dependent effect of the TREM2 R47H variant on both bone and muscle. Clinical evidence demonstrates that AD is more prevalent in female compared to male sex, but the mechanism remains unclear. BMD and body composition analysis only showed differences in female, not male, TREM2^{R47H/+} animals across 20 months of age, which prompted us to further investigate the female phenotype

by assessing an intermediate time point. Although male animals experience cancellous bone loss and mechanical strength changes at 20 months of age, female animals had much more pronounced changes in bone volume and strength already at 13 months of age, and milder differences in cortical bone volume at 20 months of age with no effect on strength. Cortical bone loss was most rapid in the $TREM2^{R47H/+}$ animals between 4 and 13 months of age, where the marrow cavity was larger, the cortical bone was thinner, but the cross-sectional area was larger. Between 13 and 20 months, the female $TREM2^{R47H/+}$ cross-sectional area and periosteal surface become smaller compared to WT. These patterns suggest that age-related periosteal expansion/endocortical resorption in the cortical bone are happening between 4 and 13 months of age in the female $TREM2^{R47H/+}$ animals. Then between 13 and 20 months of age, these patterns stall out and WT animals catch up to conclude with a similar level of bone loss at 20 months of age. These differential rates of bone loss between $TREM2^{R47H/+}$ and WT female mice may explain the lack of difference in the mechanical properties between female $TREM2^{R47H/+}$ and WT femurs at 20 months of age. However, while male $TREM2^{R47H/+}$ animals did not have differences in cortical bone volume at 4 and 20 months of age, there were mild increases in ultimate stress and failure force as measured by three-point bending only at 20 months of age. The only bone loss found in male $TREM2^{R47H/+}$ animals was in the cancellous bone of the distal femur, which was only seen at 20 months of age. This suggests that changes in TREM2 signaling in male cells may not impact bone as strongly compared to the females; and may explain why, although $ER\alpha$ mRNA levels and phospho-CREB protein levels were increased in male $TREM2^{R47H/+}$ osteoclasts, there was no effect on bone volume.

The decreased cortical bone volume likely contributes to the decreased mechanical properties seen at 13 months of age in the female TREM2^{R47H/+} animals, although the changes in the material properties and a decrease in the endocortical mineral apposition rate suggest the effect of the TREM2^{R47H/+} variant may go beyond the cell-intrinsic effect of the mutation on osteoclasts and may also impact osteoblast/osteocyte function. This has been described in a clinical case study of Nasu-Hakola disease where a male patient had a mutation in TREM2 with abnormal mineralization patterns in the trabecular bone [139]. Interestingly, this case study sample also had a higher BMD in the trabecular bone. Although the mutation in TREM2 found in this case study is different from the R47H model reported here, our findings suggest alterations to TREM2 signaling may impact osteoblasts. On the other hand, previous work in TREM2/DAP12 signaling in osteoclasts has demonstrated that a total loss of TREM2 signaling causes increases in osteoclasts as measured by histomorphometry, but no changes in osteoblasts in mice [133]. These data suggest that the changes to intracellular cell signaling as a result of variants in TREM2 may alter the paracrine signaling environment impacting osteoblasts. Osteoblasts are not known to express TREM2, hence osteoclast-osteoblast paracrine interactions may mediate effects on bone material properties and dynamic histomorphometry observed in our data. Furthermore, whether TREM2 and the R47H variant also play a role in osteocytes remains unknown. Gene expression profiling data shows TREM2 is expressed, albeit at low levels, in osteocytes and in the osteocytic cell line IDG-SW3, suggesting there may be some cell-intrinsic effects of the TREM2 R47H mutation in this cell type [233], although no evidence of TREM2 protein being present in osteocytes has been reported. Therefore, we cannot rule out the possibility that part of the TREM2^{R47H/+} mice phenotype is due to direct

consequences of the expression of the variant in osteocytes. Future studies will address the contribution of these cells to the phenotype of mice expressing the TREM2 variant.

In an attempt to find the mediator between osteoclasts and skeletal muscle, we measured the circulating levels of TGF- β , a growth factor known to be deposited in bone by osteoblastic cells and released by osteoclasts following bone resorption. However, osteocytes, which are a differentiated osteoblast embedded in the bone and create an interconnected network, are also known to be significantly impacted by TGF- β . Previous work has shown that the osteocyte network and bone volume are negatively impacted in a sex-dependent manner by loss of TGF- β signaling using a T β 2R^{-/-} mouse model, however an effect was seen in male and not female animals suggesting that either a different receptor is involved or that other mechanisms are contributing to our observed phenotype beyond loss of TGF- β signaling [234]. Other work has also defined a role for TGF- β signaling in bone material strength, suggesting the potential involvement of osteocytes on the effects of the growth factor [235]. Yet, whether this effect is sex dimorphic or consistent with the data presented herein remains unclear. Further, we show herein an age-related decrease in circulating TGF- β levels, but osteocyte scoring shows no difference in the number of osteocytes in the cortical compartment of the femur. Therefore, our data does not provide conclusive evidence for or against direct consequences of the TREM2 R47H variant on osteocytes. Rather, future studies will need to define whether TREM2 is expressed in osteocytes at the protein level, if this expression changes with age, if TREM2 interacts with TGF- β in osteocytes, and whether the R47H variant alters osteocyte function directly or indirectly.

The data presented in our study suggest the R47H variant may alter intracellular osteoclast signaling in a sex-dependent manner. In female animals, the R47H variant seems to modify the interaction of TREM2 signaling with ER α -mediated estrogen signaling via Akt. Changes in cyclin D1 also indicate the R47H variant may alter Wnt/ β -catenin signaling which is consistent with previous studies in TREM2 knockout models [133, 236]. AD is thought to be more common in females compared to males, which suggests that sex-dependent prevalence of AD may be explained by changes in ER α signaling. Consistent with previous reports in macrophages showing that cell differentiation and activity is only mildly impacted by the R47H mutation, osteoclast differentiation was mildly increased only in male osteoclasts [137]. Future work will be needed to directly evaluate whether osteoclast activity is also sex-dependent.

However, why increased AD prevalence in women is dependent on geographic location or other sex-dependent risk factors remains uncertain [237, 238]. In a mouse model of APOE4 expression, another strong genetic risk factor for AD, TREM2 expression and microglial response to plaque in the brain was also different between female and male animals [239]. Although these data were generated in microglia of the brain, they suggest that TREM2 signaling may contribute to sex-dependent differences in risk and pathology of AD, and our data suggest that this may be true in multiple tissues including bone and muscle.

Lean mass and muscle strength have been shown to be decreased in AD patients, but whether this impairment is regulated in a sex-dependent manner remains unclear [110, 111, 227]. Our data shows that female TREM2^{R47H/+} animals weighed less than WT, and this was driven primarily by decreases in fat mass which likely had some degree of

influence on the mild increase in lean mass. Surprisingly, female TREM2^{R47H/+} animals are also stronger, but these changes in body composition and strength is not likely influenced by changes in activity levels, suggesting other mechanisms may be at play. TGF- β is known to be secreted from the bone matrix via resorption and has been shown to cause skeletal muscle atrophy in mouse models of high osteoclastic resorption [226, 240]. Since our female and male animals experience bone loss by 20 months of age, we investigated whether TGF- β could play a role in these observed changes in body composition. Interestingly, although significant decreases in TGF- β in the circulation were seen in both female and male animals, strength changes were only observed in female animals. Thus, the mechanism leading to increased muscle strength in female TREM2^{R47H/+} mice may be related to the decreased pro-atrophic signals resulting from lower TGF- β levels, though this does not explain the lack of effect on male animals, therefore suggesting that additional unknown mechanisms may be involved.

Ex vivo muscle contractility measurement demonstrated increases in the soleus strength, not the EDL, suggesting that the change in strength may also be muscle specific. Aging skeletal muscle is known to undergo fiber-type specific changes, primarily affecting glycolytic, Type II fibers which are the predominant fiber type found in the EDL [241, 242]. These Type II fibers that make up the majority of the EDL have been shown to express more ACVR1B receptors for TGF- β and its family members, including activin, myostatin and GDF-11, than the Type I fibers that make up a majority of the soleus, making it unlikely that the decreased TGF- β had a strong effect on the soleus strength but not the EDL [243].

Our mRNA expression data demonstrate skeletal muscle fibers do not express TREM2, and our bone conditioned media experiment suggests bone-muscle crosstalk cannot likely explain our observed changes in skeletal muscle of female TREM2^{R47H/+} mice. Thus, another cell type in skeletal muscle may be involved in this observed phenotype. Macrophages, known to express TREM2, exist in the skeletal muscle as intramuscular macrophages. These macrophages are known to play a role in skeletal muscle regeneration and repair after injury and exercise, but also are thought to be involved in age-related skeletal muscle weakness [244]. No data has ever described a role for TREM2 in skeletal muscle during aging, although changes in intramuscular macrophage cell population are known to contribute to age-related skeletal muscle weakness. Previous work has demonstrated an increased ratio of M2/M1 macrophages in aged *vs.* young skeletal muscle, and that these macrophages associate with intramuscular adipose tissue [245]. Further, it is known that the soleus muscle has a higher proportion of intramuscular macrophages compared to the gastrocnemius [246]. Therefore, it is possible that intramuscular macrophage function altered due to the TREM2 R47H variant may explain the fiber type-specific changes in skeletal muscle strength. Here we used a model of global expression of the R47H variant, hence our study does not allow us to explicitly identify intramuscular macrophages as the cause of the muscle alterations, although we cannot exclude these cells from consideration as contributors to the phenotype. Therefore, more work is needed to clearly define the role of the intramuscular macrophage in muscle weakness and sarcopenia, and future studies will be needed to address how TREM2 expression, and the R47H variant, in these intramuscular macrophages may impact skeletal muscle mass and strength with age.

Overall, this study suggests that mechanisms active in perpetuating AD pathogenesis in the brain may also be active in other tissues that are known to be negatively affected by AD. These data demonstrate that genetic risk factors known to contribute to the pathology of AD in the brain can also cause bone loss and fragility, but not muscle weakness, independent of pathology in the brain. Further work will be needed to assess when in the aging process these mechanisms become detrimental to bone volume and fragility, and what triggers this degeneration. Additionally, although our data implicates a role of TREM2 in skeletal muscle strength, more work is needed to identify what cell types expressing TREM2 may contribute to skeletal muscle strength regulation, and the mechanism for this interaction. In this study, A β plaques, or tau neurofibrillary tangles were not present, suggesting that other age-related changes may be triggering TREM2-dependent degenerative mechanisms in tissues beyond the brain.

Conclusions

Mice carrying the global heterozygous TREM2^{R47H/+} variant have distinct age- and sex-dependent phenotype in both the bone and skeletal muscle. These data are some of the first to demonstrate that alterations or dysfunction in TREM2 signaling cause bone loss and weakness independent of central neurodegeneration. This suggests that the bone weakness seen clinically in AD may not be a result of the neurodegeneration. Rather, these data are the first to demonstrate that the mechanisms active in myeloid cells of the brain that contribute to the neuroinflammation and neurodegeneration are active in other tissues of the body independent of central pathology. Further, these data are the first to suggest that exacerbated bone loss seen in aged AD patients may be a consequence of TREM2 signaling, and may not be dependent on central neurodegeneration. The contribution of

TREM2, specifically the R47H variant, to AD associated bone loss seems to be dependent on age. This raises the question of whether TREM2 is also involved in age-related bone loss independent of AD which has never been explored. These data also suggest that TREM2 is responding to these age-associated signals that are contributing to bone loss, and the R47H variant alters this signaling. However, what ligands TREM2 is responding to in bone remains unknown. As discussed in the Introduction, APP is expressed in bone but seems to have a positive effect in bone, specifically on osteoblasts [117]. This suggests that either aging changes the effect of the presence of APP on bone, or that the TREM2 R47H variant alters the way bone interacts with APP in bone. This may be due to the pro-survival role of TREM2 previously shown in myeloid cells [247].

As described in this study, TREM2 R47H osteoclasts have increases in ER α expression but decreases in ER α target gene and increased pro-survival BCL2 gene expression, suggesting decreased sensitivity to estrogen-related apoptosis signals that may be mediated by the TREM2 R47H variant. This would suggest that TREM2 activating antibodies being studied for their therapeutic effectiveness in the brain for AD might also be beneficial for bone. However, these antibodies have been shown to increase survival of macrophages and myeloid cells, which would not be beneficial in bone as extending the survival of osteoclasts would further promote resorption and bone loss [248]. Indeed, previous studies have shown these activating antibodies to improve phagocytosis in microglia, suggesting they may increase resorption in osteoclasts [249]. However, more work will be needed to evaluate the potential effectiveness of TREM2 activating antibodies on bone and osteoclasts.

The effect of the TREM2 R47H variant on skeletal muscle was unexpected, causing increased skeletal muscle strength and decreased fat in only female mice. This is not consistent with what is seen in AD patients who experience skeletal muscle weakness as described earlier. These data indicate that the TREM2 R47H variant does not cause skeletal muscle weakness. However, these data do not rule out the potential role of TREM2 entirely in skeletal muscle loss with aging or AD. Similar to our results, previous work in a 5xFAD model of AD showed no difference in peripheral nerve input to the skeletal muscle in female mice at 12 months of age, but interestingly they showed a decrease in ambulatory time which is the opposite of what our data demonstrates [210]. This study by O'Leary et al also demonstrates decreases in swim time, suggesting a decrease in the skeletal muscle endurance and strength which may be consistent with our data demonstrating an increased fatigability of the soleus muscle from TREM2^{R47H/+} female mice compared to WT. Interestingly, skeletal muscle protein synthesis and glucose uptake has shown to be sex dependent, suggesting that these mechanisms may be impacted by TREM2^{R47H/+} and could potentially explain our sex-dependent changes in skeletal muscle strength [250, 251]. This may also be a potential mechanism to explain why female TREM2^{R47H/+} animals are more lean, accumulating less fat with age compared to WT, but more work will be needed to clearly define the role of TREM2 in adipose tissue, lean mass, and whole body metabolism.

These data are the first to demonstrate that genetic variants increasing the risk for developing AD may be active in other tissues that experience dysfunction and degeneration in AD. This opens up the potential for exploring therapeutic options that target multiple tissues affected by AD, specifically the assessment of bone and muscle function in the clinical evaluation of TREM2-targeted therapeutics. These data are some of the first to

suggest that central neurodegeneration may not be the sole regulator of bone and skeletal muscle degeneration in AD. Further, this suggests that there may be potential predictive changes in tissues such as bone and muscle that can be used to help screen for AD prior to memory loss or cognitive dysfunction. This work demonstrates that TREM2 may be a mediator of this, and it may be of interest to pursue future work in understanding how TREM2 alters bone cell function with age independent of AD-related genetic variants.

REFERENCES

1. Vaupel, J.W., F. Villavicencio, and M.-P. Bergeron-Boucher, *Demographic perspectives on the rise of longevity*. Proceedings of the National Academy of Sciences of the United States of America, 2021. **118**(9): p. e2019536118.
2. Knickman, J.R. and E.K. Snell, *The 2030 problem: caring for aging baby boomers*. Health services research, 2002. **37**(4): p. 849-884.
3. Birch, J. and J. Gil, *Senescence and the SASP: many therapeutic avenues*. Genes Dev, 2020. **34**(23-24): p. 1565-1576.
4. Franceschi, C., et al., *Inflammaging: a new immune–metabolic viewpoint for age-related diseases*. Nature Reviews Endocrinology, 2018. **14**(10): p. 576-590.
5. da Silva, P.F.L. and B. Schumacher, *Principles of the Molecular and Cellular Mechanisms of Aging*. Journal of Investigative Dermatology, 2021. **141**(4, Supplement): p. 951-960.
6. Kumari, R. and P. Jat, *Mechanisms of Cellular Senescence: Cell Cycle Arrest and Senescence Associated Secretory Phenotype*. Frontiers in Cell and Developmental Biology, 2021. **9**(485).
7. Niccoli, T. and L. Partridge, *Ageing as a risk factor for disease*. Curr Biol, 2012. **22**(17): p. R741-52.
8. Lindsay, J., et al., *Risk Factors for Alzheimer's Disease: A Prospective Analysis from the Canadian Study of Health and Aging*. American Journal of Epidemiology, 2002. **156**(5): p. 445-453.

9. Metzler-Baddeley, C., *A Review of Cognitive Impairments in Dementia with Lewy Bodies Relative to Alzheimer's Disease and Parkinson's Disease with Dementia*. Cortex, 2007. **43**(5): p. 583-600.
10. Hebert, L.E., et al., *Alzheimer disease in the United States (2010–2050) estimated using the 2010 census*. Neurology, 2013. **80**(19): p. 1778.
11. Association, A.s., *2019 Alzheimer's disease facts and figures*. Alzheimer's & Dementia, 2019. **15**(3): p. 321-387.
12. Joachim, C.L., H. Mori, and D.J. Selkoe, *Amyloid β -protein deposition in tissues other than brain in Alzheimer's disease*. Nature, 1989. **341**(6239): p. 226-230.
13. Puig, K.L. and C.K. Combs, *Expression and function of APP and its metabolites outside the central nervous system*. Experimental gerontology, 2013. **48**(7): p. 608-611.
14. Sanchez-Varo, R., et al., *Plaque-Associated Oligomeric Amyloid-Beta Drives Early Synaptotoxicity in APP/PS1 Mice Hippocampus: Ultrastructural Pathology Analysis*. Frontiers in Neuroscience, 2021. **15**.
15. Metaxas, A. and S.J. Kempf, *Neurofibrillary tangles in Alzheimer's disease: elucidation of the molecular mechanism by immunohistochemistry and tau protein phospho-proteomics*. Neural regeneration research, 2016. **11**(10): p. 1579-1581.
16. Paolicelli, R.C., et al., *Synaptic Pruning by Microglia Is Necessary for Normal Brain Development*. Science, 2011. **333**(6048): p. 1456.
17. Schafer, D.P., et al., *Microglia sculpt postnatal neural circuits in an activity and complement-dependent manner*. Neuron, 2012. **74**(4): p. 691-705.

18. Penzes, P., et al., *Dendritic spine pathology in neuropsychiatric disorders*. Nat Neurosci, 2011. **14**(3): p. 285-93.
19. Andoh, M., Y. Ikegaya, and R. Koyama, *Synaptic Pruning by Microglia in Epilepsy*. Journal of clinical medicine, 2019. **8**(12): p. 2170.
20. Wang, S. and M. Colonna, *Microglia in Alzheimer's disease: A target for immunotherapy*. Journal of Leukocyte Biology, 2019. **106**(1): p. 219-227.
21. Subramanian, J., J.C. Savage, and M.-È. Tremblay, *Synaptic Loss in Alzheimer's Disease: Mechanistic Insights Provided by Two-Photon in vivo Imaging of Transgenic Mouse Models*. Frontiers in Cellular Neuroscience, 2020. **14**.
22. Hansen, D.V., J.E. Hanson, and M. Sheng, *Microglia in Alzheimer's disease*. The Journal of cell biology, 2018. **217**(2): p. 459-472.
23. Jay, T.R., V.E. von Saucken, and G.E. Landreth, *TREM2 in Neurodegenerative Diseases*. Mol. Neurodegener, 2017. **12**(1): p. 56.
24. Wang, Y., et al., *TREM2-mediated early microglial response limits diffusion and toxicity of amyloid plaques*. Journal of Experimental Medicine, 2016. **213**(5): p. 667-675.
25. Yuan, P., et al., *TREM2 haplodeficiency in mice and humans impairs the microglia barrier function leading to decreased amyloid compaction and severe axonal dystrophy*. Neuron, 2016. **90**(4): p. 724-739.
26. Jay, T.R., et al., *TREM2 deficiency eliminates TREM2+ inflammatory macrophages and ameliorates pathology in Alzheimer's disease mouse models*. J Exp Med, 2015. **212**(3): p. 287-95.

27. Association, A.s., *2016 Alzheimer's disease facts and figures*. Alzheimer's & Dementia, 2016. **12**(4): p. 459-509.
28. Gambassi, G., et al., *Predictors of mortality in patients with Alzheimer's disease living in nursing homes*. J Neurol Neurosurg Psychiatry, 1999. **67**(1): p. 59-65.
29. Loskutova, N., et al., *Bone density and brain atrophy in early Alzheimer's disease*. Journal of Alzheimer's disease : JAD, 2009. **18**(4): p. 777-785.
30. Foidl, B.M. and C. Humpel, *Can mouse models mimic sporadic Alzheimer's disease?* Neural regeneration research, 2020. **15**(3): p. 401-406.
31. Jin, S.C., et al., *Coding variants in TREM2 increase risk for Alzheimer's disease*. Human Molecular Genetics, 2014. **23**(21): p. 5838-5846.
32. Guerreiro, R., et al., *TREM2 variants in Alzheimer's disease*. N Engl J Med, 2013. **368**(2): p. 117-27.
33. Rayaprolu, S., et al., *TREM2 in neurodegeneration: evidence for association of the p.R47H variant with frontotemporal dementia and Parkinson's disease*. Molecular Neurodegeneration, 2013. **8**(1): p. 19.
34. Kotredes, K., et al., *A multi-discipline phenotyping platform for late-onset Alzheimer's disease employed on a novel, humanized APOEε4.Trem2*R47H mouse model*. 2021, Research Square.
35. Blake, G.M. and I. Fogelman, *The role of DXA bone density scans in the diagnosis and treatment of osteoporosis*. Postgraduate medical journal, 2007. **83**(982): p. 509-517.
36. Melton, L.J., III, et al., *Bone density and fracture risk in men*. J. Bone Miner. Res, 1998. **13**(12): p. 1915-1923.

37. Melton, L.J., III, et al., *Perspective: How many women have osteoporosis*. J. Bone Min. Res, 1992. **7**: p. 1005-1010.
38. Bliuc, D., et al., *Mortality Risk Associated With Low-Trauma Osteoporotic Fracture and Subsequent Fracture in Men and Women*. JAMA, 2009. **301**(5): p. 513-521.
39. Clowes, J.A., N. Peel, and R. Eastell, *Glucocorticoid-induced osteoporosis*. Curr. Opin. Rheumatol, 2001. **13**(4): p. 326-332.
40. Weinstein, R.S., *Glucocorticoid-induced osteoporosis and osteonecrosis*. Endocrinol. Metab Clin. North Am, 2012. **41**(3): p. 595-611.
41. Carmeliet, G., L. Vico, and R. Bouillon, *Space flight: a challenge for normal bone homeostasis*. Crit Rev. Eukaryot. Gene Expr, 2001. **11**(1-3): p. 131-144.
42. Bikle, D.D. and B.P. Halloran, *The response of bone to unloading*. J. Bone Miner. Metab, 1999. **17**(4): p. 233-244.
43. Anastasilakis, A.D., et al., *Osteonecrosis of the jaw and antiresorptive agents in benign and malignant diseases: a critical review organized by ECTS*. J Clin Endocrinol Metab, 2021.
44. Park, J.H., et al., *Gradual, but Not Sudden, Dose-Dependent Increase of ONJ Risk With Bisphosphonate Exposure: A Nationwide Cohort Study in Women With Osteoporosis*. Front Endocrinol (Lausanne), 2021. **12**: p. 774820.
45. Sharma, A., et al., *Risk of Atrial Fibrillation With Use of Oral and Intravenous Bisphosphonates*. The American Journal of Cardiology, 2014. **113**(11): p. 1815-1821.

46. Wu, S.T., J.F. Chen, and C.J. Tsai, *The impact of bisphosphonates on mortality and cardiovascular risk among osteoporosis patients after cardiovascular disease*. J Formos Med Assoc, 2021. **120**(11): p. 1957-1966.
47. Naganathar, N., et al., *Alendronate use in older patients with reduced renal function: challenges and opportunities in clinical practice*. Osteoporos Int, 2021. **32**(10): p. 1981-1988.
48. Grove, E.L., B. Abrahamsen, and P. Vestergaard, *Heart failure in patients treated with bisphosphonates*. J Intern Med, 2013. **274**(4): p. 342-50.
49. Tsourdi, E., et al., *Discontinuation of Denosumab therapy for osteoporosis: A systematic review and position statement by ECTS*. Bone, 2017. **105**: p. 11-17.
50. Popp, A.W., P.K. Zysset, and K. Lippuner, *Rebound-associated vertebral fractures after discontinuation of denosumab-from clinic and biomechanics*. Osteoporos Int, 2016. **27**(5): p. 1917-21.
51. Anastasilakis, A.D., et al., *Denosumab Discontinuation and the Rebound Phenomenon: A Narrative Review*. J Clin Med, 2021. **10**(1).
52. Bellido, T., *Osteocyte-Driven Bone Remodeling*. Calcif. Tissue Int, 2014. **94**(1): p. 25-34.
53. Dallas, S.L., M. Prideaux, and L.F. Bonewald, *The osteocyte: an endocrine cell ... and more*. Endocr. Rev, 2013. **34**(5): p. 658-690.
54. Bonewald, L.F., *The Amazing Osteocyte*. J. Bone Miner. Res, 2011. **26**(2): p. 229-238.
55. Marotti, G., et al., *Morphometric investigation on osteocytes in human auditory ossicles*. Anat. Anz, 1998. **180**(5): p. 449-453.

56. Plotkin, L.I., *Apoptotic osteocytes and the control of targeted bone resorption*. Curr. Osteoporos. Rep, 2014. **12**(1): p. 121-126.
57. Davis, H.M., et al., *Cx43 overexpression in osteocytes prevents osteocyte apoptosis and preserves cortical bone quality in aging mice*. JBMR Plus, 2018. **DOI:10.1002/jbm4.10035**.
58. Davis, H.M., et al., *High mobility group box1 (HMGB1) protein regulates osteoclastogenesis through direct actions on osteocytes and osteoclasts in vitro*. J Cell Biochem, 2019. **120**(10): p. 16741-16749.
59. Plotkin, L.I., et al., *Inhibition of Osteocyte Apoptosis Prevents the Increase in Osteocytic RANKL but it does not Stop Bone Resorption or the Loss of Bone Induced by Unloading*. J. Biol. Chem, 2015. **290**(31): p. 18934-18941.
60. Plotkin, L.I., et al., *Prevention of osteocyte and osteoblast apoptosis by bisphosphonates and calcitonin*. J. Clin. Invest, 1999. **104**(10): p. 1363-1374.
61. Bellido, T. and L.I. Plotkin, *Novel actions of bisphosphonates in bone: Preservation of osteoblast and osteocyte viability*. Bone, 2011. **49**: p. 50-55.
62. Plotkin, L.I., N. Bivi, and T. Bellido, *A bisphosphonate that does not affect osteoclasts prevents osteoblast and osteocyte apoptosis and the loss of bone strength induced by glucocorticoids in mice*. Bone, 2011. **49**: p. 122-127.
63. Boyce, B.F. and L. Xing, *Biology of RANK, RANKL, and osteoprotegerin*. Arthritis Res. Ther, 2007. **9 Suppl 1**: p. S1.
64. Drake, M.T., B.L. Clarke, and S. Khosla, *Bisphosphonates: mechanism of action and role in clinical practice*. Mayo Clinic proceedings, 2008. **83**(9): p. 1032-1045.

65. Huang, X.-L., et al., *Zoledronic acid inhibits osteoclast differentiation and function through the regulation of NF- κ B and JNK signalling pathways*. International journal of molecular medicine, 2019. **44**(2): p. 582-592.
66. Suda, T., et al., *Regulation of osteoclast function*. J. Bone Miner. Res, 1997. **12**(6): p. 869-879.
67. Yasuda, H., et al., *Osteoclast differentiation factor is a ligand for osteoprotegerin/osteoclastogenesis-inhibitory factor and is identical to TRANCE/RANKL*. Proc. Natl. Acad. Sci. U. S. A, 1998. **95**(7): p. 3597-3602.
68. Lacey, D.L., et al., *Osteoprotegerin ligand is a cytokine that regulates osteoclast differentiation and activation*. Cell, 1998. **93**(2): p. 165-176.
69. Teitelbaum Steven, L., *Bone Resorption by Osteoclasts*. Science, 2000. **289**(5484): p. 1504-1508.
70. Glantschnig, H., et al., *M-CSF, TNF α and RANK ligand promote osteoclast survival by signaling through mTOR/S6 kinase*. Cell Death. Differ, 2003. **10**(10): p. 1165-1177.
71. McDonald, M.M., et al., *Osteoclasts recycle via osteomorphs during RANKL-stimulated bone resorption*. Cell, 2021.
72. Teitelbaum, S.L., *Osteoclasts: what do they do and how do they do it?* Am. J Pathol, 2007. **170**(2): p. 427-435.
73. Biskobing, D.M., X. Fan, and J. Rubin, *Characterization of MCSF-Induced Proliferation and Subsequent Osteoclast Formation in Murine Marrow Culture*. J. Bone Min. Res, 1995. **10**(number 7): p. 1025-1032.

74. Kudo, O., et al., *Proinflammatory cytokine (TNF α /IL-1 α) induction of human osteoclast formation*. The Journal of Pathology, 2002. **198**(2): p. 220-227.
75. Lam, J., et al., *TNF-alpha induces osteoclastogenesis by direct stimulation of macrophages exposed to permissive levels of RANK ligand*. J Clin Invest, 2000. **106**(12): p. 1481-1488.
76. Plotkin, L.I., A.L. Essex, and H.M. Davis, *RAGE Signaling in Skeletal Biology*. Curr Osteoporos Rep, 2019. **17**(1): p. 16-25.
77. Black, D.M. and C.J. Rosen, *Postmenopausal Osteoporosis*. New England Journal of Medicine, 2016. **374**(3): p. 254-262.
78. Eastell, R., et al., *Postmenopausal osteoporosis*. Nature Reviews Disease Primers, 2016. **2**(1): p. 16069.
79. Manolagas, S.C., C.A. O'Brien, and M. Almeida, *The role of estrogen and androgen receptors in bone health and disease*. Nat. Rev. Endocrinol, 2013. **9**(12): p. 699-712.
80. Jilka, R.L., et al., *Ovariectomy in the mouse upregulates hematopoietic precursors in the bone marrow and their progeny in the peripheral blood: a mediating role of IL-6*. J. Bone Min. Res, 1992. **7**(S1): p. S115.
81. Jilka, R.L., et al., *Estrogen deficiency induces sensitivity of the osteoclastogenic process to IL-6*. J. Bone Min. Res, 1994. **9**(S1): p. S143.
82. Martin-Millan, M., et al. *ER alpha Deletion in Cells of the Monocyte/Macrophage Lineage Increases Osteoclastogenesis and Abrogates the Pro-apoptotic Effect of E-2 on Osteoclasts*. in *JOURNAL OF BONE AND MINERAL RESEARCH*. 2008.

WILEY-BLACKWELL COMMERCE PLACE, 350 MAIN ST, MALDEN 02148,
MA USA.

83. Xie, H., et al., *Estrogen receptor-alpha36 mediates a bone-sparing effect of 17beta-estrodinol in postmenopausal women*. J. Bone Miner. Res, 2010.
84. Nakamura, T., et al., *Estrogen prevents bone loss via estrogen receptor alpha and induction of Fas ligand in osteoclasts*. Cell, 2007. **130**(5): p. 811-823.
85. Garcia, A.J., et al., *ERα signaling regulates MMP3 expression to induce FasL cleavage and osteoclast apoptosis*. Journal of Bone and Mineral Research, 2013. **28**(2): p. 283-290.
86. Nagata, S., *Fas Ligand-Induced Apoptosis*. Annual Review of Genetics, 1999. **33**(1): p. 29-55.
87. Jilka, R.L., et al., *Interleukin-6 neutralizing antibody administration prevents osteoclastogenic response to ovariectomy in the mouse*, in *Proceedings of the XIIth International Conference on Calcium Regulating Hormones*, D.V. Cohn and A. Tashjian, Editors. 1992, Elsevier: Amsterdam. p. in press.
88. Girasole, G., et al., *17b-estradiol inhibits interleukin-6 production by bone marrow-derived stromal cells and osteoblasts in-vitro: a potential mechanism for the antiosteoporotic effect of estrogens*. J. Clin. Invest, 1992. **89**: p. 883-891.
89. Narayana Murthy, P.S., et al., *Effect of ormeloxifene on ovariectomy-induced bone resorption, osteoclast differentiation and apoptosis and TGF beta-3 expression*. J. Steroid Biochem. Mol. Biol, 2006.

90. Mann, V., et al., *The antioxidant effect of estrogen and Selective Estrogen Receptor Modulators in the inhibition of osteocyte apoptosis in vitro*. *Bone*, 2007. **40**(3): p. 674-684.
91. Michael, H., et al., *Differential effects of selective oestrogen receptor modulators (SERMs) tamoxifen, ospemifene and raloxifene on human osteoclasts in vitro*. *British Journal of Pharmacology*, 2007. **151**(3): p. 384-395.
92. Kousteni, S., et al., *Reversal of bone loss in mice by nongenotropic signaling of sex steroids*. *Science*, 2002. **298**(5594): p. 843-846.
93. Kousteni, S., et al., *Nongenotropic, sex-nonspecific signaling through the estrogen or androgen receptors: dissociation from transcriptional activity*. *Cell*, 2001. **104**(5): p. 719-730.
94. Gennari, L., et al., *Selective estrogen receptor modulators for postmenopausal osteoporosis: current state of development*. *Drugs Aging*, 2007. **24**(5): p. 361-79.
95. Ellis, A.J., et al., *Selective estrogen receptor modulators in clinical practice: a safety overview*. *Expert Opin Drug Saf*, 2015. **14**(6): p. 921-34.
96. Boskey, A.L., *Bone composition: relationship to bone fragility and antiosteoporotic drug effects*. *BoneKEy reports*, 2013. **2**: p. 447-447.
97. Blair, H.C., et al., *Osteoblast Differentiation and Bone Matrix Formation In Vivo and In Vitro*. *Tissue engineering. Part B, Reviews*, 2017. **23**(3): p. 268-280.
98. Fujisawa, R. and M. Tamura, *Acidic bone matrix proteins and their roles in calcification*. *Front Biosci (Landmark Ed)*, 2012. **17**: p. 1891-903.
99. Seeman, E., *Bone Modeling and Remodeling*. *Crit Rev. Eukaryot. Gene Expr*, 2009. **19**(3): p. 219-233.

100. Sims, N.A. and T.J. Martin, *Coupling the activities of bone formation and resorption: a multitude of signals within the basic multicellular unit*. Bonekey. Rep, 2014. **3**: p. 481.
101. Allen, M.R. and D.B. Burr, *Bone modeling and remodeling*, in *Basic and Applied Bone Biology*, B. D and A. M, Editors. 2014, Elsevier. p. 75-90.
102. Valcourt, U., et al., *Non-enzymatic glycation of bone collagen modifies osteoclastic activity and differentiation*. J Biol Chem, 2007. **282**(8): p. 5691-703.
103. Viguet-Carrin, S., P. Garnero, and P.D. Delmas, *The role of collagen in bone strength*. Osteoporos Int, 2006. **17**(3): p. 319-36.
104. Unal, M., A. Creecy, and J.S. Nyman, *The Role of Matrix Composition in the Mechanical Behavior of Bone*. Curr Osteoporos Rep, 2018. **16**(3): p. 205-215.
105. Wallace, J.M., *Skeletal Hard Tissue Biomechanics*, in *Basic and Applied Bone Biology*, D.B. Burr and M.R. Allen, Editors. 2019, Elsevier. p. 125-140.
106. *2021 Alzheimer's disease facts and figures*. Alzheimer's & Dementia, 2021. **17**(3): p. 327-406.
107. Briggs, A.M., et al., *Musculoskeletal Health Conditions Represent a Global Threat to Healthy Aging: A Report for the 2015 World Health Organization World Report on Ageing and Health*. Gerontologist, 2016. **56 Suppl 2**: p. S243-55.
108. Harvey, N., E. Dennison, and C. Cooper, *Osteoporosis: impact on health and economics*. Nat Rev Rheumatol, 2010. **6**(2): p. 99-105.
109. DeTure, M.A. and D.W. Dickson, *The neuropathological diagnosis of Alzheimer's disease*. Molecular Neurodegeneration, 2019. **14**(1): p. 32.

110. Ogawa, Y., et al., *Sarcopenia and Muscle Functions at Various Stages of Alzheimer Disease*. Front Neurol, 2018. **9**: p. 710.
111. Burns, J.M., et al., *Reduced lean mass in early Alzheimer disease and its association with brain atrophy*. Arch Neurol, 2010. **67**(4): p. 428-33.
112. Zhao, L., et al., *Effects of Curculigoside on Memory Impairment and Bone Loss via Anti-Oxidative Character in APP/PS1 Mutated Transgenic Mice*. PLoS One, 2015. **10**(7): p. e0133289.
113. Dengler-Crish, C.M., M.A. Smith, and G.N. Wilson, *Early Evidence of Low Bone Density and Decreased Serotonergic Synthesis in the Dorsal Raphe of a Tauopathy Model of Alzheimer's Disease*. J Alzheimers Dis, 2017. **55**(4): p. 1605-1619.
114. Lorentzon, M. and S.R. Cummings, *Osteoporosis: the evolution of a diagnosis*. J Intern Med, 2015. **277**(6): p. 650-61.
115. Gambacciani, M. and M. Levancini, *Management of postmenopausal osteoporosis and the prevention of fractures*. Panminerva Med, 2014. **56**(2): p. 115-31.
116. Gambacciani, M., et al., *The relative contributions of menopause and aging to postmenopausal vertebral osteopenia*. J. Clin. Endocrinol. Metab, 1993. **77**: p. 1148-1151.
117. Pan, J.X., et al., *APP promotes osteoblast survival and bone formation by regulating mitochondrial function and preventing oxidative stress*. Cell Death Dis, 2018. **9**(11): p. 1077.
118. Xia, W.F., et al., *Swedish mutant APP suppresses osteoblast differentiation and causes osteoporotic deficit, which are ameliorated by N-acetyl-L-cysteine*. J Bone Miner Res, 2013. **28**(10): p. 2122-35.

119. Yang, M.-W., et al., *Curcumin improves bone microarchitecture and enhances mineral density in APP/PS1 transgenic mice*. *Phytomedicine*, 2011. **18**(2): p. 205-213.
120. Loskutova, N., A.S. Watts, and J.M. Burns, *The cause-effect relationship between bone loss and Alzheimer's disease using statistical modeling*. *Med Hypotheses*, 2019. **122**: p. 92-97.
121. Tan, Z.S., et al., *Bone Mineral Density and the Risk of Alzheimer Disease*. *Archives of Neurology*, 2005. **62**(1): p. 107-111.
122. Satoh, J.-I., et al., *Alzheimer's disease pathology in Nasu-Hakola disease brains*. *Intractable & rare diseases research*, 2018. **7**(1): p. 32-36.
123. Bliuc, D., et al., *Cognitive decline is associated with an accelerated rate of bone loss and increased fracture risk in women: a prospective study from the Canadian Multicentre Osteoporosis Study*. *Journal of Bone and Mineral Research*, 2021. **n/a**(n/a).
124. Cui, S., et al., *APP^{swe}/A β regulation of osteoclast activation and RAGE expression in an age-dependent manner*. *J Bone Miner Res*, 2011. **26**(5): p. 1084-98.
125. Tinetti, M.E., M. Speechley, and S.F. Ginter, *Risk Factors for Falls among Elderly Persons Living in the Community*. *New England Journal of Medicine*, 1988. **319**(26): p. 1701-1707.
126. Dev, K., et al., *Prevalence of Falls and Fractures in Alzheimer's Patients Compared to General Population*. *Cureus*, 2021. **13**(1): p. e12923-e12923.

127. Filipello, F., et al., *The Microglial Innate Immune Receptor TREM2 Is Required for Synapse Elimination and Normal Brain Connectivity*. *Immunity*, 2018. **48**(5): p. 979-991.e8.
128. Gervois, P. and I. Lambrichts, *The Emerging Role of Triggering Receptor Expressed on Myeloid Cells 2 as a Target for Immunomodulation in Ischemic Stroke*. *Frontiers in Immunology*, 2019. **10**.
129. Liu, W., et al., *Trem2 promotes anti-inflammatory responses in microglia and is suppressed under pro-inflammatory conditions*. *Human molecular genetics*, 2020. **29**(19): p. 3224-3248.
130. Ulrich, J.D., et al., *Elucidating the Role of TREM2 in Alzheimer's Disease*. *Neuron*, 2017. **94**(2): p. 237-248.
131. Jay, T.R., et al., *Disease Progression-Dependent Effects of TREM2 Deficiency in a Mouse Model of Alzheimer's Disease*. *J Neurosci*, 2017. **37**(3): p. 637-647.
132. Ransohoff, R.M., *How neuroinflammation contributes to neurodegeneration*. *Science*, 2016. **353**(6301): p. 777-83.
133. Otero, K., et al., *TREM2 and β -catenin regulate bone homeostasis by controlling the rate of osteoclastogenesis*. *Journal of immunology (Baltimore, Md. : 1950)*, 2012. **188**(6): p. 2612-2621.
134. Humphrey, M.B., et al., *TREM2, a DAPI2-Associated Receptor, Regulates Osteoclast Differentiation and Function*. *Journal of Bone and Mineral Research*, 2006. **21**(2): p. 237-245.

135. Korvatska, O., et al., *R47H Variant of TREM2 Associated With Alzheimer Disease in a Large Late-Onset Family: Clinical, Genetic, and Neuropathological Study*. JAMA Neurology, 2015. **72**(8): p. 920-927.
136. Cheng-Hathaway, P.J., et al., *The Trem2 R47H variant confers loss-of-function-like phenotypes in Alzheimer's disease*. Mol Neurodegener, 2018. **13**(1): p. 29.
137. Hall-Roberts, H., et al., *TREM2 Alzheimer's variant R47H causes similar transcriptional dysregulation to knockout, yet only subtle functional phenotypes in human iPSC-derived macrophages*. Alzheimer's Research & Therapy, 2020. **12**(1): p. 151.
138. Dean, H.B., E.D. Roberson, and Y. Song, *Neurodegenerative Disease-Associated Variants in TREM2 Destabilize the Apical Ligand-Binding Region of the Immunoglobulin Domain*. Frontiers in neurology, 2019. **10**: p. 1252-1252.
139. Shboul, M., et al., *Bone matrix hypermineralization associated with low bone turnover in a case of Nasu-Hakola disease*. Bone, 2019. **123**: p. 48-55.
140. Pacheco-Costa, R., et al., *High Bone Mass in Mice Lacking Cx37 Due to Defective Osteoclast Differentiation*. J. Biol. Chem, 2014. **289**(12): p. 8508-8520.
141. Wallace, J.M., et al., *Inbred strain-specific effects of exercise in wild type and biglycan deficient mice*. Annals of biomedical engineering, 2010. **38**(4): p. 1607-1617.
142. Aguilar-Perez, A., et al., *Age- and sex-dependent role of osteocytic pannexin1 on bone and muscle mass and strength*. Sci Rep, 2019. **9**(1): p. 13903.

143. Jepsen, K.J., et al., *Establishing biomechanical mechanisms in mouse models: practical guidelines for systematically evaluating phenotypic changes in the diaphyses of long bones*. J. Bone Miner. Res, 2015. **30**(6): p. 951-966.
144. Dempster, D.W., et al., *Standardized nomenclature, symbols, and units for bone histomorphometry: A 2012 update of the report of the ASBMR Histomorphometry Nomenclature Committee*. J. Bone Miner. Res, 2013. **28**(1): p. 2-17.
145. Davis, H.M., et al., *Disruption of the Cx43/miR21 pathway leads to osteocyte apoptosis and increased osteoclastogenesis with aging*. Aging Cell, 2017. **16**(3): p. 551-563.
146. Xiang, X., et al., *The Trem2 R47H Alzheimer's risk variant impairs splicing and reduces Trem2 mRNA and protein in mice but not in humans*. Mol Neurodegener, 2018. **13**(1): p. 49.
147. Poggiogalle, E., et al., *Body Composition, IGF1 Status, and Physical Functionality in Nonagenarians: Implications for Osteosarcopenia*. J Am Med Dir Assoc, 2018.
148. Argilés, J.M., et al., *Skeletal Muscle Regulates Metabolism via Interorgan Crosstalk: Roles in Health and Disease*. J Am Med Dir Assoc, 2016. **17**(9): p. 789-96.
149. Cartee, G.D., et al., *Exercise Promotes Healthy Aging of Skeletal Muscle*. Cell metabolism, 2016. **23**(6): p. 1034-1047.
150. Menshikova, E.V., et al., *Effects of exercise on mitochondrial content and function in aging human skeletal muscle*. J Gerontol A Biol Sci Med Sci, 2006. **61**(6): p. 534-40.

151. Bamman, M.M., B.M. Roberts, and G.R. Adams, *Molecular Regulation of Exercise-Induced Muscle Fiber Hypertrophy*. Cold Spring Harb Perspect Med, 2018. **8**(6).
152. Graham, Z.A., et al., *Mechanisms of exercise as a preventative measure to muscle wasting*. Am J Physiol Cell Physiol, 2021. **321**(1): p. C40-c57.
153. von Haehling, S., J.E. Morley, and S.D. Anker, *An overview of sarcopenia: facts and numbers on prevalence and clinical impact*. J Cachexia Sarcopenia Muscle, 2010. **1**(2): p. 129-133.
154. Skelton, D.A., J. Kennedy, and O.M. Rutherford, *Explosive power and asymmetry in leg muscle function in frequent fallers and non-fallers aged over 65*. Age and ageing, 2002. **31**(2): p. 119-125.
155. Yeung, S.S.Y., et al., *Sarcopenia and its association with falls and fractures in older adults: A systematic review and meta-analysis*. Journal of cachexia, sarcopenia and muscle, 2019. **10**(3): p. 485-500.
156. Kirk, B., A. Al Saedi, and G. Duque, *Osteosarcopenia: A case of geroscience*. AGING MEDICINE, 2019. **2**(3): p. 147-156.
157. Bilodeau, P.A., E.S. Coyne, and S.S. Wing, *The ubiquitin proteasome system in atrophying skeletal muscle: roles and regulation*. American Journal of Physiology-Cell Physiology, 2016. **311**(3): p. C392-C403.
158. Cohen, S., et al., *During muscle atrophy, thick, but not thin, filament components are degraded by MuRF1-dependent ubiquitylation*. Journal of Cell Biology, 2009. **185**(6): p. 1083-1095.

159. Clavel, S., et al., *Atrophy-related ubiquitin ligases, atrogin-1 and MuRF1 are up-regulated in aged rat Tibialis Anterior muscle*. *Mechanisms of Ageing and Development*, 2006. **127**(10): p. 794-801.
160. Edström, E., et al., *Atrogin-1/MAFbx and MuRF1 are downregulated in aging-related loss of skeletal muscle*. *J Gerontol A Biol Sci Med Sci*, 2006. **61**(7): p. 663-74.
161. Altun, M., et al., *Muscle wasting in aged, sarcopenic rats is associated with enhanced activity of the ubiquitin proteasome pathway*. *The Journal of biological chemistry*, 2010. **285**(51): p. 39597-39608.
162. Davis, H.M., et al., *Short-term pharmacologic RAGE inhibition differentially affects bone and skeletal muscle in middle-aged mice*. *Bone*, 2019. **124**: p. 89-102.
163. Dos Santos, M., et al., *Single-nucleus RNA-seq and FISH identify coordinated transcriptional activity in mammalian myofibers*. *Nat Commun*, 2020. **11**(1): p. 5102.
164. Léger, B., et al., *Human sarcopenia reveals an increase in SOCS-3 and myostatin and a reduced efficiency of Akt phosphorylation*. *Rejuvenation Res*, 2008. **11**(1): p. 163-175b.
165. Sandri, M., et al., *Foxo transcription factors induce the atrophy-related ubiquitin ligase atrogin-1 and cause skeletal muscle atrophy*. *Cell*, 2004. **117**(3): p. 399-412.
166. Proud, C.G., *Signalling to translation: how signal transduction pathways control the protein synthetic machinery*. *Biochem J*, 2007. **403**(2): p. 217-34.

167. Bodine, S.C., et al., *Akt/mTOR pathway is a crucial regulator of skeletal muscle hypertrophy and can prevent muscle atrophy in vivo*. Nat. Cell Biol, 2001. **3**(11): p. 1014-1019.
168. Drummond, M.J., et al., *Nutritional and contractile regulation of human skeletal muscle protein synthesis and mTORC1 signaling*. Journal of Applied Physiology, 2009. **106**(4): p. 1374-1384.
169. Brunn, G.J., et al., *Phosphorylation of the translational repressor PHAS-I by the mammalian target of rapamycin*. Science, 1997. **277**(5322): p. 99-101.
170. Chesley, A., et al., *Changes in human muscle protein synthesis after resistance exercise*. J Appl Physiol (1985), 1992. **73**(4): p. 1383-8.
171. Volpi, E., et al., *Basal muscle amino acid kinetics and protein synthesis in healthy young and older men*. JAMA, 2001. **286**(10): p. 1206-1212.
172. Drummond, M.J., et al., *Skeletal muscle protein anabolic response to resistance exercise and essential amino acids is delayed with aging*. J Appl Physiol (1985), 2008. **104**(5): p. 1452-61.
173. Welle, S., C. Thornton, and M. Statt, *Myofibrillar protein synthesis in young and old human subjects after three months of resistance training*. Am J Physiol, 1995. **268**(3 Pt 1): p. E422-7.
174. Fry, C.S., et al., *Aging impairs contraction-induced human skeletal muscle mTORC1 signaling and protein synthesis*. Skeletal muscle, 2011. **1**(1): p. 11-11.
175. Hara, K., et al., *Amino acid sufficiency and mTOR regulate p70 S6 kinase and eIF-4E BPI through a common effector mechanism*. J Biol Chem, 1998. **273**(23): p. 14484-94.

176. Cuthbertson, D., et al., *Anabolic signaling deficits underlie amino acid resistance of wasting, aging muscle*. *Faseb j*, 2005. **19**(3): p. 422-4.
177. Bai, G.H., et al., *Effects of branched-chain amino acid-rich supplementation on EWGSOP2 criteria for sarcopenia in older adults: a systematic review and meta-analysis*. *Eur J Nutr*, 2022. **61**(2): p. 637-651.
178. Ten Haaf, D.S.M., et al., *Effects of protein supplementation on lean body mass, muscle strength, and physical performance in nonfrail community-dwelling older adults: a systematic review and meta-analysis*. *Am J Clin Nutr*, 2018. **108**(5): p. 1043-1059.
179. Li, L., et al., *Effects of protein supplementation and exercise on delaying sarcopenia in healthy older individuals in Asian and non-Asian countries: A systematic review and meta-analysis*. *Food Chem X*, 2022. **13**: p. 100210.
180. Rasmussen, B.B., et al., *Insulin resistance of muscle protein metabolism in aging*. *FASEB journal : official publication of the Federation of American Societies for Experimental Biology*, 2006. **20**(6): p. 768-769.
181. Meneilly, G.S., et al., *Insulin-mediated increase in blood flow is impaired in the elderly*. *J Clin Endocrinol Metab*, 1995. **80**(6): p. 1899-903.
182. Baron, A.D., et al., *Interaction between insulin sensitivity and muscle perfusion on glucose uptake in human skeletal muscle: evidence for capillary recruitment*. *Diabetes*, 2000. **49**(5): p. 768-74.
183. Petersen, K.F., et al., *Effect of aging on muscle mitochondrial substrate utilization in humans*. *Proceedings of the National Academy of Sciences*, 2015. **112**(36): p. 11330-11334.

184. Cleasby, M.E., et al., *Local overexpression of the myostatin propeptide increases glucose transporter expression and enhances skeletal muscle glucose disposal*. American journal of physiology. Endocrinology and metabolism, 2014. **306**(7): p. E814-E823.
185. Cleasby, M.E., et al., *Functional studies of Akt isoform specificity in skeletal muscle in vivo; maintained insulin sensitivity despite reduced insulin receptor substrate-1 expression*. Mol. Endocrinol, 2007. **21**(1): p. 215-228.
186. Merz, K.E. and D.C. Thurmond, *Role of Skeletal Muscle in Insulin Resistance and Glucose Uptake*, in *Comprehensive Physiology*. p. 785-809.
187. Musi, N., et al., *Metformin increases AMP-activated protein kinase activity in skeletal muscle of subjects with type 2 diabetes*. Diabetes, 2002. **51**(7): p. 2074-81.
188. Zhang, S., et al., *Structure of the full-length human Pannexin1 channel and insights into its role in pyroptosis*. Cell Discov, 2021. **7**(1): p. 30.
189. Suwa, M., et al., *Metformin increases the PGC-1alpha protein and oxidative enzyme activities possibly via AMPK phosphorylation in skeletal muscle in vivo*. J Appl Physiol (1985), 2006. **101**(6): p. 1685-92.
190. Lexell, J., *Human aging, muscle mass, and fiber type composition*. J Gerontol A Biol Sci Med Sci, 1995. **50 Spec No**: p. 11-6.
191. Kirkendall, D.T. and W.E. Garrett, Jr., *The effects of aging and training on skeletal muscle*. Am J Sports Med, 1998. **26**(4): p. 598-602.
192. Hortobágyi, T., et al., *The influence of aging on muscle strength and muscle fiber characteristics with special reference to eccentric strength*. The Journals of

- Gerontology Series A: Biological Sciences and Medical Sciences, 1995. **50**(6): p. B399-B406.
193. Pette, D. and C. Spamer, *Metabolic properties of muscle fibers*. Fed Proc, 1986. **45**(13): p. 2910-4.
194. Ørtenblad, N., et al., *The Muscle Fiber Profiles, Mitochondrial Content, and Enzyme Activities of the Exceptionally Well-Trained Arm and Leg Muscles of Elite Cross-Country Skiers*. Front Physiol, 2018. **9**: p. 1031.
195. Liang, H. and W.F. Ward, *PGC-1 α : a key regulator of energy metabolism*. Advances in Physiology Education, 2006. **30**(4): p. 145-151.
196. Barrès, R., et al., *Non-CpG methylation of the PGC-1 α promoter through DNMT3B controls mitochondrial density*. Cell Metab, 2009. **10**(3): p. 189-98.
197. Lin, H.K., et al., *Proteasome activity is required for androgen receptor transcriptional activity via regulation of androgen receptor nuclear translocation and interaction with coregulators in prostate cancer cells*. J. Biol. Chem, 2002.
198. Yang, S., et al., *Functional effects of muscle PGC-1 α in aged animals*. Skeletal Muscle, 2020. **10**(1): p. 14.
199. Hettige, P., et al., *Comparative analysis of the transcriptomes of EDL, psoas, and soleus muscles from mice*. BMC Genomics, 2020. **21**(1): p. 808.
200. Shou, J., P.-J. Chen, and W.-H. Xiao, *Mechanism of increased risk of insulin resistance in aging skeletal muscle*. Diabetology & Metabolic Syndrome, 2020. **12**(1): p. 14.

201. Qiang, W., et al., *Aging impairs insulin-stimulated glucose uptake in rat skeletal muscle via suppressing AMPK α* . *Experimental & Molecular Medicine*, 2007. **39**(4): p. 535-543.
202. Bouzakri, K., H.A. Koistinen, and J.R. Zierath, *Molecular mechanisms of skeletal muscle insulin resistance in type 2 diabetes*. *Current diabetes reviews*, 2005. **1**(2): p. 167-174.
203. Burke, R.E., *Chapter 15 Revisiting the Notion of 'motor unit types'*, in *Progress in Brain Research*, M.D. Binder, Editor. 1999, Elsevier. p. 167-175.
204. Hepple, R.T. and C.L. Rice, *Innervation and neuromuscular control in ageing skeletal muscle*. *The Journal of Physiology*, 2016. **594**(8): p. 1965-1978.
205. Ansved, T., P. Wallner, and L. Larsson, *Spatial distribution of motor unit fibres in fast- and slow-twitch rat muscles with special reference to age*. *Acta Physiol Scand*, 1991. **143**(3): p. 345-54.
206. Langer, H.T., et al., *Muscle Atrophy Due to Nerve Damage Is Accompanied by Elevated Myofibrillar Protein Synthesis Rates*. *Frontiers in Physiology*, 2018. **9**.
207. Pikatza-Menoio, O., et al., *The Skeletal Muscle Emerges as a New Disease Target in Amyotrophic Lateral Sclerosis*. *Journal of personalized medicine*, 2021. **11**(7): p. 671.
208. Thibeau, S., et al., *Alzheimer's Disease Biomarkers Interactively Influence Physical Activity, Mobility, and Cognition Associations in a Non-Demented Aging Population*. *J Alzheimers Dis*, 2017. **60**(1): p. 69-86.
209. Yamaguchi, K., *[Falls in patients with dementia]*. *Clin Calcium*, 2008. **18**(11): p. 1588-93.

210. O'Leary, T.P., et al., *Motor function deficits in the 12 month-old female 5xFAD mouse model of Alzheimer's disease*. Behav Brain Res, 2018. **337**: p. 256-263.
211. Oblak, A.L., et al., *Comprehensive Evaluation of the 5XFAD Mouse Model for Preclinical Testing Applications: A MODEL-AD Study*. Frontiers in aging neuroscience, 2021. **13**: p. 713726-713726.
212. Vanden Dries, V., et al., *Amyloid precursor protein reduction enhances the formation of neurofibrillary tangles in a mutant tau transgenic mouse model*. Neurobiology of Aging, 2017. **55**: p. 202-212.
213. Chen, Y., et al., *Metformin attenuates plaque-associated tau pathology and reduces amyloid- β burden in APP/PS1 mice*. Alzheimer's research & therapy, 2021. **13**(1): p. 40-40.
214. Rotermund, C., G. Machetanz, and J.C. Fitzgerald, *The Therapeutic Potential of Metformin in Neurodegenerative Diseases*. Front Endocrinol (Lausanne), 2018. **9**: p. 400.
215. Wang, C.P., et al., *Differential effects of metformin on age related comorbidities in older men with type 2 diabetes*. J Diabetes Complications, 2017. **31**(4): p. 679-686.
216. Pin, F., et al., *Growth of ovarian cancer xenografts causes loss of muscle and bone mass: a new model for the study of cancer cachexia*. J. Cachexia. Sarcopenia. Muscle, 2018. **9**(4): p. 685-700.
217. Toledo, M., et al., *A multifactorial anti-cachectic approach for cancer cachexia in a rat model undergoing chemotherapy*. Journal of cachexia, sarcopenia and muscle, 2016. **7**(1): p. 48-59.

218. Huot, J.R., et al., *MC38 Tumors Induce Musculoskeletal Defects in Colorectal Cancer*. International Journal of Molecular Sciences, 2021. **22**(3).
219. Huot, J.R., et al., *ACVR2B antagonism as a countermeasure to multi-organ perturbations in metastatic colorectal cancer cachexia*. Journal of cachexia, sarcopenia and muscle, 2020. **11**(6): p. 1779-1798.
220. Au - Arnold, W.D., et al., *Electrophysiological Motor Unit Number Estimation (MUNE) Measuring Compound Muscle Action Potential (CMAP) in Mouse Hindlimb Muscles*. JoVE, 2015(103): p. e52899.
221. Sheth, K.A., et al., *Muscle strength and size are associated with motor unit connectivity in aged mice*. Neurobiol Aging, 2018. **67**: p. 128-136.
222. Pin, F., et al., *PDK4 drives metabolic alterations and muscle atrophy in cancer cachexia*. Faseb j, 2019. **33**(6): p. 7778-7790.
223. Schneider, C.A., W.S. Rasband, and K.W. Eliceiri, *NIH Image to ImageJ: 25 years of image analysis*. Nat Methods, 2012. **9**(7): p. 671-5.
224. Schiaffino, S. and C. Reggiani, *Fiber Types in Mammalian Skeletal Muscles*. Physiological Reviews, 2011. **91**(4): p. 1447-1531.
225. Bonewald, L., *Use it or lose it to age: A review of bone and muscle communication*. Bone, 2019. **120**: p. 212-218.
226. Waning, D.L., et al., *Excess TGF-beta mediates muscle weakness associated with bone metastases in mice*. Nat. Med, 2015. **21**(11): p. 1262-1271.
227. Boyle, P.A., et al., *Association of muscle strength with the risk of Alzheimer disease and the rate of cognitive decline in community-dwelling older persons*. Archives of neurology, 2009. **66**(11): p. 1339-1344.

228. Daulatzai, M.A., *Early Stages of Pathogenesis in Memory Impairment during Normal Senescence and Alzheimer's Disease*. Journal of Alzheimer's Disease, 2010. **20**: p. 355-367.
229. Zhou, S.L., et al., *TREM2 Variants and Neurodegenerative Diseases: A Systematic Review and Meta-Analysis*. J Alzheimers Dis, 2019.
230. Xing, J., A.R. Titus, and M.B. Humphrey, *The TREM2-DAP12 signaling pathway in Nasu-Hakola disease: a molecular genetics perspective*. Research and reports in biochemistry, 2015. **5**: p. 89-100.
231. Otero, K., et al., *TREM2 and beta-catenin regulate bone homeostasis by controlling the rate of osteoclastogenesis*. J. Immunol, 2012. **188**(6): p. 2612-2621.
232. Guo, Q., et al., *Modeling Alzheimer's disease in mouse without mutant protein overexpression: cooperative and independent effects of A β and tau*. PloS one, 2013. **8**(11): p. e80706-e80706.
233. Youlten, S.E., et al., *Osteocyte transcriptome mapping identifies a molecular landscape controlling skeletal homeostasis and susceptibility to skeletal disease*. Nat Commun, 2021. **12**(1): p. 2444.
234. Dole, N.S., et al., *TGFbeta regulation of perilacunar/canalicular remodeling is sexually dimorphic*. J Bone Miner Res, 2020.
235. Dole, N.S., et al., *Osteocyte-Intrinsic TGF-beta Signaling Regulates Bone Quality through Perilacunar/Canalicular Remodeling*. Cell Rep, 2017. **21**(9): p. 2585-2596.

236. Zheng, H., et al., *TREM2 Promotes Microglial Survival by Activating Wnt/ β -Catenin Pathway*. The Journal of neuroscience : the official journal of the Society for Neuroscience, 2017. **37**(7): p. 1772-1784.
237. Zhu, D., A. Montagne, and Z. Zhao, *Alzheimer's pathogenic mechanisms and underlying sex difference*. Cell Mol Life Sci, 2021. **78**(11): p. 4907-4920.
238. Nebel, R.A., et al., *Understanding the impact of sex and gender in Alzheimer's disease: A call to action*. Alzheimers Dement, 2018. **14**(9): p. 1171-1183.
239. Stephen, T.L., et al., *APOE genotype and sex affect microglial interactions with plaques in Alzheimer's disease mice*. Acta Neuropathol Commun, 2019. **7**(1): p. 82.
240. Regan, J.N., et al., *The Role of TGFbeta in Bone-Muscle Crosstalk*. Curr Osteoporos Rep, 2017. **15**(1): p. 18-23.
241. Miljkovic, N., et al., *Aging of skeletal muscle fibers*. Ann Rehabil Med, 2015. **39**(2): p. 155-62.
242. Tarantino, U., et al., *Osteoporosis and sarcopenia: the connections*. Aging Clin. Exp. Res, 2013. **25 Suppl 1**: p. S93-S95.
243. Mendias, C.L., et al., *Contractile properties of EDL and soleus muscles of myostatin-deficient mice*. Journal of applied physiology (Bethesda, Md. : 1985), 2006. **101**(3): p. 898-905.
244. Saclier, M., et al., *Monocyte/macrophage interactions with myogenic precursor cells during skeletal muscle regeneration*. The FEBS Journal, 2013. **280**(17): p. 4118-4130.
245. Cui, C.-Y., et al., *Skewed macrophage polarization in aging skeletal muscle*. Aging Cell, 2019. **18**(6): p. e13032.

246. Reidy, P.T., et al., *Aging impairs mouse skeletal muscle macrophage polarization and muscle-specific abundance during recovery from disuse*. American Journal of Physiology-Endocrinology and Metabolism, 2019. **317**(1): p. E85-E98.
247. Ulland, T.K., et al., *TREM2 Maintains Microglial Metabolic Fitness in Alzheimer's Disease*. Cell, 2017. **170**(4): p. 649-663.e13.
248. Cheng, Q., et al., *TREM2-activating antibodies abrogate the negative pleiotropic effects of the Alzheimer's disease variant TREM2(R47H) on murine myeloid cell function*. J. Biol. Chem, 2018. **293**(32): p. 12620-12633.
249. Schlepckow, K., et al., *Enhancing protective microglial activities with a dual function TREM2 antibody to the stalk region*. EMBO Molecular Medicine, 2020. **12**(4): p. e11227.
250. Smith, G.I., et al., *Sexually dimorphic effect of aging on skeletal muscle protein synthesis*. Biology of Sex Differences, 2012. **3**(1): p. 11.
251. Gómez-Pérez, Y., et al., *Gender Dimorphism in High-Fat-Diet-Induced Insulin Resistance in Skeletal Muscle of Aged Rats*. Cellular Physiology and Biochemistry, 2008. **22**(5-6): p. 539-548.

CURRICULUM VITAE

Alyson Lola Essex

Education

Doctor of Philosophy from Indiana University - Anatomy & Cell Biology

Aug. 2016 – May 2022

Indiana University School of Medicine, Indiana University- Purdue University,
Indianapolis (IUPUI), Indianapolis IN

Doctoral Minor in Policy Analysis for Biomedical Sciences

Bachelor of Science – Microbiology and Immunology

Aug. 2013 – Dec.2016

University of Miami, Coral Gables FL

Minors in Chemistry and Classics; Cognate in Abnormal Psychology

Research Experience

Graduate Research Assistant, Plotkin Lab and Bonetto Lab

May 2018 – May 2022, IU School of Medicine, Indianapolis, IN

“Dementia associated variant in TREM2 present with sex-dependent musculoskeletal phenotype”

“Effect of osteocytic miR-21 on bone and muscle parameters *in vivo*”

“The potential therapeutic role for bisphosphonates in chemotherapy-induced cachexia”

Research Assistant, Strbo Lab

2015 – 2016, University of Miami, Coral Gables FL

“Role of Perforin-2 at the maternal-fetal interface.”

Honors

Presidential Management Fellow – Class of 2022

President of the Graduate and Professional Student Government at IUPUI

Indiana University School of Medicine Graduation Speaker – Spring 2022

Invited Speaker at the Indiana University Inauguration of Pamela Whitten

Speaker for the Indiana University School of Medicine 2022 Commencement

Indiana University Board of Trustees Student Trustee Selection Committee Member

Indiana University Graduate Faculty Council Member

Vice President of the Graduate and Professional Student Government at IUPUI

IUPUI Faculty Council *ex officio* student representative

Anatomy & Cell Biology Representative for the Biomedical Graduate Student

Advocacy Association (BGSAA)

Awards

Finalist for the Presidential Management Fellows Class of 2022

Pre-Doctoral Fellowship on NIH T32-AR065971 Musculoskeletal Grant

ASBMR Young Investigator Travel Award

Beckman Coulter Reagents Grant

Graduate and Professional Education Grant (GPEG) Award

Publications

Essex AL, Huot JR, Deosthale P, Wagner A, Figueras J, Davis A, Damrath J, Pin F, Wallace J, Bonetto A, Plotkin L. TREM2 R47H variant causes distinct age- and sex-dependent musculoskeletal alterations in mice. *Journal of Bone and Mineral Research (JBMR)*. 2022.

Essex AL, Desothale P, Huot JR, Moment N, Bonetto A, Plotkin LI. miR21 deletion in osteocytes has direct and indirect effects on skeletal muscle in a sex-dimorphic manner in mice. *BMC Biology of Sex Differences*, Under Review. 2022.

Deosthale P, Hong JM, Essex AL, Rodriguez W, Tariq D, Sidhu H, Marcial A, Bruzzaniti A, Plotkin LI. Sex-specific differences in direct osteoclastic *versus* indirect osteoblastic effects underlay the low bone mass of Pannexin1 deletion in TRAP-expressing cells in mice. *Bone Rep*. 2022 Jan 4;16:101164. doi: 10.1016/j.bonr.2021.101164.

Pin, F., Prideaux, M., Huot, J. R., Essex, A. L., Plotkin, L. I., Bonetto, A., & Bonewald, L. F. (2021). Non-bone metastatic cancers promote osteocyte-induced bone destruction. *Cancer Letters*, 520, 80-90. doi:<https://doi.org/10.1016/j.canlet.2021.06.030>

Huot, J. R., Pin, F., Essex, A. L., & Bonetto, A. (2021). MC38 Tumors Induce Musculoskeletal Defects in Colorectal Cancer. *International Journal of Molecular Sciences*, 22(3). doi:10.3390/ijms22031486

Essex, A. L., Pin, F., Huot, J. R., Bonewald, L. F., Plotkin, L. I., & Bonetto, A. (2019). Bisphosphonate Treatment Ameliorates Chemotherapy-Induced Bone and Muscle Abnormalities in Young Mice. *Front Endocrinol (Lausanne)*, 10, 809. doi:10.3389/fendo.2019.00809

Aguilar-Perez, A., Pacheco-Costa, R., Atkinson, E. G., Deosthale, P., Davis, H. M., Essex, A. L., . . . Plotkin, L. I. (2019). Age- and sex-dependent role of osteocytic pannexin1 on bone and muscle mass and strength. *Sci Rep*, 9(1), 13903. doi:10.1038/s41598-019-50444-1

Davis, H. M., Deosthale, P. J., Pacheco-Costa, R., Essex, A. L., Atkinson, E. G., Aref, M. W., . . . Plotkin, L. I. (2019). Osteocytic miR21 deficiency improves bone strength independent of sex despite having sex divergent effects on osteocyte viability and bone turnover. *Febs j*. doi:10.1111/febs.15066

Davis, H. M., Essex, A. L., Valdez, S., Deosthale, P. J., Aref, M. W., Allen, M. R., . . . Plotkin, L. I. (2019). Short-term pharmacologic RAGE inhibition differentially affects bone and skeletal muscle in middle-aged mice. *Bone*, 124, 89-102. doi:https://doi.org/10.1016/j.bone.2019.04.012

Huot, J. R., Essex, A. L., Gutierrez, M., Barreto, R., Wang, M., Waning, D. L., . . . Bonetto, A. (2019). Chronic Treatment with Multi-Kinase Inhibitors Causes Differential Toxicities on Skeletal and Cardiac Muscles. *Cancers (Basel)*, 11(4). doi:10.3390/cancers11040571

Plotkin, L. I., Essex, A. L., & Davis, H. M. (2019). RAGE Signaling in Skeletal Biology. *Curr Osteoporos Rep*, 17(1), 16-25. doi:10.1007/s11914-019-00499-w

Presentations

Nick Momeni, Alyson Essex, Padmini Deosthale, Lilian Plotkin. (November 2021)
“Bone loss after acute sex-hormone removal via gonadectomy prior to skeletal maturity

most striking in male but not female animals” 7th Annual Marian University College of Osteopathic Medicine Research Day; Best Poster Presentation Award- Second Place.

Alyson L. Essex, Padmini Deosthale, Alison Wagner, Jorge Figueras, Azaria Davis, J. D. Damrath, Ziyue Liu, Joseph Wallace, Andrea Bonetto, Lilian I. Plotkin. (October 2021) “*Brain to Bone: Neurodegeneration risk-factor TREM2 R47H mutation accelerates bone loss and then stalls out in female mice*” ASBMR Annual Meeting, Poster Presentation. San Diego, California.

Alyson L. Essex, Padmini Deosthale, Alison Wagner, Jorge Figueras, Azaria Davis, J. D. Damrath, Ziyue Liu, Joseph Wallace, Andrea Bonetto, Lilian I. Plotkin. (September 2021) “*Brain to Bone: Neurodegeneration risk-factor TREM2 R47H mutation accelerates bone loss and then stalls out in female mice*” Endocrine Fellows Forum (EFF), Poster Presentation. Virtual due to the COVID-19 pandemic.

Azaria Davis, Alyson Essex, Padmini Deosthale, Joseph Wallace, Andrea Bonetto, Lilian I. Plotkin. (November 2020) “*Genetic Mutations in TREM2 as a Link Between Neurodegeneration and Bone.*” ABRCMS Poster Presentation. Virtual due to the COVID-19 pandemic.

Azaria Davis, Alyson Essex, Padmini Deosthale, Joseph Wallace, Andrea Bonetto, Lilian I. Plotkin. (October 2020) “*Genetic Mutations in TREM2 as a Link Between Neurodegeneration and Bone*” APSA South Atlantic Regional Meeting Oral Presentation. Virtual due to the COVID-19 pandemic.

Alyson L. Essex, Padmini Deosthale, Alison Wagner, J. D. Damrath, Joseph Wallace, Monte Willis, Andrea Bonetto, Lilian I. Plotkin. (September 2020) “*Beyond the Brain: Neurodegeneration risk-factor TREM2 R47H mutation causes distinct sex-*

dependent bone and cardiovascular phenotype in the absence of neuropathology.”
ASBMR Annual Meeting, Oral Presentation. Virtual due to the COVID-19 pandemic.

Alyson L. Essex, Padmini Deosthale, Alison Wagner, J. D. Damrath, Joseph Wallace, Monte Willis, Andrea Bonetto, Lilian I. Plotkin. (June 2020) “*Beyond the Brain: Neurodegeneration risk-factor TREM2 R47H mutation causes distinct sex-dependent bone and cardiovascular phenotype in the absence of neuropathology.*” ECTS - GEMSTONE Digital Masterclass, Oral Presentation. Virtual due to the COVID-19 pandemic.

Alyson Essex, Hannah Davis, Padmini Deosthale, Andrea Bonetto, Lilian Plotkin. (September 2019) “*Lack of osteocytic-miR21 promotes skeletal muscle mass growth in a sex-specific manner.*” ASBMR Annual Meeting; ASBMR Muscle Pre-meeting, Poster Presentation. Orlando, Florida.

Lilian I. Plotkin, Padmini Deosthale, Jung Min Hong, Harry Sidhu, Alyson Essex, Angela Bruzzaniti. (September 2019) “*Sex-specific increases in osteoclast differentiation and function by Pannexin1 channel deletion in TRAP-expressing cells.*” ASBMR Annual Meeting, Poster Presentation. Orlando, Florida.

Alyson Essex, Hannah Davis, Padmini Deosthale, Andrea Bonetto, Lilian Plotkin. (August 2019) “*Lack of osteocytic-miR21 promotes skeletal muscle mass growth in a sex-specific manner.*” Bone and Muscle Interactions: the Mechanical and Beyond. Role of Soluble Factors in Muscle-Bone Interactions. Oral and Poster Presentation. Indianapolis, Indiana.

Alyson Essex, Hannah Davis, Sinai Valdez, Fabrizio Pin, Lilian Plotkin, Andrea Bonetto. (March 2019) “*Rescuing age-associated decline in muscle mass by inhibition of*

the receptor for advanced glycosylation end products, RAGE” Advances in Skeletal Biology Muscle Meeting Poster Presentation. Gainesville, Florida.

Alyson Essex, Hannah Davis, Sinai Valdez, Fabrizio Pin, Lilian Plotkin, Andrea Bonetto. (September 2018) “*Rescuing age-associated decline in muscle mass by inhibition of the receptor for advanced glycosylation end products, RAGE*” *Late-Breaking Abstract*. ASBMR Annual Meeting Poster Presentation. Montreal, Canada.

Hannah M. Davis, Rafael Pacheco-Costa, Mohammad W. Aref, Sinai Valdez, Alyson Essex, Emily G. Atkinson, Julian E. Dilley, Padmini J. Deosthale, Mircea Ivan, Teresita Bellido, Matthew Allen, Lilian I. Plotkin. (September 2018) “*Sex divergent role of osteocytic miR21 in the maintenance of osteocyte viability and regulation of bone turnover.*” *Plenary Poster*. ASBMR Annual Meeting Poster Presentation. Montreal, Canada.